5. SITE 221

The Shipboard Scientific Party[1]
With Additional Reports From
Robert E. Coleman, U. S. Geological Survey, Menlo Park, California
and
Norman Hamilton, University of Southamptom, United Kingdom

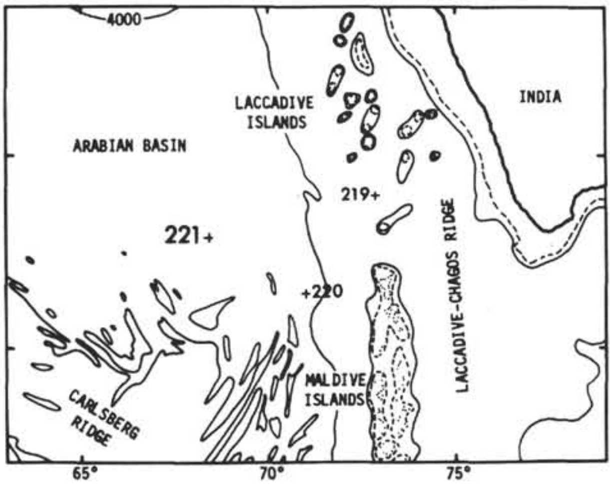

Figure 1. *Position of Site 221 and adjacent Leg 23 sites (shown by +). Contours at 200, 1000, and 4000 meters, from Laughton et al. (1971).*

SITE SUMMARY

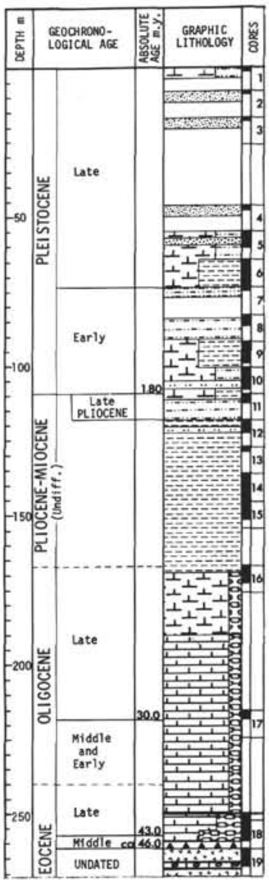

SITE DATA

Dates: 0520 18 Mar–1320 20 Mar 72

Time: 56 hours

Position (Figure 1): 7°58.18′N, 68°24.37′E

Holes Drilled: 1

Water Depth by Echo-Sounder: 4650 corr. meters

Total Penetration: 270 meters

Total Core Recovered: 76.6 meters from 19 cores

Age of Oldest Sediment: Middle Eocene

Basement: Basalt

ABSTRACT

Located on the Arabian Abyssal Plain near its southernmost termination, this site recorded continuous Middle Eocene through Pleistocene deep-water sedimentation above oceanic basalt. A chert layer is developed at the base of the Eocene strata. The Eocene through Miocene sequence shows the transition from biogenic ooze to brown clay sedimentation which typifies depositional sites as they move from a ridge crest to a deep-ridge flank position. Above this sequence is an undifferentiated Pliocene-Miocene through Pleistocene interval of terrigenous and calcareous turbidites. The former were derived from the Indus Canyon, and the latter from elsewhere.

---

[1] Robert B. Whitmarsh, National Institute of Oceanography, Wormley, Godalming, Surrey, United Kingdom; Oscar E. Weser, Scripps Institution of Oceanography, La Jolla, California: Syed Ali, State University of New York, Stony Brook, New York; Joseph E. Boudreaux, Texaco Inc., New Orleans, Louisiana; Robert L. Fleisher, University of Southern California, Los Angeles, California; Dan Jipa, M.I.M.G. Institutul Geologic, Bucharest, Romania; Robert B. Kidd, Southampton University, Southampton, United Kingdom (Present address: National Institute of Oceanography, Wormley, Godalming, Surrey, United Kingdom); Tapas K. Mallik, Geological Survey of India, Calcutta, India; Albert Matter, Geologisches Institut, Universität Bern, Bern, Switzerland; Catherine Nigrini, Lexington, Massachusetts; Hassan N. Siddiquie, Geological Survey of India, Calcutta India (Present address: National Institute of Oceanography, Goa, India); Peter Stoffers, Laboratorium für Sedimentforschung, Universität Heidelberg, Heidelberg, Germany.

BACKGROUND AND OBJECTIVES

Before the Indian Ocean drilling began, a low priority hole had been proposed at 8°55'N, 63°05'E. The main objective of drilling the site was to sample basement at a point just outside the zone of most recent crustal spreading in the Arabian Sea. McKenzie and Sclater (1971) believed that the onset of the present spreading episode in the Arabian Sea should be marked by a sudden shoaling of the depth to igneous basement. Such a step in the basement is apparently visible on a *Conrad*-9 seismic reflection profile close to 8°55'N, 63°05'E (Ewing et al., 1969). However, the proposed site suffered from the disadvantages that the acoustic basement was not visible at the foot of the basement step and that it involved extra steaming time. For these reasons this site had been rejected by the JOIDES Indian Ocean Advisory Panel.

However, on leaving Site 220 it was apparent that time was available for a site at the southern end of the Arabian Abyssal Plain. Such a site could allow for a comparison of distal sediments of the abyssal plain with those to be drilled at the next site on the Indus Cone. A further reason, explained below, for a site in this region was the discovery that the strong smooth, or slightly irregular acoustic basement at Site 220 was Lower Eocene chert, just as at Site 219.

A *Vema*-19 profile roughly along lat 8°N showed that a similar reflector underlies the southeastern part of the Arabian Abyssal Plain. Westwards, this reflector merges with the rough basement which eventually emerges as the Carlsberg Ridge (Figure 2). In this context, it was also very interesting to read the paper of Neprochnov (1961) in which he used the reflections from near-surface explosions to map the sediment thickness in the Arabian Sea. In particular, he remarks that "a typical feature of most of the seismic records is the presence of a strong reflection . . . The amplitude of these waves is comparable to the amplitude of the waves reflected off the bottom and sometimes even exceeds it." The nature of this "key reflection" was consistent from station to station, and it was only absent from 4 stations, of which one lay in the Oman Basin and two more were within about 280 km of the crest of the Carlsberg Ridge over crust, which in all likelihood, is younger than Early Eocene (Figure 3). It appeared very likely from what we had already discovered at Sites 219 and 220 that both the smooth *Vema* reflector and Neprochnov's key reflection were Eocene chert. Confirmation of this in the main Arabian Basin would greatly assist in clarifying the sea floor spreading history of the area. Site 221 was therefore chosen at a point where the smooth reflector on the *Vema*-19 track lay about 0.5 sec below the sea bed, well within reach of the drill.

The Indus Cone is a triangular-shaped prism of sediment with the apex near the mouth of the Indus River in the north Arabian Sea. The sea floor is monotonously flat everywhere except where dissected by channels in the north or by the foothills of the Carlsberg Ridge in the south. The Cone and Arabian Abyssal Plain are bounded on three sides by sea floor elevations. The eastern margin is the continental margin of India and the west flank of the Laccadive-Maldive Ridge. The Carlsberg Ridge forms the

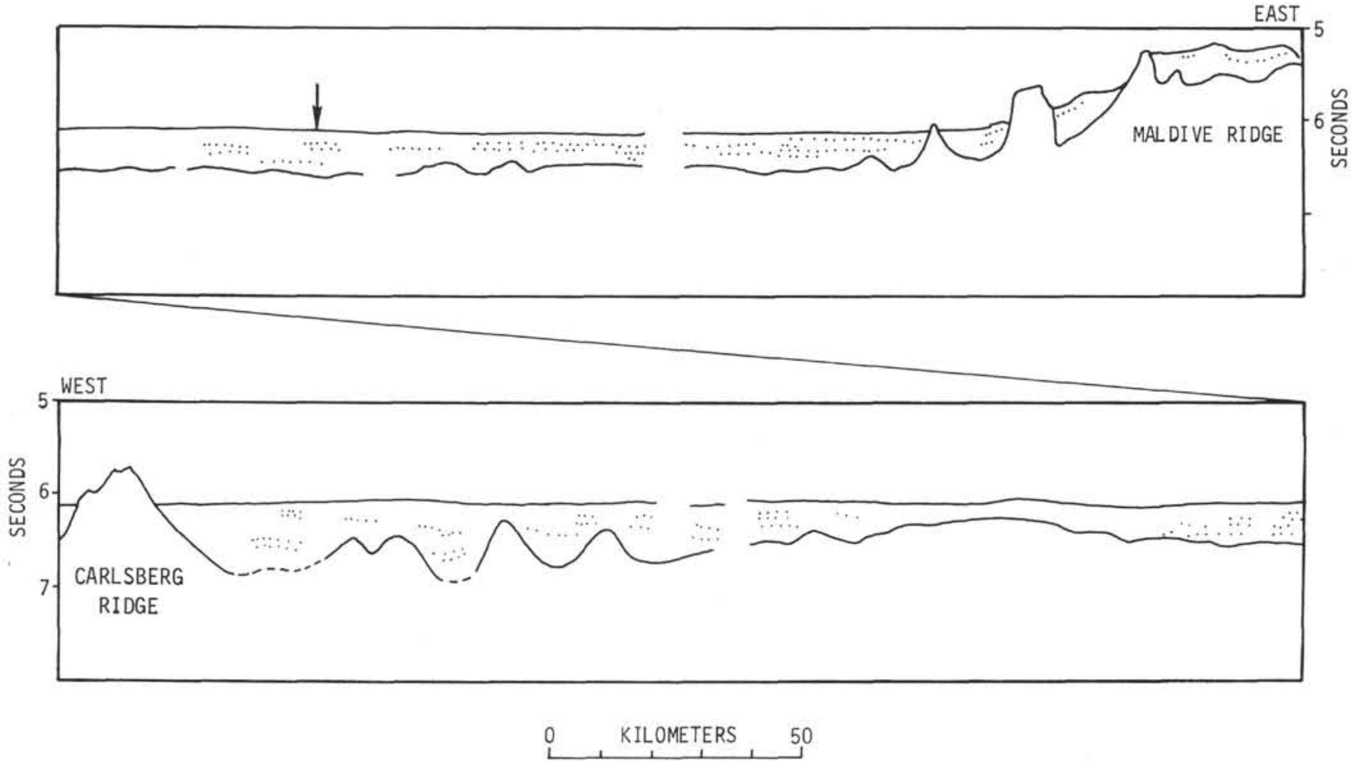

Figure 2. *Tracing of a seismic reflection record across the Arabian Basin and Maldive Ridge obtained along latitude 8°N west of the Laccadive-Chagos Ridge. Note how the acoustic basement beneath the turbidites of the basin is smooth in the east and rough in the west. The arrow marks the proposed position of Site 221. Seismic profile obtained on cruise* Vema-19, *courtesy of Lamont-Doherty Geological Observatory.*

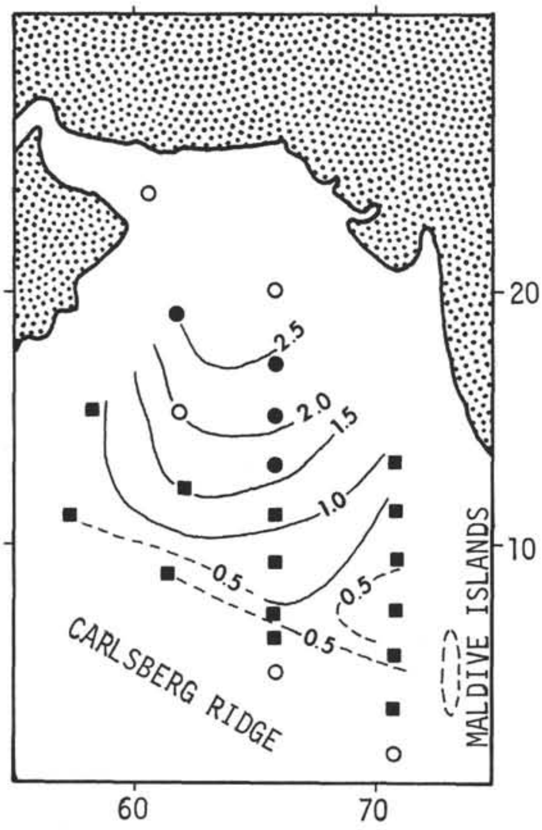

Figure 3. *Thicknesses of sediment above a key reflector in the Arabian Basin (from Neprochnov, 1961). The contour interval is 0.5 sec (about 500 meters). O = key reflection absent;* ● *= key reflection present, no deeper reflections observed;* ■ *= key reflection present, deeper reflections also observed.*

southern boundary and the Owen Ridge (this name was given by the shipboard scientists to the Owen Fracture Zone north of 15°N) the western boundary. The work of Neprochnov showed that the abyssal plain sediments thicken northwards to at least 2.5 km around 18°N (Figure 3). Nearer the mouth of the Indus, seismic refraction work of Closs et al. (1969) showed up to 6 km of sediment overlying a layer with a velocity between 4 and 5 km/sec. The age of the Indus Cone sediments was unknown, although Ewing et al. (1969) had suggested a mid-Miocene age, contemporaneous with the uplift of the Himalayas at that time and with the vast thickness of the Siwalik alluvium deposits found in the foothills of the Himalayas (Wadia, 1968). Gansser (1966) favors a younger age, contemporaneous with the late Quaternary uplift (Morphogenic Phase) of these mountains. Presumably, the Indus Cone is still forming today since the Indus River annually carries 0.44×10^{15} grams of sediment into the Arabian Sea (Holeman, 1968).

The objectives of drilling this site were, therefore, to:

1) Sample and date the strong smooth reflector and the igneous basement if it lies at a deeper level.

2) Determine the history and nature of the Arabian Abyssal Plain sediments.

3) Obtain a geological section at a site more representative of the main Arabian Basin.

4) Obtain paleomagnetic samples for paleolatitude determinations ashore.

Since the site was a new one no constraints had been imposed by the JOIDES Advisory Panel on Pollution Prevention and Safety.

OPERATIONS

The track from Site 220 to Site 221 was chosen so as to pass over a narrow north-south trough up to 5000 meters deep indicated on the bathymetric chart of Laughton (unpublished). The track was continued 280 km to the west of the trough before turning north so as to twice cross the edge of the Lower Eocene cherts since the *Conrad*-9 profile showed that the chert reflector was absent west of the trough. This boundary is identifiable because the chert acoustically masks the underlying volcanic basement, but when it is absent, the rough volcanic basement became apparent.

Glomar Challenger approached Site 221 from the south on 18 March. The approximate site position had been chosen from a *Vema*-19 east-to-west profile (Figure 2). In the region of the intersection of the two tracks, the airgun profile was very uniform and showed essentially flat lying strata underlying the Arabian Basin.

The ship approached the site at 10 knots. After a suitable site had been seen on the reflection profile, speed was reduced to 5 knots and the streamed gear brought on board. A course was then steered by dead reckoning to bring the ship back over the chosen site. There was some delay in laying a good beacon since an initial 13.5 Khz beacon failed while it was still falling through the water column. The launching of a second 16 Khz beacon was delayed by a jammed quick-release hook. The captain had requested that the beacon be laid while the ship was stationary because, due to a breakdown of the computer, the positioning system would only work in the manual mode.

Two basic scientific objectives guided the drilling and coring program at this site: (1) to study in detail a sequence of presumed turbidite beds in the upper part of the hole and (2) to sample a deep presumed chert reflector and, if possible, obtain a sample of the underlying basalt. Core statistics are summarized in Table 1.

With the first objective in mind, it was planned to continuously core from the surface down to approximately 140 meters. For better recovery, the extended core barrel was used on the first coring attempt. Only water was recovered. On the second attempt (which is noted as Core 1 in Table 1) the recovery was zero and the plastic "sock" was torn. That this occurred despite the presence of a small patch of silty clay nanno ooze in the core catcher attests to the presence of mostly sand at the ocean floor. Subsequently, only conventional core barrels were used.

The next two cores had zero recovery; however, sand was recovered from the core catcher, suggesting that a thick sequence of loose sand was being drilled but not retained by the plastic "sock." Of greater concern was the fact that in addition to the strong torque met while cutting Core 2, excessive weight (up to 5000 lb) was necessary at a shallow depth to penetrate the section, thus endangering the bottom hole assembly. Circulation was broken slightly for the third core. Also, mud was spotted to wash out the hole.

TABLE 1
Coring Summary, Site 221

Core	Date/Time Core on Deck (Time Zone-5)	Depth Below Sea Floor (m)	Cored (m)	Recovered (m)
	18 Mar:			
1[a]	2135	0-8	8.0	CC
2	2310	8-17	9.0	CC
	19 Mar:			
3[b]	0030	17-26	9.0	CC
4[c]	0250	46-55	9.0	0.2
5	0415	55-64	9.0	4.8
6	0550	64-73	9.0	8.9
7	0720	73-82	9.0	CC
8	0845	82-91	9.0	2.9
9	1005	91-100	9.0	8.5
10	1140	100-109	9.0	8.1
11	1310	109-118	9.0	2.2
12	1440	118-127	9.0	3.7
13	1615	127-136	9.0	CC
14	1810	136-145	9.0	9.3
15	2010	145-154	9.0	6.0
16[c]	2205	167-176	9.0	6.3
	20 Mar:			
17[c]	0045	215-224	9.0	2.0
18[c]	0320	252-261	9.0	8.8
19[d]	0910	261-270	9.0	4.9
Totals			170.0	76.6

[a] Bit torqued up, extended core barrel scoured by bit.

[b] Pumps on from here.

[c] Drilled before coring.

[d] Took 5 hours.

With the above poor recovery record and the critical situation of the drill string, the section was drilled ahead for 20 meters with the hope of finding a more clayey interval. This decision was justified as succeeding cores contained sediments including interbedded clay beds. Minimum circulation had to be retained, however, to penetrate with the 0 to 5000 lbs of bit weight being used. Continuous cores were taken down through Core 15. With increasing depth, drilling was accompanied by an increase in the bit weight to 10,000 or 12,000 lbs.

After the turbidite sequence had been penetrated, the second objective was pursued, and drilling proceeded in intervals of 13, 39, and 28 meters, separated by single cores. Core 18, at a depth of 252 meters, encountered both chert and basalt. Another basalt core, cut at a rate of 1.5 meters/hour, was obtained to verify that the basalt did not represent a thin sill. After this the hole was terminated at a depth of 270 meters.

Examination of the drill bit after pulling pipe, showed it to be in excellent condition except for a few broken teeth.

Glomar Challenger left Site 221 at 1820 hours 20 March. After streaming gear on a southerly course, the ship returned to pass over the beacon and then set course for 11°00′N, 68°30′E. The reason for this northerly excursion from the direct track to Site 222 was to try and identify the east-west trending magnetic anomalies which exist in this area. Clocks were retarded one hour at midnight 21 March.

LITHOLOGY

Table 2 outlined below depicts the major lithologic units and subunits and their relative approximate depths and thicknesses.

Unit I

This unit is characterized by graded sandy and silty beds intercalated in carbonate detrital silt-nanno ooze or carbonate detrital clay-nanno ooze. On the core summary forms only clearly defined graded beds are illustrated. The strong coring disturbance and limited core recovery, especially in the higher parts of the unit, appear to have prevented other graded intervals from being observed.

The dominant lithology here is a fine-grained gray nanno ooze which has a major clay and silt fraction. Clastic grains, e.g., mica, quartz, feldspar, carbonate particles (including some carbonate rhombs), and clay minerals are the major constituents of this clay/silt fraction. Only rarely is relatively pure nanno ooze present, and this is green where it occurs.

Intercalated in the clay and silt nanno oozes are coarser clastic graded beds and laminae, some of which are dominated by detrital materials similar to those in the oozes, e.g., mica, quartz, feldspar, and abraded calcite rhombs, which have a much diminished nanno content. Other clastic beds have a high content of aragonite pellets, carbonate needles, plant debris, and mega and microfossils. Nannofossils present in these graded sediments are considered to be reworked. This interpretation is strengthened by the presence of discoasters (a pre-Pleistocene fossil) in these Pleistocene beds. Heavy minerals are found in the graded beds, particularly within the basal few centimeters. At present, it appears likely that the oozes may also be reworked sediments. However, as the evidence is not conclusive, they are not given a textural designation but instead retain the designation of ooze.

Many samples taken for grain-size, X-ray mineralogy, and carbon-carbonate analysis in unit I were from graded beds. A detailed compositional analysis of these clastic beds appears in Jipa and Kidd (this volume).

The graded beds have sharp lower boundaries but it is difficult to determine their upper-limits. therefore, wherever the visual grading ends, upper-boundaries are indicated by dashed lines on the core forms.

Above Core 4, only core catcher samples were recovered; these were mainly silty sands. On the basis of the drill string response, these sands are believed to be representative of the upper 55 meters of sediment at this site. However, as this is by no means certain, only the core catcher lithologies are shown on the graphic hole summary.

The boundary between unit I and unit II is placed in Core 11, where there is a marked downward decrease in nannofossil content.

Unit II

Unit II is transitional between unit I and the brown clay of unit III. Nanno ooze is absent and nannofossils only

TABLE 2
Lithologic Summary, Site 221

Lithology			Thickness (m)	Subbottom Depth (m)	Cores
Units		Subunits			
I	Gray CARBONATE-RICH DETRITAL CLAY/SILT-NANNO OOZE with graded DETRITAL SAND and PELLETAL CARBONATE SAND		111	0-111	1-11
II	Gray CARBONATE-RICH DETRITAL SILT/CLAY with graded beds of SAND and SILT		ca. 16	111-127	11-13
III	Brown CLAY		ca. 43	127-170	14-16
IV	Orange MICARB-RICH NANNO OOZE and CHALK with traces of zeolite and/or volcanic glass	a. MICARB-RICH NANNO OOZE b. MICARB-RICH NANNO CHALK c. MICARB-NANNO CHALK with siliceous nodules	20 65 6 91	170-261	16-18
V	THOLEIITIC BASALT with one thin LIMESTONE bed		9	261-270	19

occur in traces. It is a transitional unit in that it contains graded sand and silt units similar to those in unit I set in a fine-grained clastic sequence which is transitional into the brown clay of unit III. The lower boundary of unit II has been arbitrarily taken as being below Sample 13, CC. The smear slides of this core catcher are more akin to the graded beds above than to the brown clay below (having prominent mica and plant debris) even though the sediment is brown in color. The unit lithology, therefore, is one of coarse-graded clastic beds set in a gray carbonate-rich detrital silty clay or clay.

Unit III

This unit is characterized by its homogeneous clay texture, mostly brown coloration, general absence of fossil material (trace of nannos only), low carbonate content, and traces of ferromanganese particles and zeolites. Local sand laminae and patches occur within minor bioturbated intervals, the derivation of which is uncertain. If not due to downhole slumping during coring operations, they would almost surely have to represent early distal products of the Indus Cone.

The base of the unit is defined by a transitional zone of increasing nannofossils. The nannofossils show a fairly abrupt increase between 35 and 60 cm in Section 2 of Core 16,as indicated by results of the carbonate analyses tabulated on the Core 16 summary form.

Unit IV

Pale orange micarb-nanno ooze and chalk typify the sediments in this unit. One to 5 percent zeolites plus traces of volcanic glass, and carbonate needles, were recorded. The carbon-carbonate data indicate that in some cases up to 25 percent noncarbonate material occurs in this unit. The micarb here is, almost without exception, fine-grained in the size range of fine silt and smaller. The subunit divisions have been arbitrarily made to divide ooze (a) from chalk (b) and both these from chalk with siliceous nodules (c). In subunit IVc, which encompasses the lower portion of Core 18, bioturbation, streaks of volcanic glass, foraminifera, and fish remains occur. Radiolaria are found in the siliceous nodules. The nodules appear to harden towards the base and may be an expression of the diagenesis of opaline silica to chert described by Heath and Moberly (1971). The lower boundary of the unit is seen in the core catcher of Core 18 where tholeiitic basalt with a glassy chilled top covered by a very clean volcanic ash is encountered. No evidence of sediment baking occurs here, but a thin solid chert layer is present in the core catcher. A minute normal fault present at the base of the chalks exhibits drag-folding, indicative of movement when the sediment was still plastic. Carbon-carbonate analyses in this unit range from 71 to 90 percent.

Unit V

This unit is a very dark gray, partially vesicular, tholeiitic basalt. The igneous rock is uniformly massive and exhibits a distinct diabasic texture. The rock shows six minor chilled margins and fractures filled with calcite. Generally, there is no secondary alteration and the rock is considered remarkably fresh. The absence of baking in the sediment above the contact would suggest this to be a thick flow which was already in place and cooled before sedimentation of the chalks occurred. A thin crystalline limestone bed occurred at the base of Core 19, Section 3, but no microfossils could be distinguished in it.

In thin section, feldspar laths produce a nearly complete interlocking net with the intergranular areas filled with clinopyroxene; however, the pyroxenes do not coalesce. Vesiculation makes up less than 2 percent of the rock with an average size of ~0.2 mm. The clinopyroxene is colorless with a moderate to small 2v optic axial angle. No reactions with olivine or orthopyroxene could be detected. Rough modal analyses give plagioclase ~40 to 50 percent, clinopyroxene ~60 to 50 percent, and minor opaques. No glass is present.

Due to limited space, the tables of grain size, carbon-carbonate, X-ray, and *p*H and salinity are presented with the data of other sites in Appendices I, II, III, and IV, respectively at the end of the volume.

PRELIMINARY NOTE ON THE HEAVY MINERALS OF THE TURBIDITES AT SITE 221[2]

Method

Ten samples of silts and sandy silts were washed, and heavy minerals were separated from the greater than 63 micron fraction in bromoform (sp. gr. 2.89). The separated fraction was mounted in Caedax and about 300 grains were counted.

Heavy Mineral Assemblage

The major constituents of the heavy mineral suite are colored and colorless mica (cf. muscovite and biotite, respectively), hornblende, garnet, kyanite, epidote, clinozoisite, calcite, and opaques. The minor constituents are zircon, tourmaline, monazite, dolomite, rutile, and tremolite/actinolite.

Provenance

The heavy mineral assemblage suggests derivation from a high rank metamorphic (kyanite, garnet, epidote, clinozoisite, hornblende–blue green variety, muscovite, and biotite) and acid igneous (hornblende, monazite, muscovite, zircon, euhedra, tourmaline, etc.) terrain (Pettijohn, 1957). Both the brown and bluish-green hornblende are present in the heavy mineral suite suggesting that these have been derived from two different sources (acid igneous and high rank metamorphic). Presence of both angular and rounded garnet likewise suggests that these also represent a dual source, and the latter has been derived from reworked sediments and has already passed through more than one cycle of sedimentation. The occurrence of large broken calcite grains, which are very low in the mineral stability order, is taken to tentatively suggest that the sediments were largely transported in suspension rather than in traction. The source for calcite should be near the source from which the sands were derived.

Mineral Variation

The heavy mineral assemblage of the 10 samples taken from the depth range 17 to 122 meters shows significant variations (Figure 4). Increase in the micas (both muscovite and biotite) leads to a decrease in hornblende and other heavy minerals. While the heavy mineral suite from 17, 26, 58, and 121 meter depth has a complex mineral assemblage (hornblende, garnet, kyanite, epidote, etc.), the suite from 83, 98.5, 104, 108, and 120 meter consists of micas only. The heavy mineral suite, consisting entirely of micas, encompasses the Lower Pleistocene and upper Upper Pliocene sediment interval. Both the overlying lower Upper Pleistocene (58 m) cores and also those in the upper Upper Pliocene (120 m) indicate a mixed or transitional heavy mineral suite. The predominance of mica in the heavy mineral suite of the Lower Pleistocene sands may also be related to the changing climate in the source areas. The significance of the variations in the heavy mineral suites is not clear but probably these are related to changes in a wide range of factors, i.e., source area, climate of the source area, channels, and the nature of the turbidity current itself.

BIOSTRATIGRAPHY

Foraminifera

Planktonic foraminifera are very rare or absent throughout most of the interval cored at Site 221. Nondiagnostic Neogene planktonic species are present sporadically as low as Sample 6, CC; benthic species throughout this interval are, when present, largely of deep-water origin, but at some levels (4, CC; 5-4, 39-41 cm; 6-3, 27-29 cm) the faunas include neritic species, indicating probable turbidite transport. Rare Eocene specimens in Core 5, Section 3, 110-112 cm have been redeposited. Between Samples 6, CC and 16, CC, foraminifera are essentially absent. Samples 17-1, 136-138 cm and 17, CC contain rare Oligocene foraminifera, but no zonal assignment could be made. Core 18 contains a few Middle Eocene species, consisting largely of solution-resistant forms of probable P.13-P.14 age.

Nannofossils

Hole 221 was drilled in sediments ranging in age from Late Pleistocene to Middle Eocene and underlain by basalt with intercalated crystallized limestone in which the nannofossils are too poorly preserved to date. An environment conducive to nannofossil productivity and preservation occurs throughout most of the stratigraphic sequence with the exception of the interval from the base of Core 11 to the base of Core 15. Sediments in these cores represent an environment below the nannofossil compensation depth of the Arabian Sea.

Several nannofossil zones are present in Pleistocene Cores 1 through 10. The *Gephyrocapsa oceanica* Zone (Boudreaux and Hay, 1969 and Hay et al., 1967) appears in Cores 1, 2, and 3, and the *Gephyrocapsa caribbeanica* Zone (ibid) is present in Core 4 and Core 5, Section 2. Cores 1, 2, 3, 4, 5, and 6 represent the Late Pleistocene interval. The lower Pleistocene *Pseudoemiliania lacunosa* Zone is present in Core 7. A flood of *Coccolithus doronicoides* appears in Core 10 and represents the last recognizable flora common to the Lower Pleistocene. Most of the Pleistocene cores contain very rare Pliocene and Miocene discoasters, probably redeposited by turbidity currents.

The Late Pliocene is recognized in Sample 11-2, 79-80 cm by the presence of common *Discoaster brouweri* and associated Upper Pliocene flora. The base of Core 11 and Cores 12, 13, 14, and 15 contain sediments deposited below the nannofossil compensation depth, and a Pliocene age is tentatively assigned to at least the upper portion of this cored interval. The interval between Core 15 and Core 16 was not continuously cored.

---

[2] H. N. Siddiquie.

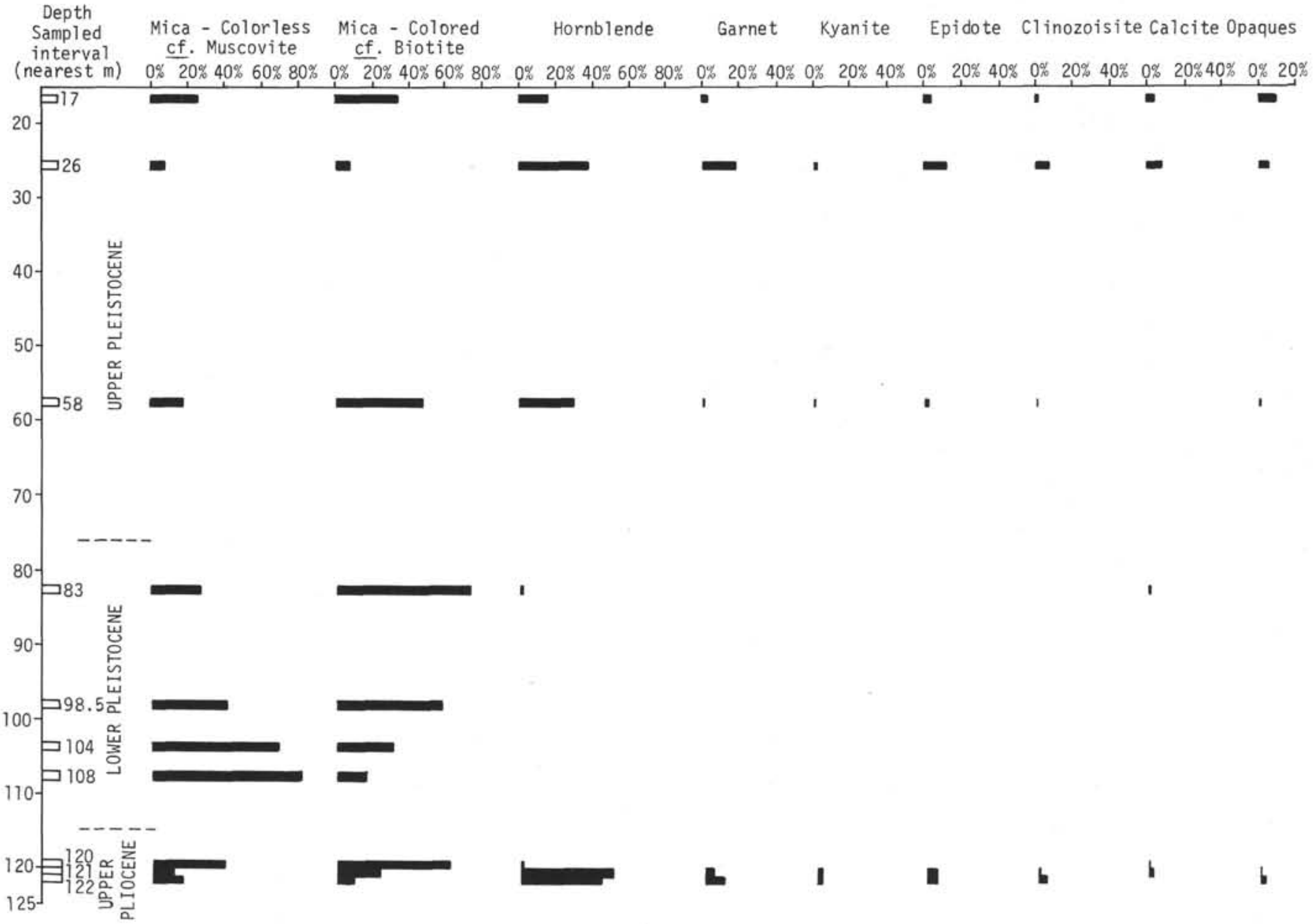

Figure 4. *The distribution of heavy minerals in some of the Site 221 turbidite sands.*

The Late Oligocene interval is well represented in Sample 16-1, 118-119 cm as verified by the presence of *Sphenolithus ciperoensis, Discoaster deflandrei, Sphenolithus moriformis, Discoaster woodringi,* and *Reticulofenestra laevis.* A nannofossil ooze is present at the base of Core 16, and sedimentation occurred in a favorable preservation environment.

The interval between Cores 16 and 17 also was not continuously cored. Sample 17, CC contains nannofossil ooze with *Sphenolithus predistentus*, and a Middle Oligocene age is assigned to this interval.

Twenty-eight meters was drilled between Cores 17 and 18. Chert and basalt were recovered from the core catcher of Core 18, and nannofossil-bearing sediments occur in the interval above the chert and basalt. Diagnostic nannofossils present in these sediments (Samples 18-6, 148-149 cm and 18, CC) include *Sphenolithus spiniger* (Bukry, 1971), *Sphenolithus obtusus* (Bukry, 1971), *Discoaster saipanensis, Discoaster barbadiensis,* and *Chiasmolithus grandis*. A Middle Eocene age is assigned to the sediment layer immediately overlying the chert and basalt. Core 19 contains dense basalt and one thin intercalated sediment layer (Section 3, 145-147 cm) composed of crystallized calcitic material. Nannofossils are virtually absent within the intercalated sediment layer; therefore, the age of this sediment layer could not be determined.

Radiolaria

Radiolaria are either absent or so rare as to preclude age determinations. At the top of the hole, the radiolarians are probably masked by detrital material. Beneath this, there is a brown clay section in which (a) sedimentation rates were so slow that radiolarians were dissolved before burial, and/or (b) during brown clay time, the waters above Site 221 were unsuitable for high radiolarian productivity.

Within Core 18, siliceous nodules were observed; one, from Core 18, Section 6, 58-60 cm, was sampled and contains a rich and well-preserved radiolarian fauna belong to the *Podocyrtis mitra* Zone (Middle Eocene).

Fish debris was noted in Cores 14, 15, and 17.

Biostratigraphic Summary

The relatively thick Pleistocene interval penetrated at Site 221 is composed of turbidite sediments rich in nannofossils. The four zones of *Gephyrocapsa oceanica, Gephyrocapsa caribbeanica, Coccolithus doronicoides,* and *Pseudoemiliania lacunosa* are present in this interval. Planktonic foraminifera and Radiolaria are very rare to absent throughout all of the Pleistocene. Rare benthonic foraminifera are found in the two lower nannofossil zones. Reworked Pliocene and Miocene discoasters are rare through most of this interval.

Turbidite sediments are also present in the Pliocene interval. The apparent extinction level of *Discoaster brouweri* in Sample 11-2, 79 to 80 cm is used to determine the Pliocene/Pleistocene boundary. Sediments in the lower portion of Core 11 and in Cores 12, 13, 14, and 15 were deposited below the calcium carbonate compensation depth (CCD). Clay with graded sand units is present in Cores 11, 12, and 13. Brown clay is present in Cores 14 and 15 and in the upper portion of Core 16. Nannofossils, foraminifera, and radiolarians are very rare or absent from the base of Core 11 through Core 15; therefore, it is impossible to delineate the Pliocene/Miocene boundary. Most of the brown clay present in Cores 14 and 15 is probably Miocene in age.

A rich nannofossil ooze occurs throughout the lower two-thirds of Core 16. All fossiliferous sediments in this core were deposited during the Late Oligocene as verified by the presence of *Sphenolithus ciperoensis.* The upper portion of Core 16 contains brown clay similar to that present in Cores 14 and 15 but lighter in color. Nannofossils are present throughout Core 16, whereas foraminifera and Radiolaria are very rare, and nannofossils appear to gradually increase in abundance toward the base.

Nannofossil ooze and chalk is present in Sample 17, CC and occurs within the *Sphenolithus predistentus* Zone of Middle Oligocene. Foraminifera and Radiolaria are very rare and nondiagnostic in this interval.

Core 18 was drilled in Upper to Middle Eocene nannofossil chalk with chert at the base. Foraminifera are present in Core 18. A siliceous nodule found in Sample 18-6, 58-60 cm is rich in well-preserved radiolarians belonging to the *Podocyrtis mitra* Zone of Middle Eocene.

Core 19 penetrated basalt with one thin layer of intercalated limestone. The intercalated limestone contains only rare broken fragments of nannofossils; therefore, age dating by conventional paleontological means is impossible.

Sedimentation Rate

Only two sedimentary sequences at Site 221 contained fossils sufficient to provide the basis for calculating sedimentation rates (Figure 5). The Middle Eocene to Middle Oligocene nannofossil oozes and chalks of Cores 17 and 18 (218 to 261 m) accumulated at a rate of 3 to 5 m/m.y. Upper Oligocene nannofossil floras, similar to those observed in Core 16, are present in the top two sections of Core 17, and an unconformity may be present in the latter core. This would imply a very high sedimentation rate for the Late Oligocene, however, in view of the absence of foraminiferal tests in Core 16 and the lithologic similarity of the Late and Middle Oligocene, it seems more reasonable to consider the Core 17 occurrences as contamination. Relative rates of Late and Middle Oligocene sedimentation cannot be determined because of the drilled interval between Cores 16 and 17; similarly, sedimentation rates in the Late Oligocene through Early Pliocene cannot be determined because of the absence of fossils.

In contrast to the slow Oligocene sedimentation, accumulation was rapid in the Pleistocene. A single Upper Pliocene core does not provide sufficient control to calculate a rate for this period, but late Pleistocene sedimentation (0 to 100 m) occurred at a rate of 170 m/m.y.

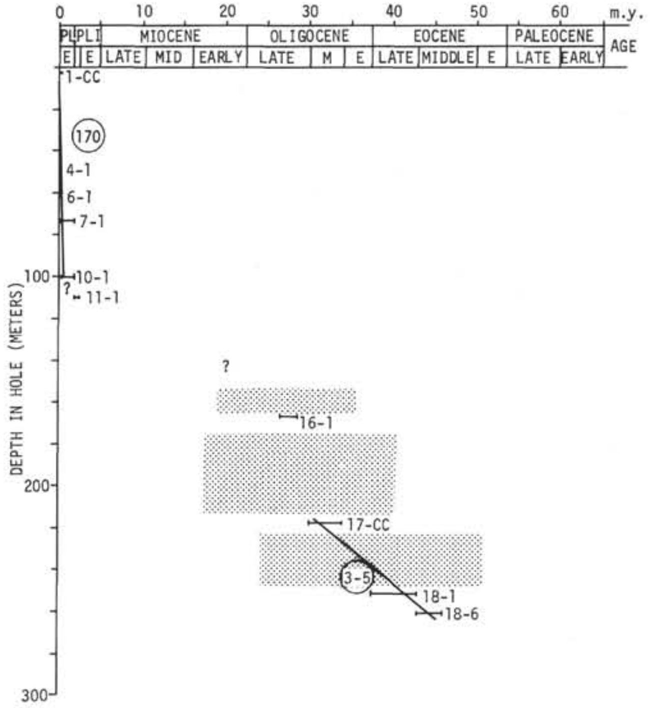

Figure 5. *Sedimentation Rate Curve, Site 221. Plotted bars are those sufficient to control slopes of lines. Stippled pattern represents some uncored intervals. See Chapter 2, Explanatory Notes, for explanation of age ranges and other symbols.*

GEOCHEMISTRY

The detrital clayey silt with graded silt and sand beds cored in the upper 127 meters at Site 221 contain relatively high amounts of iron, vanadium, chromium, manganese, and titanium compared to nanno ooze recovered from the basal 100 meters (Figure 6). Samples analyzed from the top and bottom of a graded unit reveal a relationship between trace metal content and grain size of the sediments (Table 3). The higher trace metal concentration in the finer grained fraction may be due to absorption by clay minerals.

The trace element content of the brown clay found from 127 to 170 meters reveals that this material is rich in copper, chromium, manganese, nickel, and vanadium compared to their presence in the basal 100 meters, which is dominantly nanno ooze. Pimm et al. (1971) noted an excessive amount of titanium and manganese in Pacific brown clays which they interpreted as indicating derivation from a basaltic source. At Site 221, the titanium and manganese values are much lower in comparison to the Pacific brown clays. This may suggest that the brown clays of Site 221 were derived from a different type of source.

The small amounts of trace metals found in the nanno ooze and chalk in the lower part of the hole confirm that there is no detrital material in these cores.

PHYSICAL PROPERTIES

Sediment Density, Porosity, and Water Content

No density measurements were made on the basement rocks of Site 221. The highest values recorded from the

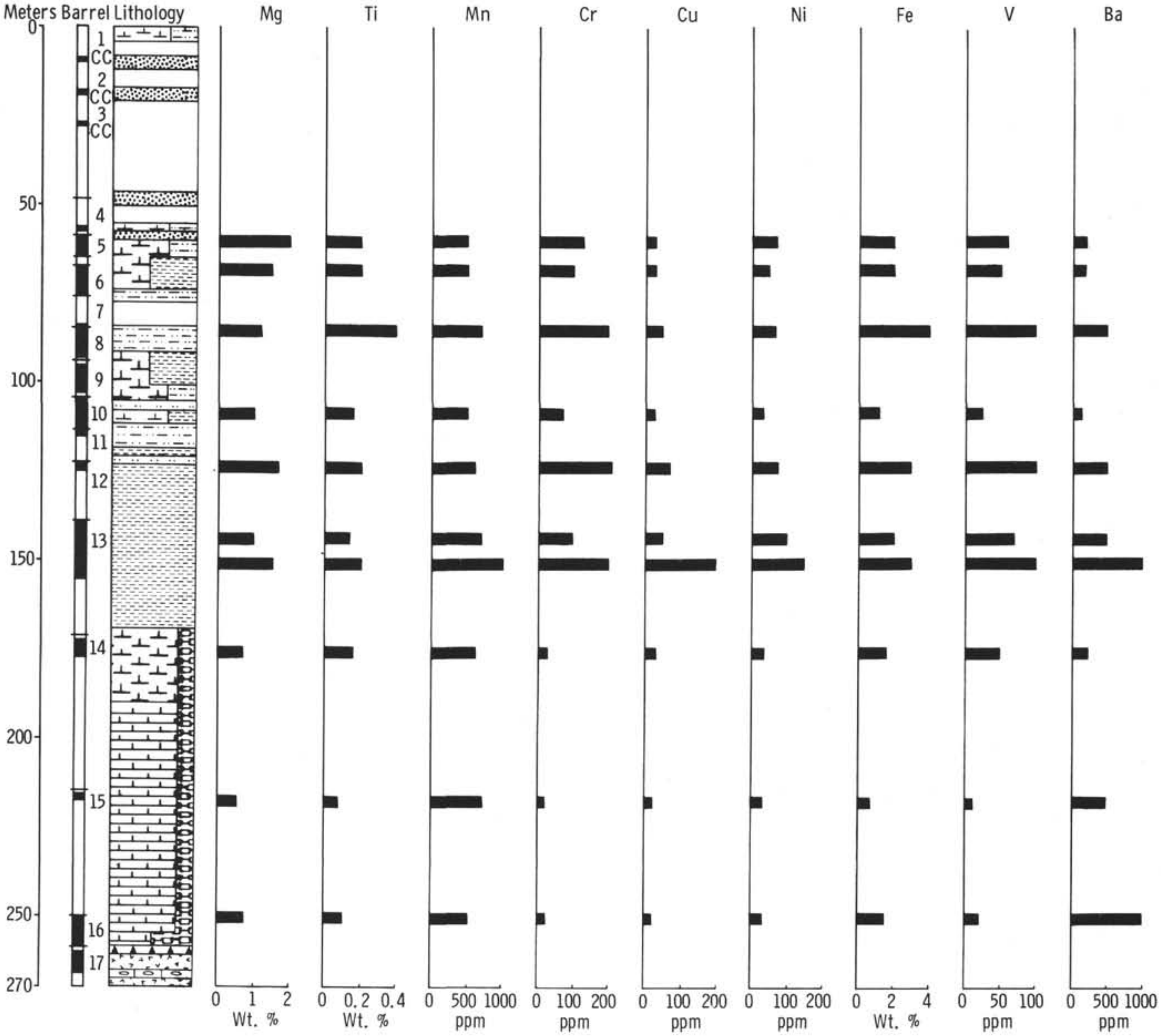

Figure 6. *Chemistry of the sediments from Site 220.*

TABLE 3
Relationship of Selected Trace Elements to Grain Size

	Fe (%)	Mn (ppm)	Cr (ppm)	Cu (ppm)	Ni (ppm)	V (ppm)
Detrital clay (top of bed) – Sample 8-2, 4-5 cm	5	700	200	50	70	100
Detrital silty clay (bottom of bed) – Sample 8-2, 75-76 cm	3	500	150	30	50	70

sediments surprisingly, are within an interval of marked density fluctuation at the top of the hole, where peaks of over 2.0 g/cc occur.

Below 128 meters, the density plot is less variable. This change approximates the lithological boundary where intercalated graded beds cease to occur, and the sequence continues downwards with homogeneous brown clay followed by micarb nanno oozes and chalks. The unit III brown clay is, in fact, less variable than is indicated by the graphical plots since Core 14 is a disturbed soupy core with water content as high as 68 percent and porosity ranging between 60 and 70 percent. Core 15 displays what can be taken as true values of density, porosity, and water content at 1.7 to 1.8 g/cc and about 30 percent and 55 percent, respectively.

These values change little in the ooze and chalk sequence below unit III, but a slight contrast in density occurs at the boundary between units II and III in Core 16, Section 2.

The higher sand content causes the peak values and general high density of units I and II. On the core logs, individual graded beds show gradients of increasing density towards their bases followed by a sharp drop off below, e.g., Core 5, Section 2, Core 5, Section 4, Core 9, Section 6, and Core 12, Section 2. Further, a degree of density variation with sediment color can be noted. The fecal pellet-rich light-colored graded beds, e.g., in Core 5, Section 4, have maximum densities of around 1.8 g/cc, probably due to high aragonite content, whereas, the darker colored beds with higher ferromagnesian mineral content reach over 2.0 g/cc. Also, the light-colored background lithology has lower density values than the darker sections, e.g., Core 5. Water content varies from around 40 percent in the silt sand beds to between 20-30 percent in the background detrital clays and silt nanno oozes.

Compressional Wave Velocity

The plot of this parameter varies little from an average value of 1.6 km/sec. It remains within the range 1.45-1.74 km/sec throughout most of the sedimentary sequence apart from a value of 2.17 km/sec at the top of Core 18, which has no apparent lithological basis, and apart from the topmost velocitv measurement (1.41 km/sec).

A sharp rise to 4.48 km/sec at the base of the sediment sequence is due to the chert layer at this level. This is followed by lower values down to 3.22 km/sec in the volcanic glass lying above the oceanic basement. The basalt has velocity values of around 4.9 km/sec.

Detailed compressional wave velocity measurements were made in graded beds from units I and II for comparison with observed GRAPE density gradients. Velocity fluctuations were found to be random and probably only within the range of experimental error in the method used. Nevertheless, some of the higher velocity values recorded in the Site Summary log, e.g., 1.8 km/sec in Core 5, Section 4, occur within the silt and sand interbeds.

Specific Acoustic Impedance

On the Site Summary logs, the plot of impedance values, in general, mirrors the velocity graph except that, as GRAPE density values in the basalt are absent, the expected high impedance values at the base of the hole are not plotted. The major increase recorded at the base of the hole is caused by the chert layer above the basalt.

The brown clay of unit III has a specific acoustic impedance between 2.6 and 2.7. A short step increase to 2.75 occurs at the top of unit IV, and a steady gradient follows towards 2.9 at the base of the oozes and chalks.

Above 128 meters, the fluctuations in specific acoustic impedance reflect the fluctuations in velocity and density within graded beds. Few velocity measurements were made on the remaining, but more representative, parts of the cores. At a scale of tens of centimeters it can be shown that the observed density gradients in the graded beds are matched by similar velocity gradients, and the high density and velocity values are always in the silt and sand interbeds. This would explain the fine reflecting horizons, which occur on the geophysical records within the Plio-Pleistocene sequence, as being due to these intercalated beds.

CORRELATION OF REFLECTION PROFILES AND LITHOLOGIES

At this site, it was relatively easy to both read off reflection times from the airgun profile and to assign a lithology change to each reflector. This was due to the uniformity and low relief of all the reflectors.

On the profile obtained on departure over the beacon (Figure 7), a well-stratified upper layer is seen to overlie a slightly folded and less-stratified (more transparent) layer which exhibits a laterally discontinuous reflector in the middle. The main reflector (acoustic basement) underlies the second layer. It has a generally horizontal attitude but is more irregular than the top of the second layer. The main reflection apparently consists of dipping plane reflections separated laterally by hyperbolic echoes denoting a rough surface.

Reflections occurred at 0.16, 0.21, and 0.30 seconds of two-way time below the sea bed. The uppermost reflection is associated with the top of the brown clay, which lay somewhere in the interval 123 to 136 meters, while the weak discontinuous reflection, at 0.21 seconds, corresponds to the density contrast between brown clay and the underlying nannofossil ooze at 170 meters. The main reflection is due to the chert and basalt. The basalt was immediately below the chert in the borehole, and the main reflection consisted of hyperbolic echoes. Elsewhere, where a plane reflection without hyperbolae is seen, the basalt presumably lies at a greater depth below the chert which hides it acoustically. These data are summarized in Figure 8, from which it is apparent that the mean velocity to basement is 1.74 km/sec.

It is interesting to note that the intensity of folding of the reflectors apparently decreases upwards from the chert to the top of the brown clay. The Plio-Pleistocene turbidites rest unconformably over the gently folded brown clays.

PALEOMAGNETIC MEASUREMENTS

The series of 19 samples measured from this site are representative of all the major lithological units cored. They include seven samples of detrital silts from the turbidite sequence of Late Pliocene to Late Pleistocene age, five samples from the brown clay facies of presumed Miocene age, one sample of nanno chalk (Middle Eocene) from the penultimate section above the contact with the basalts, and six samples of amygdaloidal basalts. These latter samples are from 5 of the succession of at least 10 flows that were cored. Table 4 summarizes the magnetic remanence measurements.

The detrital silts have a mean intensity of magnetization of 5.2 × 10^{-6} G/cm^3. On the whole, the remanence directions of these samples appear moderately stable on partial alternating field (Af) demagnetization. Evidence from the behavior of Sample 5-3, 8 cm during progressive demagnetization (Table 5 and Figure 9) reinforces this

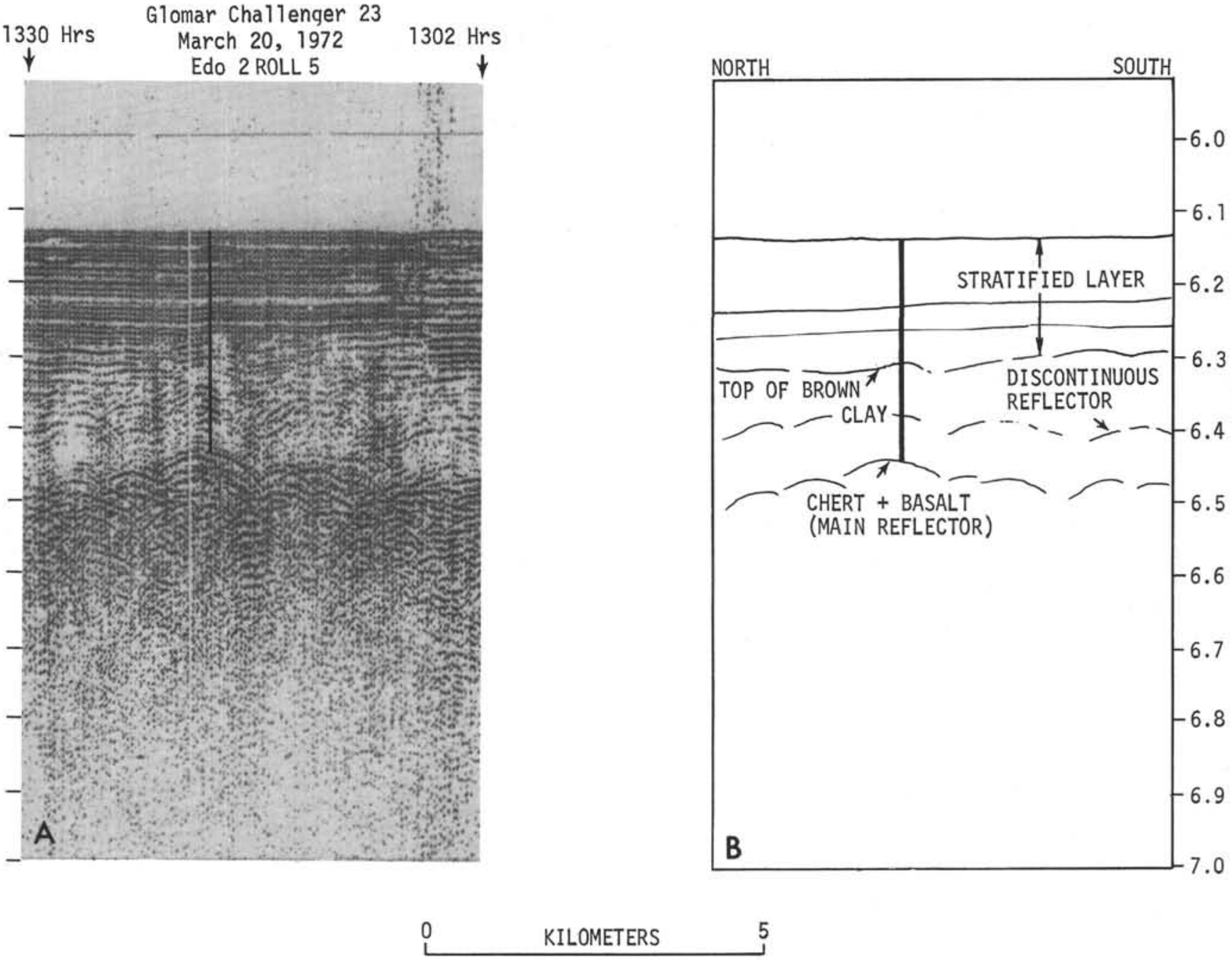

Figure 7. (a). *Profile obtained on departure while passing directly over the sea bed acoustic beacon. The vertical line marks the position of the approximate penetration of the drill bit.* (b). *The interpretation of Figure 7A used to construct Figure 8. The vertical line has tenth second divisions.*

observation. However, there remains an appreciable scatter in inclination values; but, if the steep inclination value of Sample 5-3, 147 cm is omitted, then the Pleistocene detrital silt samples have a mean absolute inclination of 15.2 ± 5.9°. Such a value agrees with the expected inclination (15.6°) for this latitude at the present time.

Similar variability in the NRM directions characterizes the underlying brown clay samples from Core 15, accepting that they have a common azimuthal orientation within the core. Evidence of a change in polarity is indicated by the negative inclinations of Samples 15-3, 81 cm, 15-4, 22 cm, and 15-4, 122 cm, but this is not associated with a comparable declination change. On partial Af demagnetization at 50 oersted, it is apparent that four of the five samples show a tendency to move towards an inclination value around 25-30degrees (Figure 10). Such a systematic change in direction is illustrated during the progressive demagnetization of Sample 15-2, 21 cm, the results of which are included in Table 5, and the intensity decay curve shown on Figure 9. It is reasonable to assume, therefore, that the brown clays are partially stable after the removal of the soft component. If this is so, then the calculated mean absolute inclination of 22.5 ± 6.0° may be reliable.

Mean intensity of magnetization of the brown clays is 3.2 ± 1.4 × 10^{-5} G/cm^3, which is nearly an order of magnitude stronger than that of the overlying detrital silts. This is probably a grain-size effect.

The single Middle Eocene nanno chalk sample is associated with a negative inclination that is steepened on partial demagnetization. Within the underlying basaltic sequence, normal polarity predominates, but the inclination values are varied and remain so after partial demagnetization. No explanation, other than that of the presence of a viscous magnetization component, can be offered to explain the three low inclination values. Table 5 and Figure 9 give the result of the progressive demagnetization of Sample 19-2, 22 cm. For this sample, the directional changes appear to be somewhat random for peak demagnetizing field values in excess of 150 oersted, indicating instability. Samples 19-2, 147 cm and 19-3, 37 cm, which are from the same flow, show some consistency in both declination and inclination of their remanence. The mean NRM intensity of the basalts is 1.2 ± 0.3 × 10^{-3}

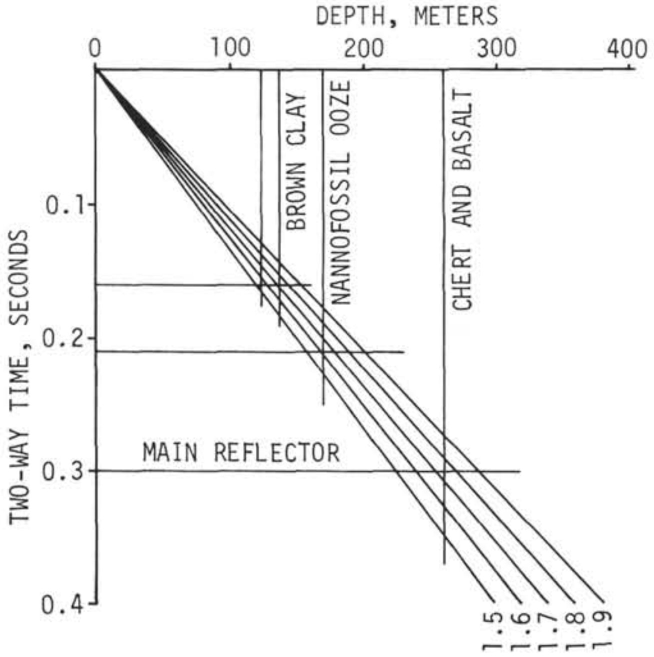

Figure 8. *Plot of reflection times beneath Site 221 against the depths of significant changes in lithology found in the cores. Lines are drawn with slopes corresponding to mean velocities of 1.5, 1.6, 1.7, 1.8, and 1.9 km/sec.*

G/cm^3. A value which is less than half that found for the basalts of Site 220.

IDENTIFICATION OF SEA FLOOR SPREADING MAGNETIC ANOMALIES NEAR SITE 221[3]

No magnetic anomalies older than anomaly 5 have been identified in the southeastern part of the Arabian Sea. Although an east-west trend is discernible between anomaly profiles north of Site 221, there was no distinctive anomaly or group of anomalies to enable McKenzie and Sclater (1971) to identify anomalies on the Heirtzler et al. (1968) time scale. In view of the fact that the *Glomar Challenger* track through Site 221 is aligned approximately north-south for 450 km, and because the sediments lying just above oceanic basement were dated paleontologically at this site, an attempt was made to identify anomalies along this track.

On the basis of micropaleontology, the oldest sediments at Site 221 are of Middle Eocene age, approximately 46 m.y. old according to Berggren's (1972) time scale. The Heirtzler geomagnetic time scale, therefore, predicts that the youngest possible anomaly at Site 221 will be anomaly 17.

The observed anomaly profile was projected onto a north-south line (Figure 11) and was compared with calculated anomaly profiles using spreading rates of 1.0, 1.6, 2.5, 4, and 6.5 cm/yr. Other parameters of the calculated profile are given in the caption of Figure 11. A constraint on the fitting was, that north of the Carlsberg Ridge, McKenzie and Sclater (1971) had found that during the period of time from the normal polarity epoch which occurred between anomalies 23 and 24 up to anomaly 26, the spreading rate was 6.5 cm/yr. No anomalies between 5 and 23 were recognized by these authors in the Indian Ocean except on the flanks of the southeast Indian Ridge, where the spreading rate was 2.5 and 3.25 cm/yr between anomalies 7 and 17.

In view of the above constraint, valid so long as there was no plate boundary between Site 221 and the Owen Fracture Zone, the only possible fit to the observed profile seems to be that shown in Figure 11. This fit is consistent with the results of McKenzie and Sclater in that a spreading rate of 6.5 cm/yr is required after anomaly 23. The spreading rate appears to have changed from 2.5 to 6.5 cm/yr at about the time of anomaly 23. The rate between anomalies 17 and 23 is in close agreement with that found between anomalies 7 and 17 on the southeast Indian Ridge. The only major discrepancy in the fit is that anomaly 19 is missing from the observed profile. It is unlikely that this anomaly was missed because of the discontinuity in the profile at Site 221. From Figure 11 the predicted age of the oceanic crust at the site is 48 m.y., in fair agreement with the paleontological dates, especially considering that undated interbeds of sediment were found within the basalt at this site. The wider implications of the above identifications of magnetic anomalies are discussed by Whitmarsh (Chapter 14).

SUMMARY AND CONCLUSIONS

Geological Setting

Located 1000 km due west of the southern tip of India, Site 221 is situated in the Arabian Sea at a depth of 4650 meters. Topographically, it is on the southeastern portion of the Arabian Abyssal Plain. Sixty km to the south, the plain terminates against the rough lower flank of the Carlsberg Ridge, and approximately 150 km to the east, it abuts the lower margin of the Laccadive-Chagos Ridge.

In the vicinity of Site 221, the surface of the abyssal plain has a southward slope of 0.7 m/km. At the base of the sediment section, the oceanic crust has a northward slope of 2.0 m/km. These opposing slopes define a northward thickening sediment wedge.

A buried abyssal hill topography, with a relief of 40 to 80 meters, can be seen to form the igneous basement surface in the vicinity of Site 221. The site itself was situated above the crest of such a hill in a region where a broad gentle swell 100 meters high and 15 km wide is developed on the basement surface. The low amplitude abyssal hill topography extends approximately 50 km south of the drill site where it meets the rougher topography of the Carlsberg Ridge. There the hills and ridges, which are broader and higher, have a relief of 200 to 400 meters. On the *Glomar Challenger* seismic records, the termination of the Arabian Abyssal Plain is seen to extend about 10 km into this rougher topography (see Figure 12). With progressive onlap it is easy to visualize how succeeding turbidite flows bury successively higher (i.e., younger) foothills of this Ridge.

Site 221 was drilled at the almost exact point where the southern edge of Eocene chert development occurs. Thus, in the vicinity of the drilled site, the hyperbolic reflectors of the rough basaltic topography are well-developed. However, in traversing to the north, these reflectors

---

[3] R. B. Whitmarsh.

TABLE 4
Summary of Magnetic Data, Site 221

	NRM			Af Demagnetization			
Sample (Interval in cm)	Intensity (G/cm^3)	Relative Declination (degrees)	Inclination (degrees)	Peak Field (oersted)	Intensity (G/cm^3)	Relative Declination (degrees)	Inclination (degrees)
Sediments							
5-3, 8	1.6×10^{-5}	186.0	19.5	50	1.5×10^{-5}	187.8	13.8
5-3, 147	1.7×10^{-6}	29.4	53.3	50	9.6×10^{-7}	58.3	72.0
5-4, 42	4.4×10^{-6}	61.1	1.1	50	2.9×10^{-6}	69.4	3.0
6-2, 77	1.4×10^{-6}	265.7	17.1	50	1.3×10^{-6}	253.1	10.8
8-1, 124	7.0×10^{-6}	107.6	48.5	50	5.9×10^{-6}	114.8	37.7
10-5, 140	2.6×10^{-6}	131.6	4.6	50	2.9×10^{-6}	133.0	10.7
12-2, 48	3.2×10^{-6}	163.0	30.8	50	3.8×10^{-6}	163.7	23.0
15-2, 21	2.8×10^{-5}	300.7	59.4	50	1.2×10^{-5}	19.8	39.2
15-2, 122	2.1×10^{-5}	42.4	9.4	50	3.6×10^{-6}	26.1	13.6
15-3, 81	1.3×10^{-5}	298.6	-6.1	50	2.8×10^{-6}	284.2	–31.1
15-4, 22	1.2×10^{-5}	21.4	-42.2	50	4.8×10^{-6}	322.0	–23.0
15-4, 122	8.5×10^{-5}	11.1	–12.6	50	2.1×10^{-5}	10.0	–5.5
18-5, 134	1.7×10^{-5}	15.5	21.9	100	1.9×10^{-6}	261.6	–32.3
Basalts							
19-2, 10	1.1×10^{-3}	77.4	1.0	100	1.8×10^{-4}	77.6	4.1
19-2, 22	1.0×10^{-3}	140.7	12.9		8.0×10^{-4}	149.7	1.3
19-2, 147	4.3×10^{-4}	306.9	39.2	100	2.5×10^{-4}	284.6	38.2
19-3, 37	1.2×10^{-3}	332.6	16.0	100	8.0×10^{-4}	327.5	23.5
19-3, 125	9.4×10^{-4}	307.9	40.5	100	2.4×10^{-4}	302.8	29.4
19-4, 124	2.8×10^{-3}	49.8	3.2	100	2.0×10^{-3}	53.4	-0.7

TABLE 5
Af Demagnetization Results, Site 221

Sample	Peak Field (oersted)	Intensity (G/cm^3)	Relative Declination (degrees)	Inclination (degrees)
5-3, 8 cm	NRM	1.6×10^{-5}	186.0	19.5
	25	1.6×10^{-5}	186.8	16.0
	50	1.5×10^{-5}	187.8	13.8
	75	1.3×10^{-5}	186.3	13.3
	100	1.1×10^{-5}	187.9	13.1
	150	7.5×10^{-6}	189.0	18.0
	200	4.1×10^{-6}	188.4	8.1
15-2, 21 cm	NRM	2.8×10^{-5}	300.7	59.4
	25	2.1×10^{-5}	313.1	57.5
	50	1.2×10^{-5}	19.8	39.2
	75	9.1×10^{-6}	19.3	30.2
	100	6.7×10^{-6}	23.7	28.0
	150	5.9×10^{-6}	25.9	9.2
	200	6.9×10^{-6}	338.1	-8.0
19-2, 22 cm	NRM	1.0×10^{-3}	140.7	12.9
	50	1.1×10^{-3}	141.7	10.2
	100	8.0×10^{-4}	149.7	1.3
	150	2.1×10^{-4}	154.7	1.1
	225	1.0×10^{-4}	142.0	-11.8
	300	5.7×10^{-5}	164.4	29.1
	375	7.7×10^{-5}	127.9	19.6
	450	3.2×10^{-5}	238.2	-22.6
	525	1.5×10^{-4}	259.0	25.7
	600	1.3×10^{-4}	241.3	25.6

gradually become fainter. Consequently, about 50 km north of the site, only that portion of the sediment wedge which is above the chert can be seen on the seismic records.

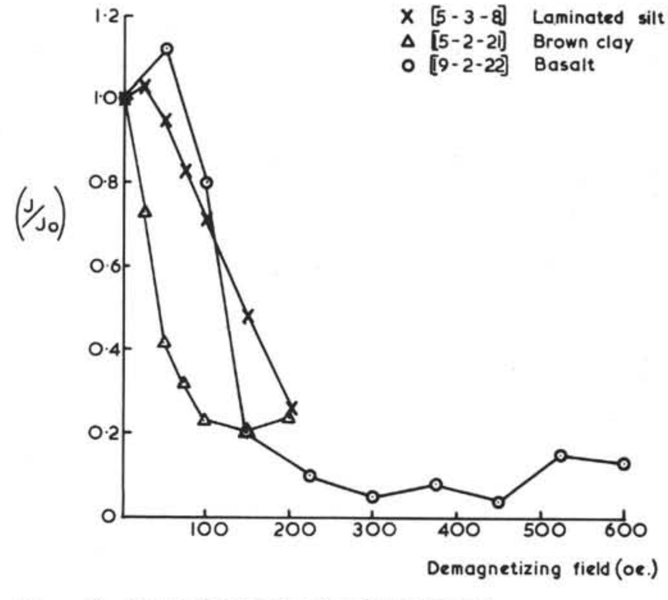

Figure 9. *Normalized intensity decay curves.*

The loss of total sediment representation in this wedge becomes increasingly greater northward because crustal ages increase in this direction.

The Stratigraphic Column

Late Pleistocene through Middle Eocene time is represented by 261 meters of sediment at this site. A program of intermittent coring and drilling recovered 71.7 meters from 18 cores taken in these sediments. Below

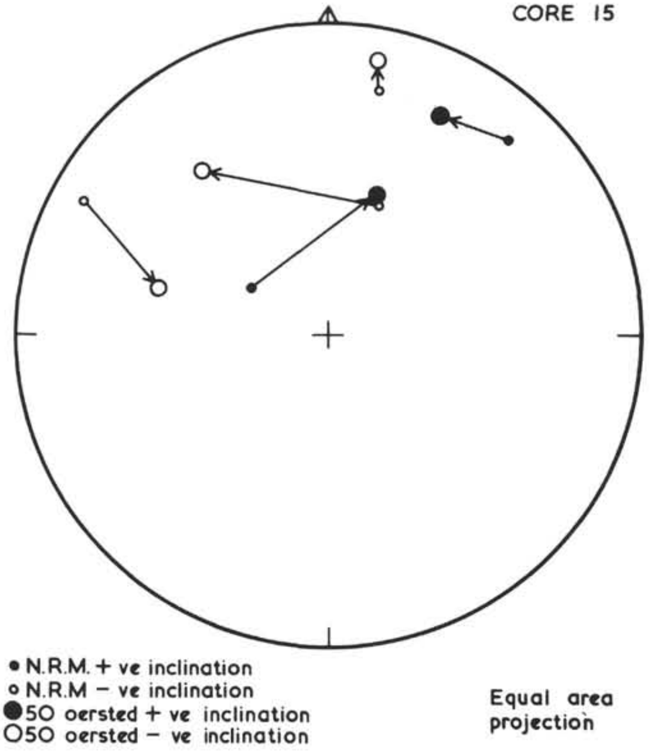

Figure 10. *Direction changes after partial demagnetization of brown clay samples from Core 15.*

them, Core 19 recovered 4.9 meters of basalt plus one thin limestone layer. The sediment column can be divided into one transitional, and three distinctive, lithologic units.

The topmost unit, extending down to 111 meters, corresponds to the highly stratified interval seen on the profiler record (see Figure 7). Its age ranges from Late Pleistocene to Late Pliocene time.

Not much lithologic data concerning the upper half of unit I is available as only 4 core catcher samples were recovered. However, on the basis of the drill string behavior plus the core catcher samples, it is reasonable to assume that much of this interval consists of detrital sands. The smear slide data suggest that compositionally they are akin to sands probably derived from the Indus Submarine Canyon found at Site 222. Consequently, one must postulate that they have traveled nearly 1700 km on the Indus Cone and Arabian Abyssal Plain, presumably by turbidity current transport. Such travel probably occurred along one or more of the many submarine channels noted on the echo sounder records.

The source and transport mechanism for sediments in the lower half of unit I is less obvious. Lithologically, this interval is complex, containing three sediment types: (a) clay to silty nanno ooze, (b) pelletal carbonate sands, and (c) detrital silty clays and sands. The type (c) sands resemble those in the upper half of unit I and presumably have a similar source and mode of transport. Type (c) silty clays are probably associated with these sands. The pelletal

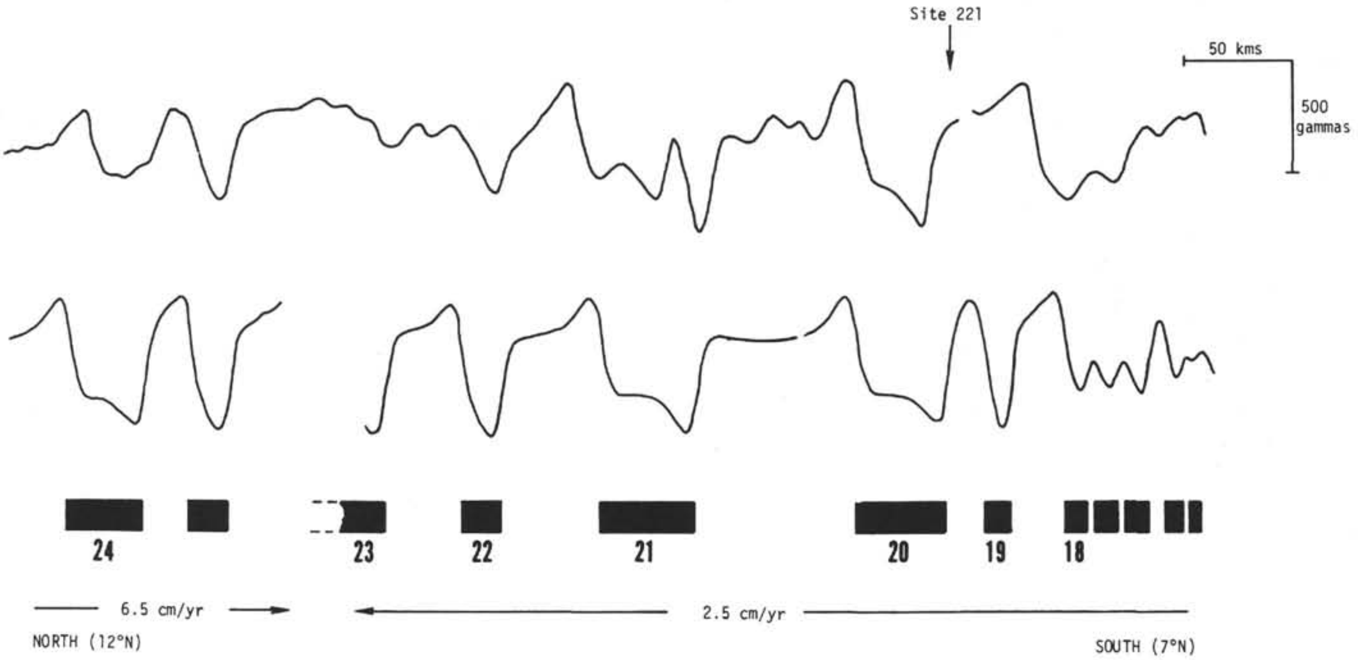

Figure 11. *The upper curve is the magnetic anomaly profile observed by* Glomar Challenger *projected onto a north-south line through Site 221. The lower profile is a synthetic profile generated by a ridge striking 105° at 13°S but observed at 8°N, 68°E with a magnetic strike of 090°. The magnetic layer lay between 5 and 7 km below sea level. Periods of normal polarity are numbered according to the scheme of Heirtzler et al. (1968). The spreading rates are indicated beneath the model.*

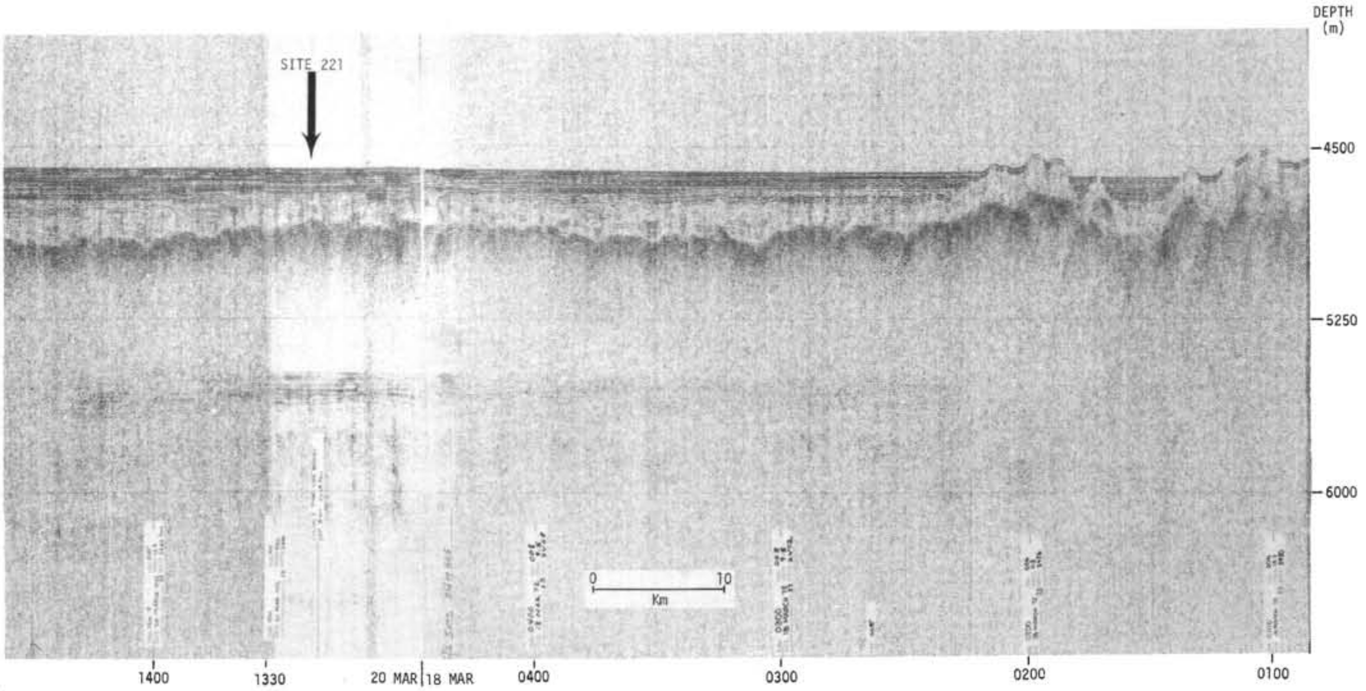

Figure 12. Challenger *seismic profiler record at Site 221. Flat-lying stratified interval abutting transparent sediments at 0120 hr, 18 March 1972, represents termination of Arabian Abyssal Plain.*

carbonate sands, which have a high aragonite content, are quite similar to those from the foot of the continental slope west of Bombay described by von Stackelberg (1972) as having a turbidite origin. At that location, as at Site 221, their source appears to be from Indian shelf areas near Bombay. The nanno oozes, which are the dominant sediment type of this interval, present a more difficult problem. Although they may possibly be typical pelagic sediments, various lines of evidence (see Weser, Chapter 12) suggest it is more likely that they[4] are also of turbidite origin (or perhaps from other gravity controlled mechanisms such as turbid layer transport) and presumably have the same general source area as the pelletal carbonate sands. On this assumption, and because these finer-grained deposits constitute approximately 70 percent of the lower half of unit I, it must be concluded that most[5] of this interval of Arabian Abyssal Plain sediments is not derived from the Indus Submarine Canyon but from the western Indian shelf. The possibility exists that this may be true for much of the eastern Indus Cone and Arabian Abyssal Plain.

The deposition of over 100 meters of Pleistocene turbidites at this Site indicates a sedimentation rate well in excess of that for normal deep-water pelagic deposition. The calculated mean Pleistocene sedimentation rate here of 55 m/m.y. is much higher than the 7 m/m.y. rate calculated for a comparable time interval at nearby Site 220 (which is 600 m shallower). This high rate with attendant rapid sediment burial explains why, in spite of O_2 rich waters being present at depths prevailing at this site (see von Stackelberg, op. cit.), the oxidation of organic matter was inhibited. As a result, the sediment colors are gray, and the organic carbon content averages 0.45 percent (three times that of nearby Site 220).

Unit II is an approximately 16-meter transitional interval containing the detrital type (c) Indus Submarine Canyon sediments of unit I and the brown clays of unit III. No Indian shelf derived pelletal sands or oozes are present. The presence of some turbidite sands contributes to its stratified nature on the seismic profile (Figure 7). A Late Pliocene age was determined for the top of this unit, but no age could be determined for its base.

Unit III is essentially an approximately 43-meter-thick brown clay interval which contains some gray clay intervals and a few streaks and lenses of sand. Although the unit is unfossiliferous, the overlying Upper Pliocene turbidites and the underlying Upper Oligocene nannofossil oozes place limiting age constraints on it between approximately 2.5 and 23.5 million years. With a sediment thickness of approximately 43 meters representing this considerable time span, the sedimentation rate of this unit was only 2 m/m.y. Such a rate typifies pelagic brown clays in other oceans. In addition to this pelagic attribute, the unit III sediments also contain rare zeolites and a trace of ferromanganese micronodules. A further pelagic aspect of this interval is its transparent signature on the seismic profiler record. The presence of only a trace of nannofossils suggests continual deposition below the calcium carbonate compensation depth (CCD).

The gray clays imply that the influence of Indus Submarine Canyon derived turbidites extends into Unit III.

---

[4] Because the evidence for a clastic origin is not obvious, the terminology rules require that they retain a pelagic (i.e., ooze), rather than a clastic textural designation.

[5] By assuming an influx rate of true pelagic clays and nannos commensurate to that established for the same age sediment at Site 220, one can calculate that, at most, 10 percent of these sediments are of a nonturbidite pelagic origin.

It is not possible to say whether the sand fraction in this unit is truly part of the stratigraphic column or a drilling artifact. Even considering that its presence is real, sediments derived from the Indus Submarine Canyon trace a pattern of generally increasing coarseness from unit III through unit I. Such a pattern is to be anticipated at a distal turbidite site as individual southward flowing turbidity currents progressively encroach on a gently northward dipping surface. Unfortunately, the absence of fossils precludes defining precisely when the products of these currents first onlapped this site; the most reasonable speculation is that it was probably sometime in the Middle Miocene. The relationship of turbidites in the Arabian Basin onlapping in a southerly direction indicates that the initial products of Indus Cone sedimentation become progressively older to the north. With the possibility, as outlined above, of a Middle Miocene age for their initial appearance at Site 221, it is not unreasonable to relate initial Indus Cone sedimentation prior to a mid-Miocene Himalayan Orogeny (Ewing et al., 1969).

The change from the pelagic clays of unit III to the nanno oozes and chalks of unit IV is transitional over an interval of about 1 meter. The reason for the loss of calcareous fossils is not apparent. One could consider structural subsidence or a change in depth of the CCD as possible causes. One structural factor which no doubt played a part is the aspect of plate tectonics which predicates that the depth of the oceanic crust increases with time because of lithospheric cooling (Sclater and Fracheteau, 1970). As approximately 23 million years of elapsed time separate the oldest Site 221 fossils and the onset of brown clay deposition, 1500 meters of subsidence due to such cooling is called for. Structural deformation in the form of subsidence as a result of collision between the Indian and Eurasian plates is another possibility. Physiochemical changes causing a rise in the CCD level may also be a factor. Sedimentation rates for unit IV sediments present several interesting aspects. Low initial rates during a part of Middle Eocene through Middle Oligocene time are succeeded by higher Late Oligocene rates. Admittedly, the presence of long drilled intervals between cores with the core barrel open causes one to question the precise location of the data points which control the sedimentation curve. However, a certain degree of validity may be assigned to the shape of this curve because Site 220, only 280 km away, had a similarly shaped curve. The reason for the increased sedimentation rate of the Upper Oligocene interval is, at present, inexplicable insofar as this rate was succeeded by a period of slowly deposited brown clay. Again, any of a number of factors may have been responsible.

Even more difficult to rationalize is the relatively slow (3 to 5 m/m.y.) deposition of the Middle Eocene to Middle Oligocene section. At Site 220, a slow rate for this interval can be explained by assuming an original ridge crest depositional site which by Middle Eocene time had already begun its conveyor belt journey into deeper water. But, at Site 221 this same geologic interval presumably represents deposition at a ridge crest location and, therefore, the preceding argument does not apply. Four equally plausible reasons can be given to explain this anomalous situation.

First, as the site was drilled on the crest of an abyssal hill rising from a broad swell, the possiblity of winnowing is present. Occasional thin laminated bedding in unit IV may reflect winnowing action. Second, using this same topographic aspect to influence current activity, initial sedimentation was inhibited until pelagic deposits filling in the surrounding low area eliminated the topographic prominence at this site. Opposing this possibility is the absence of a weathered zone at the top of the basalt. Third, as a possible minor factor, diagenetic alteration of an originally larger content of Eocene siliceous fossils may have reduced the thickness of the total sediment interval thereby causing an apparent decrease in the sedimentation rate. Some evidence for this is found in the presence of zeolites and chert nodules in the Eocene section which overlies an unaltered siliceous fossil-rich zone just above the basalt (i.e., Core 18). Fourth, late volcanic activity buried earlier sediment deposits. Favoring this view is the presence of a thin sediment layer in the basalt and the possibility that the topographic swell at Site 221 is a constructional feature resulting from volcanism. Opposing it is the finding that the magnetic signature of the crust at this site calls for an age of 48 million years, which approximates the ~46 million year paleontologic age of the oldest sediments.

Although neither of the four alternatives can be proven, what does seem obvious on the seismic record is that the thickness of unit IV at this site is somewhat less than the average for the immediately surrounding area.

The occurrence of chert at this site is limited to a 5-cm bed between the base of the unit IV chalks and the top of the basalt. Scattered chert nodules occur within a 5-meter interval above this bed. Geochronologically, the age of the chert bed is approximately 46 m.y., which approximates the age of its shallowest occurrence at Site 220. At the latter site, the chert spanned a 204-meter interval, which timewise ranged from 43 ± 1 to 51 m.y. However, as the maximum age of sediments at Site 221 is only ~46 m.y., one would anticipate a thinner chert development there. Actually, the location of Site 221 may well be at the extreme edge of chert development for the particular segment of oceanic plate upon which it is situated. The near contemporaneity of youngest age of chert development at Sites 220 and 221 indicates that this interval, which is a good acoustic reflector, may be a fairly reliable time marker for at least this portion of the Arabian Sea.

Not yet discussed is the basalt interval beneath the chert layer. A penetration of 9.5 meters was made into the basalt, although only 5 meters were recovered. The basalt was derived from a typical tholeiitic melt. On the basis of the identification of chilled zones, at least ten flows could be identified. The absence of a baked or altered zone at the base of the sediment section suggests the flow is not part of a sill. Again, as at Site 220, sediment, this time as a thin (4 cm) altered bed, occurs one meter above the base of the basalt interval. Although highly altered, nannofossils could be seen in the sediment. Unfortunately, they are nondiagnostic as regards an age determination, and therefore, the time gap separating this sediment layer from the continuous sediment sequence above, is unknown. It does again illustrate the necessity of deep basalt penetration to make certain crustal age determinations are valid.

Regarding the age of the basalt at this site, it has already been noted that a 46 m.y. paleontological date, derived just above the basalt, compares favorably with a 48 m.y.

date based on fair correlations of the magnetic anomalies with calculated profiles. As previously stated, there are suggestions, based on depositional rates, that a portion of the basal sediment record may be missing and that, therefore, the above figures are minimal dates. At times, it is possible to resolve questions regarding anomalous crustal ages by comparing the actual depth to basalt encountered at a site with that predicted from a theoretical seafloor spreading, age-depth curve. Such a comparison gives a corrected actual depth of 4900 meters at Site 221 versus a predicted depth of slightly over 5000 meters, a difference within the limits of error of this technique.

The above comparison suggests that little, if any, structural movement has occurred at Site 221. As mentioned earlier, the presence of a broad 100-meter-high swell there could be explained just as easily by magmatic activity as by crustal deformation.

Evidence for deformed bedding planes is readily apparent on the seismic records. There is also a small fault in the sediments just above the basalt. Again, one could relate these to compressive stresses imposed on the sediments by plate collision. However, an examination of the seismic data shows the amplitude of sediment deformation decreases upward in the section, disappearing completely by the time the Early Pliocene turbidites were deposited. The suggestion is strong that the progressive elimination of basement relief occurs by preferential deposition of slightly more sediments in the troughs than on the abyssal hills, an aspect typical of pelagic deposition.

Depositional History

The oldest rocks recovered at this site consist of 20- to 100-cm-thick tholeiitic basalt flows which contain a thin limestone bed. Unfortunately, age diagnostic fossils in the limestone are lacking. Overlying the basalt is a thin ash layer which, in turn, has a thin chert bed rich in radiolarians above it. A Middle Eocene age was assigned to the lowermost nannofossil chalks which lie above the chert.

The deposition of such chalks and ooze continued until Late Oligocene time. Except for the presence of radiolarians and sponge spicules, and associated chert nodules plus a few foraminifera, the chalks consist almost entirely of nannofossils. The light color and high carbonate content of the sediments attest to their relative purity. An absence of all but the most solution resistant forms of foraminifera plus a slow rate of sedimentation indicates deposition was always in fairly deep water. The presence of highly productive upwelling waters at the surface, usually indicated by abundant biogenous tests, apparently occurred for only a brief period during initial sedimentation at this site.

During Late Oligocene time, the pelagic regime changed from one of nanno ooze to brown clay deposition, which persisted into an undifferentiated portion of Pliocene-Miocene time. The change took place over a distance of only one meter.

At an undetermined point in Neogene time, onlapping turbidites from the Indus Cone reached the southern portion of the Arabian Sea at this site, initially mixing with the pelagic deposits. Finally, in Late Pliocene time, the onlapping turbidity current deposits, many derived from areas of carbonate sedimentation along the shelf of western India, dominated the sedimentary regime. On the basis of data from nearby sites, true pelagic sedimentation contributes, at most, 10 percent to the cone sediments. A mix of multisource turbidites and pelagic deposits has apparently persisted to the present day.

In summary, during 44 of the 46 m.y. of recorded history at Site 221, pelagic sedimentation accounted for about half of the total sediment cover. This deposition served to partially subdue the irregular basaltic topography. The last 2 m.y., a period of mostly turbidite sedimentation, served to build up the other half of the sediment cover. By the mechanism of gravity flow, these sediments served to fill in the remaining topographic irregularities and develop a smoothly sloping sea floor surface.

REFERENCES

Berggren, W. A., 1972. A Cenozoic time-scale–some implications for regional geology and paleobiogeography: Lethaia., v. 5, p. 195-215.

Boudreaux, J. E. and Hay, W. W., 1969. Calcareous nannoplankton and biostratigraphy of the Late Pliocene-Pleistocene-Recent sediments in the *Submarex* cores: Rev. Espanola Micropaleontol., v. 1, no. 3, p. 249-292.

Bukry, D. 1971. Cenozoic calcareous nannofossils from The Pacific Ocean: San Diego Soc. Nat. Hist. Trans., v. 16, no. 14, p. 303-328.

Closs, H., Bungenstock, H., and Hinz, K., 1969. Results of seismic refraction measurements in the northern Arabian Sea, a contribution to the International Indian Ocean Expedition (in German): METEOR Expedition C2(1), p. 1-28.

Ewing, M., Eittreim, S., Truchan, M., and Ewing, J. I., 1969. Sediment distribution in the Indian Ocean: Deep-Sea Res., v. 16, p. 231-248.

Folk, R. L. and Ward, W. C., 1957. Brazos River bar: a study in the significance of grain size parameters: J. Sediment. Petrol., v. 31, p. 514-529.

Gansser, A., 1966. The Indian Ocean and the Himalayas: Ecologae Geol. Helv., v. 59(2), p. 831-848.

Hay, W. W., Mohler, H. P., Roth, P. H., Schmidt, R. R., and Boudreaux, J. E., 1967. Calcareous nannoplankton zonation of the Cenozoic of the Gulf Coast and Caribbean-Antillean area and transoceanic correlation; Gulf Coast Assoc. Geol. Soc. Trans., v. 17, p. 428-480.

Heath, G. R. and Moberly, R., 1971. Cherts From the western Pacific, Leg 7, Deep Sea Drilling Project. *In* Winterer, E. L., Riedel, W. R., et al., Initial Reports of the Deep Sea Drilling Project, volume 7: Washington (U. S. Government Printing Office), p. 99.

Heirtzler, J. R., Dickson, G. O., Herron, E. M., Pitman, W. C., and Le Pichon, X., 1968. Marine magnetic anomalies, geomagnetic field reversals, and motions of the ocean floor and continents: J. Geophys. Res., v. 73, p. 2119-2139.

Holeman, J. H., 1968. The sediment yield of the major rivers of the world: Water Resources Res., v. 4, p. 737.

Laughton, A. S., Matthews, D. H., and Fisher, R. L., 1971. The structure of the Indian Ocean. *In* The Sea, A Maxwell (Ed.): New York (John Wiley & Sons Inc.), v. 4(2) p. 543-586.

McKenzie, D. P., Sclater, J. G., 1971. The evolution of the Indian Ocean since the Late Cretaceous: Geophys. J. Roy. Astro. Soc., v. 25, p. 437-528.

Neprochnov, Yu. P., 1961. Sediment thickness of the Arabian Sea Basin (in Russian): Dokl. Akad. Nauk. USSR, v. 139(1), p. 177-179.

Passega, R., 1964. Grain size representation by CM patterns as a geological tool: J. Sediment. Petrol., v. 34, p. 830-847.

Pettijohn, F. J., 1957. Sedimentary rocks: New York, London (Harper and Row), 718 p.

Pimm, A. C., Garrison, R. E., and Boyce, R. E., 1971. Sedimentology synthesis lithology, chemistry and physical properties of sediments in the northwestern Pacific Ocean: Initial Reports of the Deep Sea Drilling Project, Volume 6. Washington (U. S. Government Printing Office), p. 1131-1253.

Sclater, J. G. and Franceteau, J., 1970. The implications of terrestrial heat flow observations on current tectonic and geochemical models of the crust and upper mantle of the earth: Geophy. J. Roy. Astro. Soc., v. 20, p. 509-542.

von Stackelberg, U., 1972. Faziesverteilung in Sedimenten des indisch-pakistanischen Kontinentalrandes (Arabisches Meer): "Meteor" Forsch.-Ergeb., Reihe C, No. 9, p. 1-73, Berlin–Stuttgart.

Wadia, D. H., 1968. The geology of India: New York (The MacMillan Co.), p. 536.

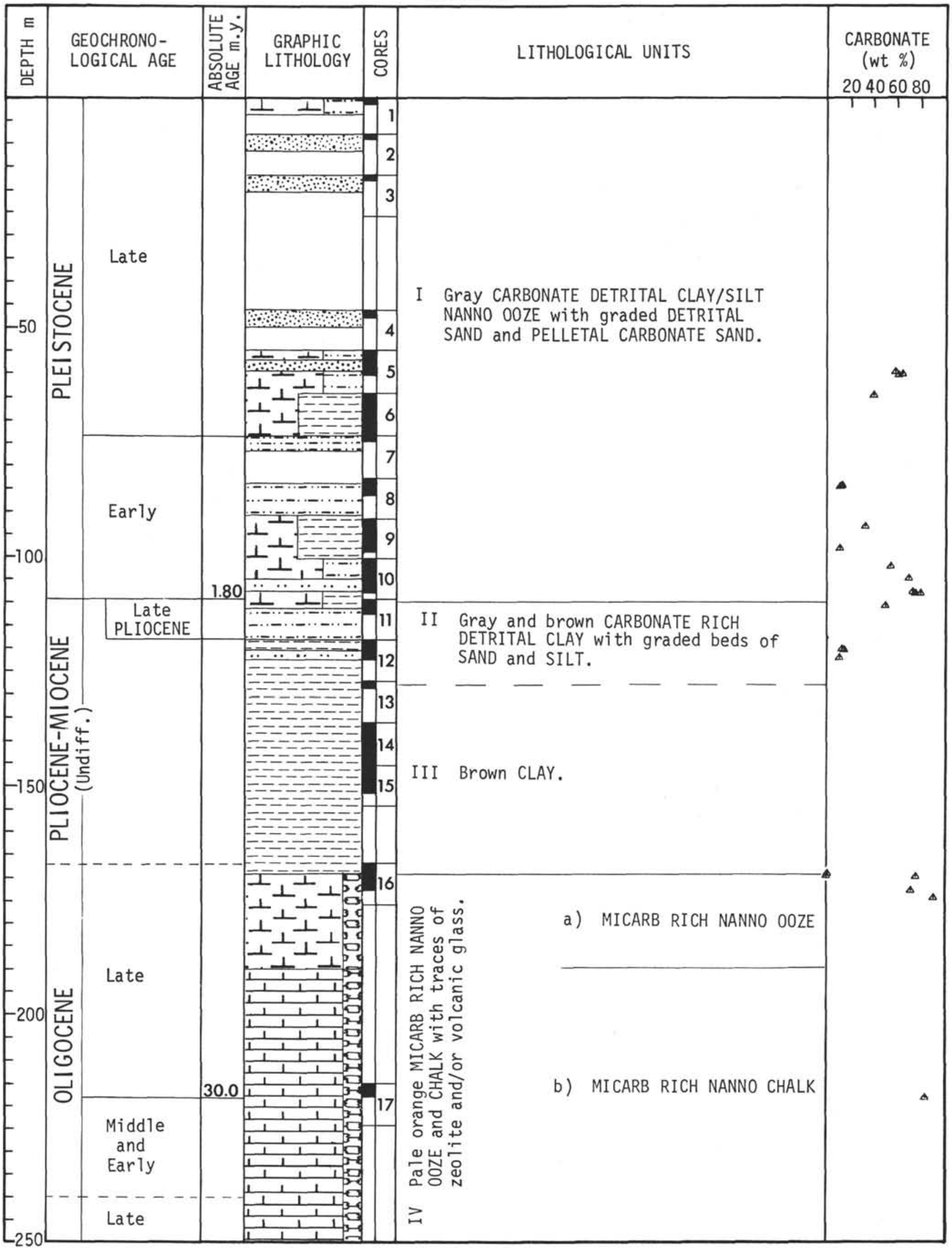

SITE 221

DEPTH m
GEOCHRONO-LOGICAL AGE
ABSOLUTE AGE m.y.
GRAPHIC LITHOLOGY
CORES
LITHOLOGICAL UNITS
CARBONATE (wt %)
20 40 60 80
50
100
150
200
250
PLEISTOCENE
Late
Early
1.80
Late PLIOCENE
PLIOCENE-MIOCENE (Undiff.)
OLIGOCENE
Late
30.0
Middle and Early
Late
1
2
3
4
5
6
7
8
9
10
11
12
13
14
15
16
17
I Gray CARBONATE DETRITAL CLAY/SILT NANNO OOZE with graded DETRITAL SAND and PELLETAL CARBONATE SAND.
II Gray and brown CARBONATE RICH DETRITAL CLAY with graded beds of SAND and SILT.
III Brown CLAY.
IV Pale orange MICARB RICH NANNO OOZE and CHALK with traces of zeolite and/or volcanic glass.
a) MICARB RICH NANNO OOZE
b) MICARB RICH NANNO CHALK

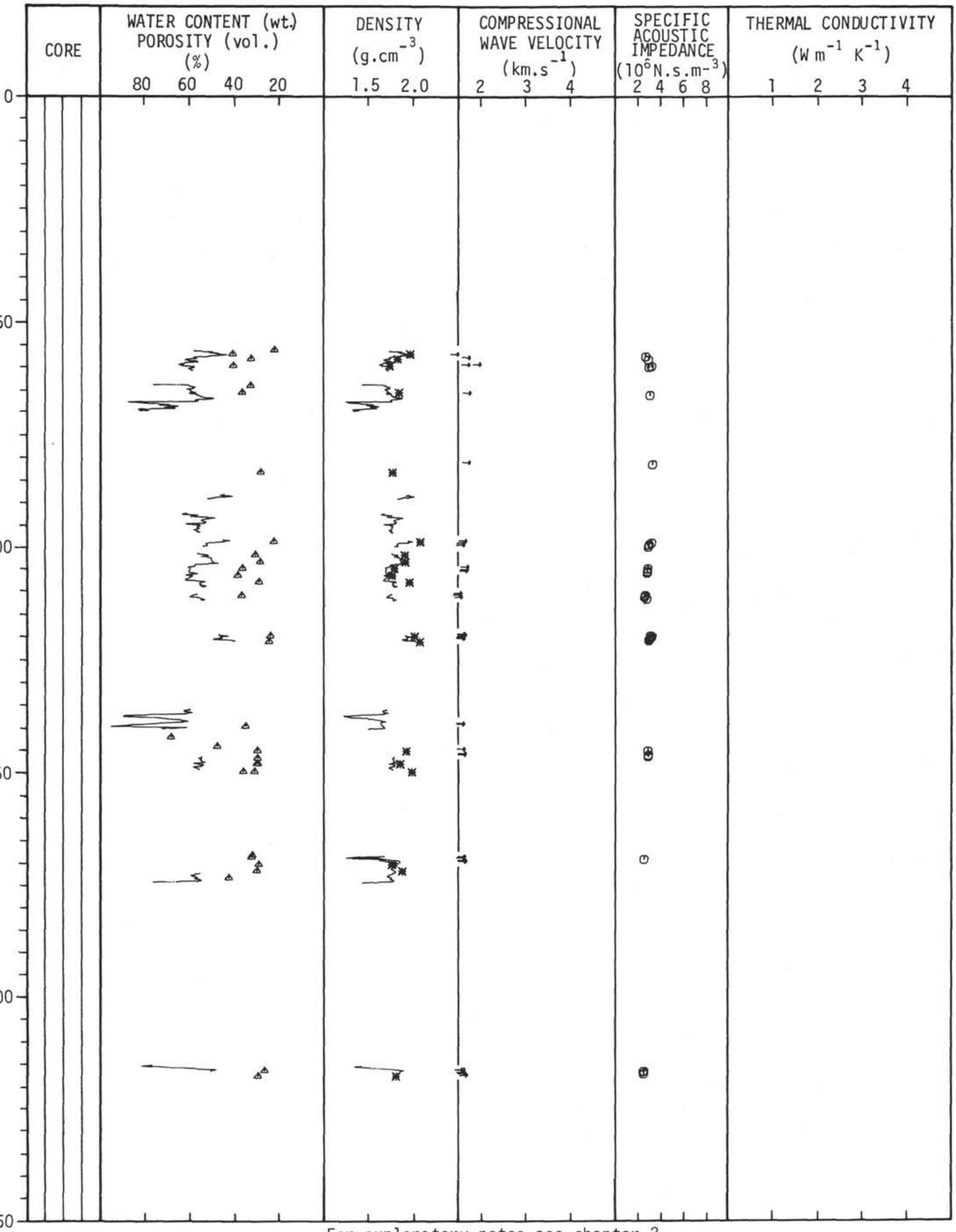

For explanatory notes see chapter 2.

SITE 221

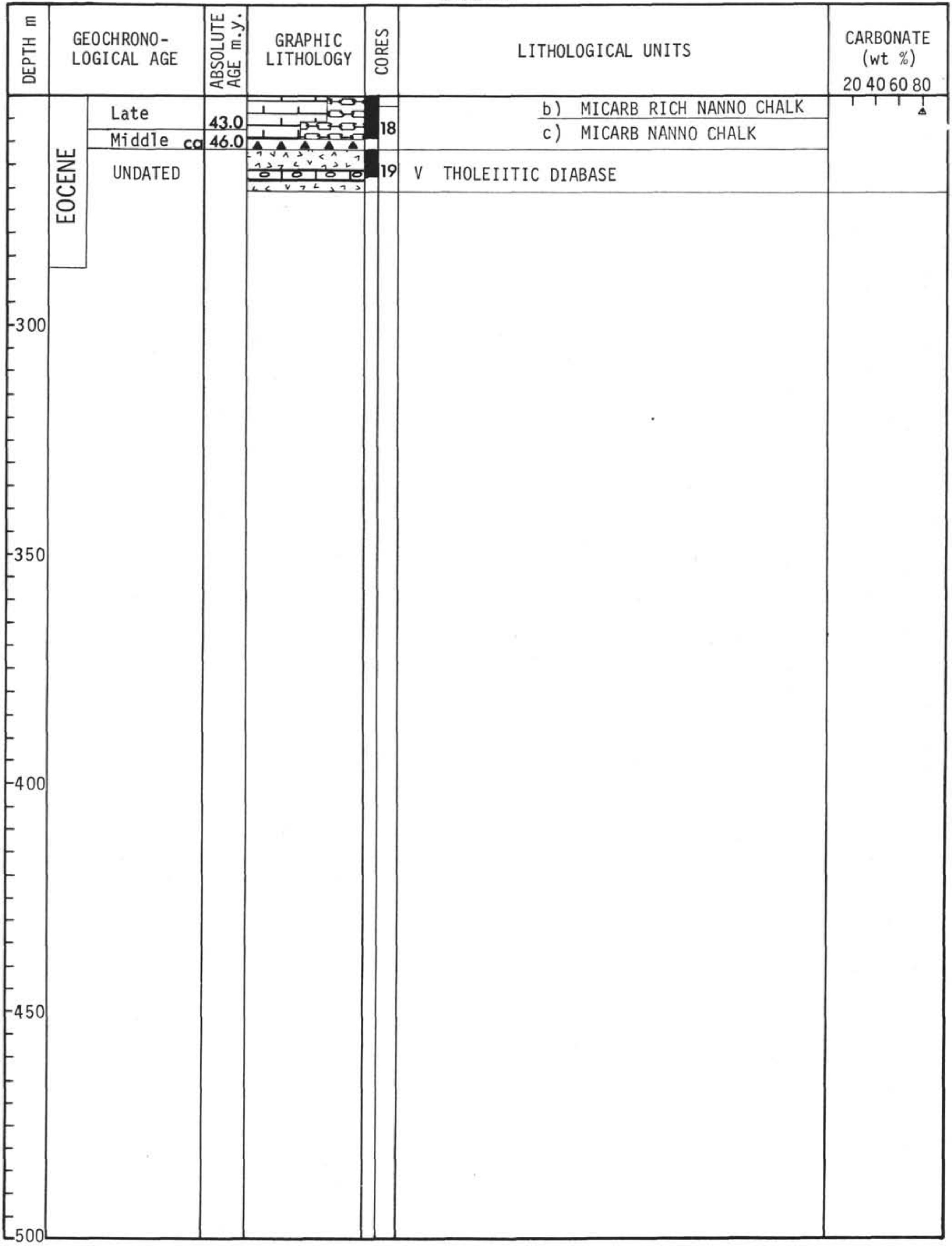
DEPTH m
GEOCHRONO-LOGICAL AGE
ABSOLUTE AGE m.y.
GRAPHIC LITHOLOGY
CORES
LITHOLOGICAL UNITS
CARBONATE (wt %)
20 40 60 80
EOCENE
Late
Middle
UNDATED
43.0
ca 46.0
18
19
b) MICARB RICH NANNO CHALK
c) MICARB NANNO CHALK
V THOLEIITIC DIABASE
300
350
400
450
500

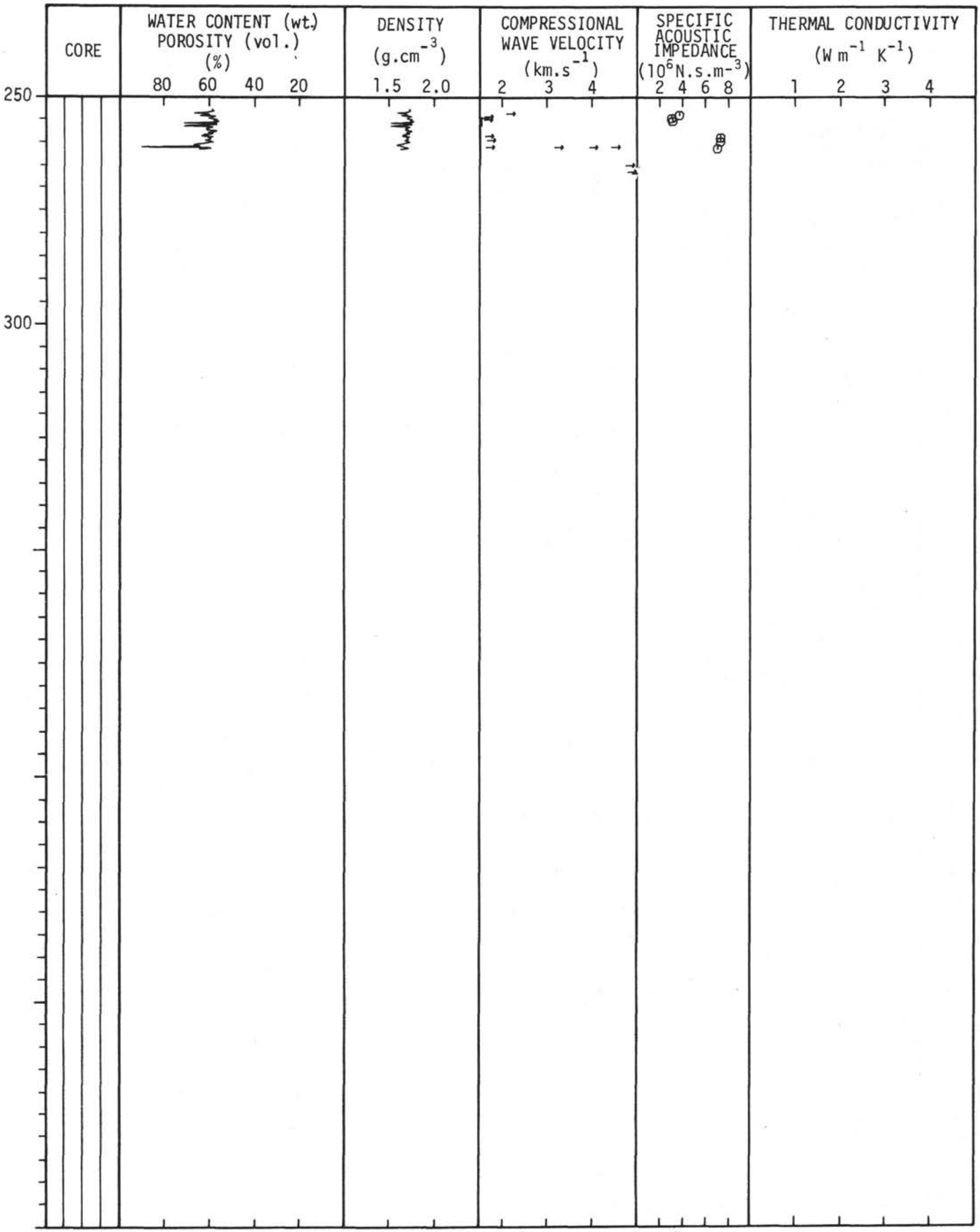

For explanatory notes see chapter 2.

Site 221 Hole Core 1 Cored Interval: 0-8

AGE	ZONE F	ZONE N	ZONE R	FOSSIL CHARACTER FORAMS	FOSSIL CHARACTER NANNOS	FOSSIL CHARACTER RADS	FOSSIL CHARACTER OTHERS	SECTION	METERS	LITHOLOGY	DEFORMATION	LITHO. SAMPLE	LITHOLOGIC DESCRIPTION
LATE PLEISTOCENE		Gephyrocapsa oceanica			Abundant and well preserved	Absent		Core Catcher		A	CC		Gray CARBONATE SILTY CLAY NANNO OOZE. Sediments are soft and massive. Dominant lithology SS: core catcher CARBONATE SILTY CLAY NANNO OOZE Composition: Nannos 55% Carbonate (coarse) 30% Mica 5% Volcanic glass 5% Carbonate needles 5% Remarks: Because the grain-size data for GRADED SEQUENCE is reported in a separate chapter (Jipa and Kidd, this volume) they are omitted from the core forms.

Site 221 Hole Core 2 Cored Interval: 8-17

AGE	ZONE F	ZONE N	ZONE R	FOSSIL CHARACTER FORAMS	FOSSIL CHARACTER NANNOS	FOSSIL CHARACTER RADS	FOSSIL CHARACTER OTHERS	SECTION	METERS	LITHOLOGY	DEFORMATION	LITHO. SAMPLE	LITHOLOGIC DESCRIPTION
LATE PLEISTOCENE		Gephyrocapsa oceanica			Rare and moderately well preserved	Absent		Core Catcher		N	CC		CARBONATE RICH DETRITAL SILTY SAND. Sediments soft and massive. Dominant lithology SS: core catcher CARBONATE RICH SILTY SAND Composition: Detrital silty sand 73% Carbonate 17% Nannos 10% Forams Trace

Explanatory notes in chapter 2

Site 221 Hole Core 3 Cored Interval: 17-26

AGE	ZONE F	ZONE N	ZONE R	FOSSIL CHARACTER FORAMS	FOSSIL CHARACTER NANNOS	FOSSIL CHARACTER RADS	FOSSIL CHARACTER OTHERS	SECTION	METERS	LITHOLOGY	DEFORMATION	LITHO. SAMPLE	LITHOLOGIC DESCRIPTION
LATE PLEISTOCENE		Gephyrocapsa oceanica			Rare and moderately well preserved	Absent		Core Catcher		N			CARBONATE RICH DETRITAL SILTY SAND. Sediments soft and massive. Dominant lithology SS: core catcher CARBONATE RICH DETRITAL SILTY SAND Composition: Detrital silty sand 78% Carbonate 17% Nannos 5% Radiolarians Trace

Site 221 Hole Core 4 Cored Interval: 46-55

AGE	ZONE F	ZONE N	ZONE R	FOSSIL CHARACTER FORAMS	FOSSIL CHARACTER NANNOS	FOSSIL CHARACTER RADS	FOSSIL CHARACTER OTHERS	SECTION	METERS	LITHOLOGY	DEFORMATION	LITHO. SAMPLE	LITHOLOGIC DESCRIPTION
LATE PLEISTOCENE		Gephyrocapsa caribbeanica		Very rare, non-diagnostic	Rare and moderately well preserved	Absent		Core Catcher		N		CC	SILTY SAND Dominant lithology SS: core catcher SILTY SAND Composition: Detrital silty sand 77% Carbonate 10% Nannos 10% Forams 3%

Explanatory notes in chapter 2

Site 221 Hole Core 5 Cored Interval: 55-64

AGE	ZONE			FOSSIL CHARACTER			
	F	N	R	FORAMS	NANNOS	RADS	OTHERS
LATE PLEISTOCENE		Gephyrocapsa caribbeanica Coccolithus doronicoides	Undifferentiated PLEISTOCENE	Rare to absent, non-diagnostic	Abundant and well preserved	Absent	Minor Eocene Neritic benthic spp.

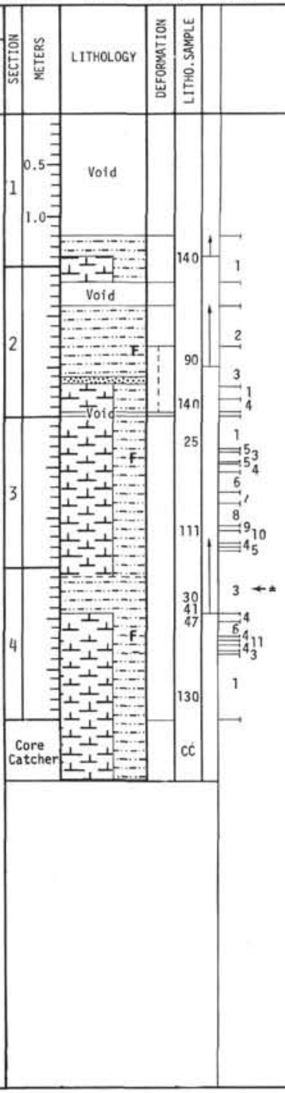

LITHOLOGIC DESCRIPTION

Gray DETRITAL SILTY CLAY NANNO OOZE.

Some intervals exhibit graded bedding.

Dominant lithology SS: Section 3-111 cm
DETRITAL SILTY CLAY NANNO OOZE
Composition:

Nannos	50%
Silty clay	38%
Carbonate	7%
Forams	5%

Minor lithology SS: Section 4-47 cm
DETRITAL PELLET RICH NANNO SILT
Composition:

Nannos	25%
Pellets	24%
Clayey silt	19%
Carbonate	10%
Shell debris	10%
Forams	7%
Calcite needles	3%
Radiolarians	Trace
Sponge spicules	Trace

Color legend:

1 = dark green gray	5GY 4/1
2 = olive gray	5Y 4/1
3 = green gray	5GY 6/1
4 = green gray	5G 6/1
5 = brown gray	5YR 4/1
6 = dusky yellow green	5GY 5/2
7 = light brown gray	5YR 6/1
8 = pale olive	10Y 6/2
9 = light blue gray	5B 7/1
10 = light green gray	5G 8/1
11 = gray yellow green	5GY 7/2

* faecal pellet rich graded bed.

Shore-based laboratory results

Carbonate: Sections 3-133 cm = 58%, 4-31 cm = 64%, 4-46 cm = 60%.

X-ray mineralogy: Section 4-33 cm

Calcite	10%
Dolomite	1%
Aragonite	63%
Quartz	6%
Plagioclase	3%
Mica	14%
Chlorite	2%
Clinoptilolite	1%
Amphibole	1%

Explanatory notes in chapter 2

Site 221 Hole Core 6 Cored Interval: 64-73

AGE	ZONE			FOSSIL CHARACTER			
	F	N	R	FORAMS	NANNOS	RADS	OTHERS
LATE PLEISTOCENE		Coccolithus doronicoides		Very rare to absent	Abundant and well preserved	Absent	Neritic benthic foraminifera

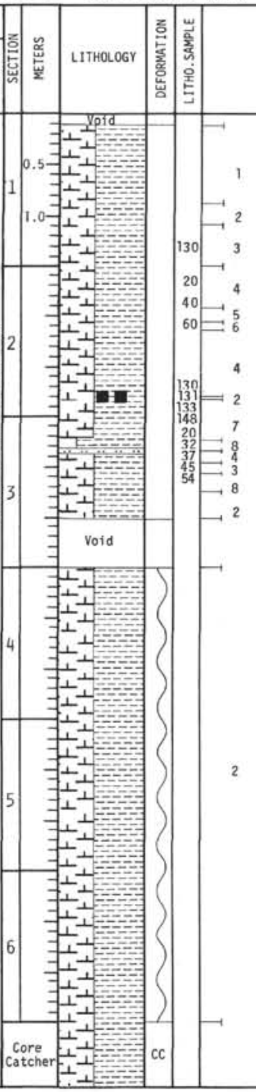

LITHOLOGIC DESCRIPTION

Gray NANNO DETRITAL CLAY.

Locally there are transitions into more silty laminae. Massive firm bedding, moderate deformation, thin laminae and bioturbation in places.

Dominant lithology SS: Section 2-60 cm
NANNO DETRITAL CLAY
Composition:

Clay	65%
Nannos	35%

Minor lithology SS: Section 3-32 cm
CARBONATE NANNO RICH DETRITAL SILT
Composition:

Detrital silt	58%
Nannos	20%
Carbonate	20%

Color legend:

1 = gray olive	10Y 4/2
2 = green gray	5G 6/1
3 = dusky yellow green	5GY 5/2
4 = green gray	10GY 5/2
5 = gray yellow green	5GY 7/2
6 = light blue gray	5B 7/1
7 = dark green gray	5G 4/1
8 = dark green gray	5GY 4/1

Shore-based laboratory results

Carbonate
Section 1-40 cm = 40%

Explanatory notes in chapter 2

Site 221 Hole Core 7 Cored Interval: 73-82

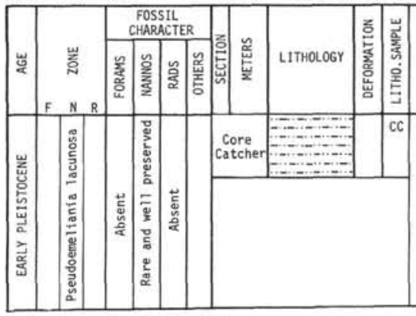

LITHOLOGIC DESCRIPTION

DETRITAL SILTY CLAY

Sediments soft and massive.

Explanatory notes in chapter 2

Site 221 Hole Core 8 Cored Interval: 82-91

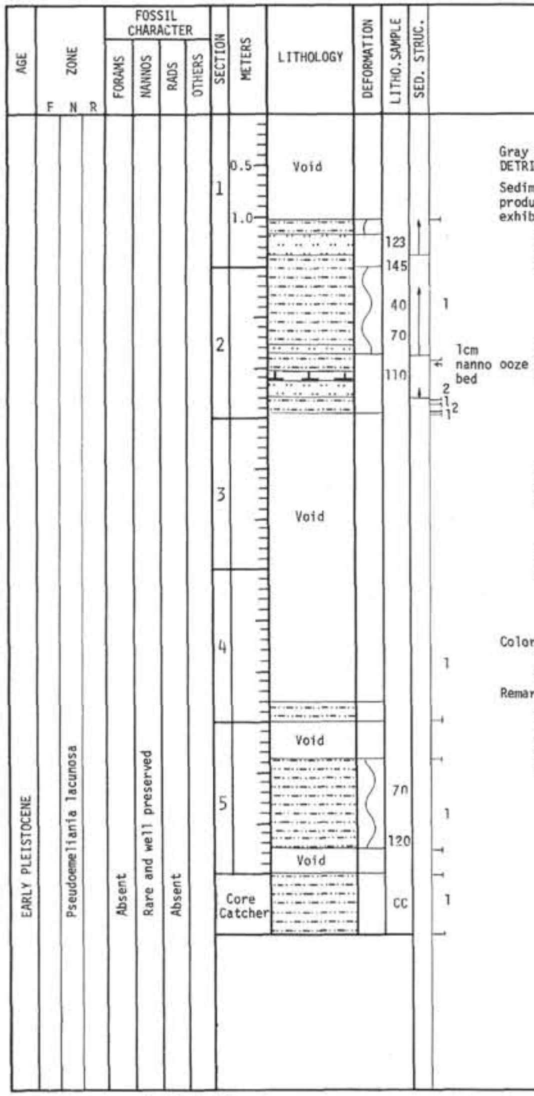

LITHOLOGIC DESCRIPTION

Gray DETRITAL SILTY CLAY and CARBONATE RICH DETRITAL SILT.

Sediments generally firm but with flow structure produced by coring. The carbonate rich beds exhibit graded bedding. Rare NANNO OOZE laminae.

Dominant lithology SS: Section 2-40 cm
DETRITAL SILTY CLAY
Composition:

Detrital silty clay	87%
Carbonate	8%
Nannos	5%
Plant fragments	Trace

Minor lithology SS: Section 1-123 cm
NANNO CARBONATE RICH DETRITAL SILT
Composition:

Detrital silt	68%
Carbonate	17%
Nannos	12%
Pellets	Trace
Carbonate needles	Trace

Minor lithology SS: Section 2-110 cm
DETRITAL CLAY RICH NANNO OOZE
Composition:

Nannos	85%
Detrital clay	15%

Minor lithology SS: Section 5-123 cm
CARBONATE DETRITAL SILT
Composition:

Detrital silt	53%
Carbonate	45%
Nannos	Trace

Color legend:
1 = dark green gray 5GY 4/1
2 = dusky yellow green 5GY 5/2

Remarks:
Prominence of voids suggests that the drilling has only retained graded bed lithologies and that the true dominant lithology may contain a higher percentage of nannos as in cores below Core 8 and above Core 7.

<u>Shore-based laboratory results</u>

Carbonate: Sections 2-47 cm = 13%, 2-67 cm = 13%, 2-83 cm = 11%.

Grain size:	Sections		
	2-5 cm,	2-66 cm,	2-88 cm
Sand	0%	2%	9%
Silt	62%	67%	70%
Clay	38%	31%	21%

X-ray mineralogy:	Sections		
	2-1 cm,	2-29 cm,	2-55 cm
Calcite	9%	11%	8%
Dolomite	2%	1%	1%
Quartz	20%	20%	22%
K-feldspar	2%	2%	5%
Plagioclase	6%	6%	10%
Mica	54%	51%	48%
Chlorite	8%	9%	6%

Explanatory notes in chapter 2

Site 221 Hole Core 9 Cored Interval: 91-100

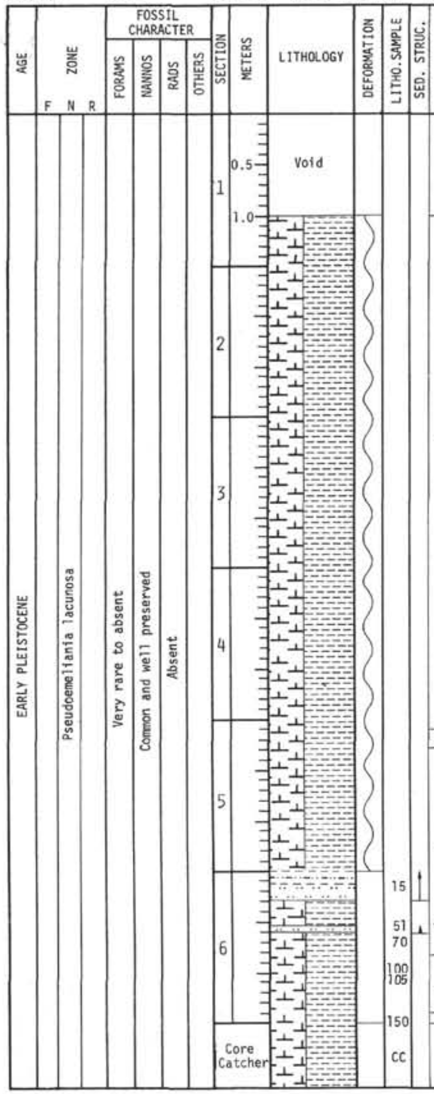

LITHOLOGIC DESCRIPTION

Gray NANNO DETRITAL CLAY.

Occasional thin graded beds above with increased silt content. Generally badly disturbed and soupy. Basal section firm with only moderate disturbance. In section 6, graded sequences present often with bioturbation at base and laminated at top. Similar sequences probably destroyed by coring deformation in sections 1-5.

Dominant lithology SS: Section 6-70 cm
NANNO DETRITAL CLAY
Composition:

Detrital clay	65%
Nannos	30%
Carbonate	5%
Carbonate needles	Trace

Minor lithology SS: Section 6-15 cm
DETRITAL RICH CARBONATE NANNO CLAYEY SILT
Composition:

Nannos	45%
Carbonate (coarse)	30%
Detrital clayey silt	15%
Carbonate (fine)	10%
Pellets	Trace

Color legend:

1 =	dark green gray	5G 4/1
2 =	olive gray	5Y 4/1
3 =	gray olive green	5GY 3/2
4 =	dusky yellow green	5GY 5/2

1 cm carb. detr. slt. shows grd. bedng.

Shore-based laboratory results

Carbonate
Section 2-39 cm = 33%
Section 5-76 cm = 11%

Explanatory notes in chapter 2

Site 221 Hole Core 10 Cored Interval: 100-109

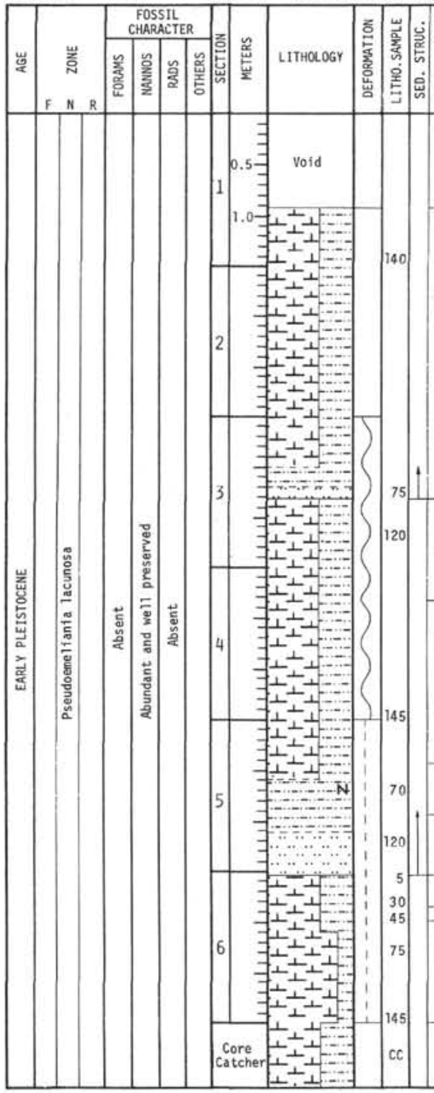

LITHOLOGIC DESCRIPTION

Green CARBONATE RICH DETRITAL SILTY CLAY NANNO OOZE with graded beds of DETRITAL CARBONATE PELLETAL CLAYEY SILT and SILTY SAND.

Sediments firm to disturbed, graded sequences often laminated. Bioturbation prominent at some levels as top of section 5. Faecal pellets prominent in graded units but none where bioturbation is present - probably of clastic origin, as they occur with other redeposited components.

Dominant lithology SS: Section 3-120 cm
CARBONATE RICH DETRITAL SILTY CLAY NANNO OOZE
Composition:

Nannos	50%
Detrital silty clay	22%
Carbonate	15%
Pellets	10%
Mica	3%
Forams	Trace
Carbonate needles	Trace

Minor lithology SS: Section 6-5 cm
DETRITAL PELLETAL CLAYEY SILT
Composition:

Pellets	40%
Detrital clayey silt	20%
Carbonate grains	10%
Carbonate needles	10%
Nannos	10%
Forams	5%
Shell debris	3%
Sponge spicules	Trace

Color legend:

1 =	dusky yellow green	5GY 5/2
2 =	gray yellow green	5GY 7/2
3 =	green gray	5GY 6/1
4 =	dark green gray	5G 4/1

Shore-based laboratory results

Carbonate: Sections 2-15 cm = 54%, 3-133 cm = 70%, 5-115 cm = 73%, 5-149 cm = 75%, 6-4 cm = 79%.

X-ray mineralogy: Sections

	5-87 cm,	5-136 cm
Calcite	16%	10%
Dolomite	1%	0%
Aragonite	68%	78%
Quartz	4%	4%
Plagioclase	1%	1%
Mica	8%	7%
Chlorite	1%	1%

Explanatory notes in chapter 2

Site 221 Hole Core 11 Cored Interval: 109-118

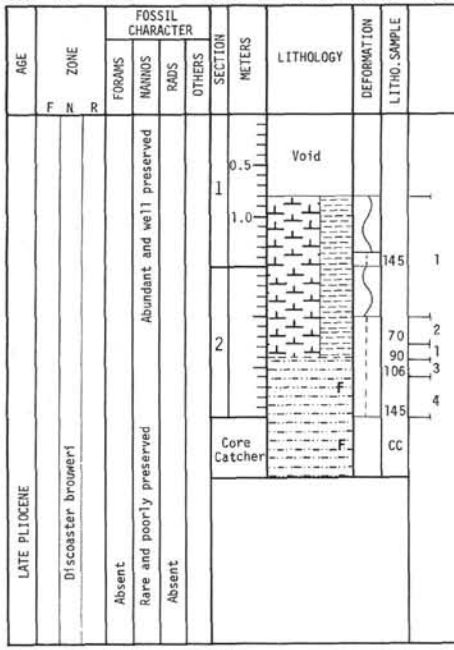

LITHOLOGIC DESCRIPTION

Gray CARBONATE RICH DETRITAL CLAY NANNO OOZE and CARBONATE RICH DETRITAL SILTY CLAY.

Sediments soft, disturbed or mottled throughout with sand in patches.

Dominant lithology SS: Section 1-145 cm
CARBONATE RICH DETRITAL CLAY NANNO OOZE
Composition:

Nannos	55%
Detrital clay	33%
Carbonate grains (fine and coarse)	12%

Dominant lithology SS: Section 2-145 cm
CARBONATE RICH DETRITAL SILTY CLAY
Composition:

Detrital silty clay	69%
Carbonate grains	20%
Shell debris	5%
Forams	3%
Carbonate needles	2%
Nannos	Trace

Color legend:

1 =	green gray	5G 6/1
2 =	gray yellow green	5GY 7/2
3 =	dusky yellow green	5GY 5/2
4 =	dark green gray	5GY 4/1

Shore-based laboratory results

Carbonate
Section 1-120 cm = 50%

Explanatory notes in chapter 2

Site 221 Hole Core 12 Cored Interval: 118-127

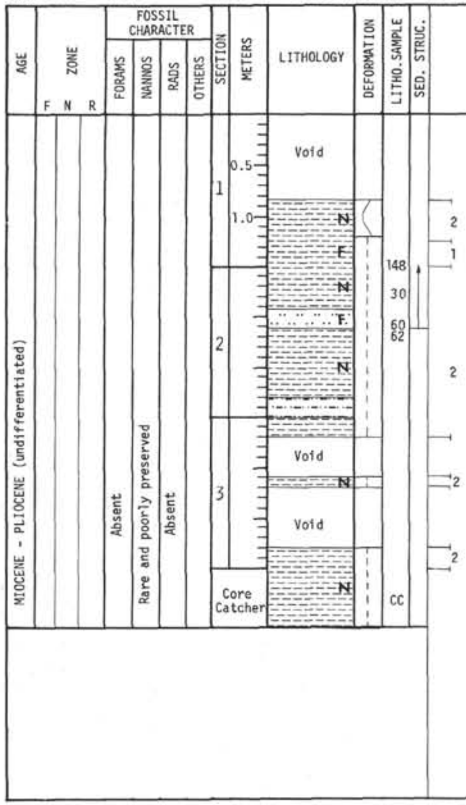

LITHOLOGIC DESCRIPTION

Gray CARBONATE RICH DETRITAL CLAY

Section 5 contains graded SANDY SILT bed. Sediments homogenous, stiff to soupy with the medium to fine graded sandy silt bed showing coring disturbance.

Dominant lithology SS: Section 1-148 cm
CARBONATE RICH DETRITAL CLAY

Detrital clay	75%
Carbonate	15%
Plant fragments	7%
Nannos	3%
Forams	Trace
Carbonate needles	Trace

Minor lithology SS: Section 2-62 cm
PLANT RICH DETRITAL SILTY SAND
Composition:

Detrital silty sand	65%
Plant debris	20%
Carbonate	7%
Shell debris	7%
Forams	Trace

Color legend:

1 =	olive gray	5Y 4/1
2 =	olive black	5Y 2/1

Shore-based laboratory results

Carbonate: Sections 2-20 cm = 13%, 2-45 cm = 15%, 3-60 cm = 11%.

Grain size: Sections

	2-19 cm,	2-44 cm,	2-60 cm
Sand	0%	0%	19%
Silt	19%	54%	69%
Clay	81%	46%	12%

X-ray mineralogy: Sections

	2-1 cm,	2-63 cm
Calcite	12%	12%
Dolomite	2%	2%
Quartz	21%	22%
Plagioclase	5%	4%
Mica	51%	51%
Chlorite	9%	9%
K-feldspar	0%	1%

Site 221 Hole Core 13 Cored Interval: 127-136

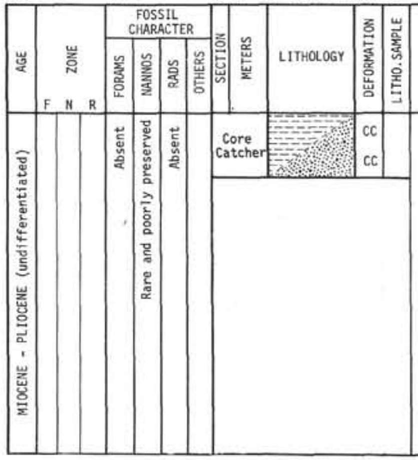

LITHOLOGIC DESCRIPTION

Brown CARBONATE RICH DETRITAL CLAY

Massive and soft.

Dominant lithology SS: core catcher 1
CARBONATE RICH DETRITAL CLAY
Composition:

Detrital clay	83%
Carbonate	12%
Plant debris	3%
Nannos	Trace

Minor lithology SS: core catcher 2
SANDY SILT
Composition:

Sandy silt	89%
Carbonate	7%
Plant debris	2%
Nannos	Trace
Sponge spicules	Trace

Explanatory notes in chapter 2

Site 221 Hole Core 14 Cored Interval: 136-145

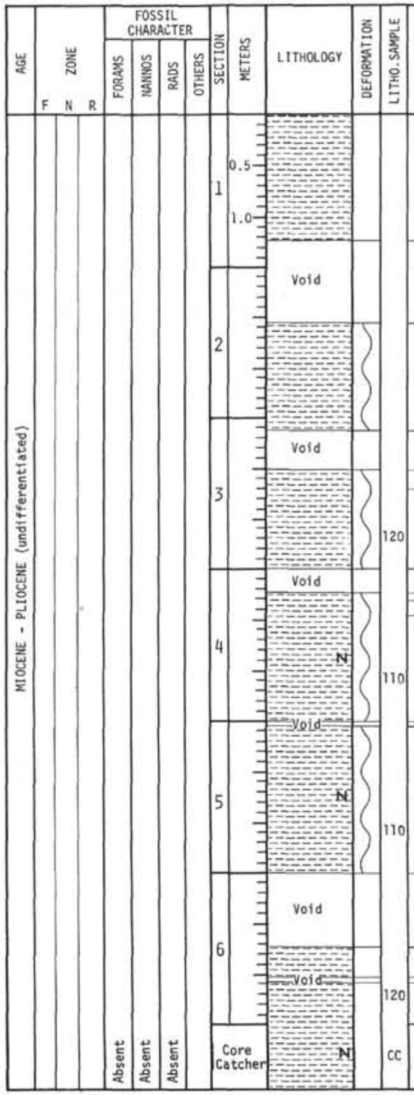

LITHOLOGIC DESCRIPTION

Brown CLAY

Well-laminated locally but generally badly deformed and soupy.

Dominant lithology SS: Section 4-110 cm
CLAY
Composition:

Clay	99%
Carbonate	Trace
Nannos	Trace

Color legend:
1 = moderate yellow brown 10YR 5/4
2 = light blue gray 5B 7/1

Explanatory notes in chapter 2

Site 221 Hole Core 15 Cored Interval: 145-154

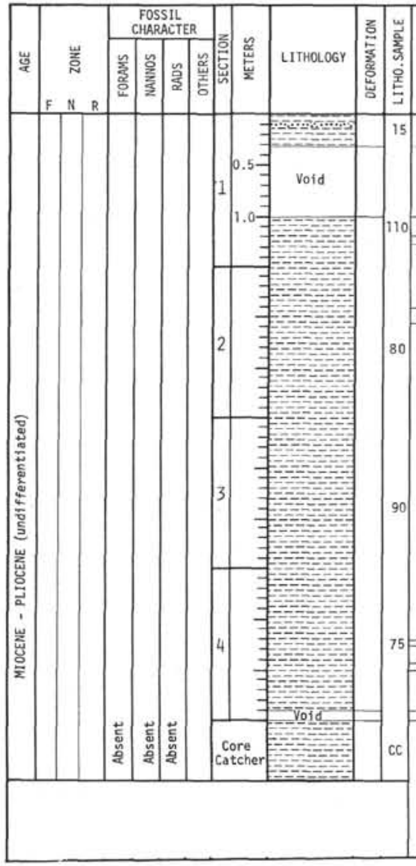

LITHOLOGIC DESCRIPTION

Brown CLAY and rare gray SILTY SAND laminae.

Compact, massive with local sandy laminae. Sand also present in bioturbated intervals.

Dominant lithology SS: Section 3-90 cm
CLAY
Composition:

Clay	97%
Zeolites	2%
Ferromanganese minerals	Trace
Nannos	Trace

Minor lithology SS: Section 2-80 cm
SILTY SAND
Composition:

Silty sand	94%
Carbonate	5%
Forams	Trace

Color legend:
1 = moderate yellow brown 10YR 5/4
2 = olive gray 5Y 4/1
3 = gray olive 10Y 4/2

X-ray mineralogy: Section 3-97 cm

Quartz	22%
K-feldspar	2%
Plagioclase	8%
Kaolin	5%
Mica	27%
Chlorite	6%
Montmorillonite	7%
Palygorskite	19%
Gypsum	4%

Shore-based laboratory results

X-ray mineralogy: Section 3-94 cm

Quartz	21%
Plagioclase	7%
Kaolin	5%
Mica	18%
Chlorite	4%
Montmorillonite	7%
Palygorskite	37%
Goethite	Trace

Explanatory notes in chapter 2

Site 221 Hole Core 16 Cored Interval: 167-176

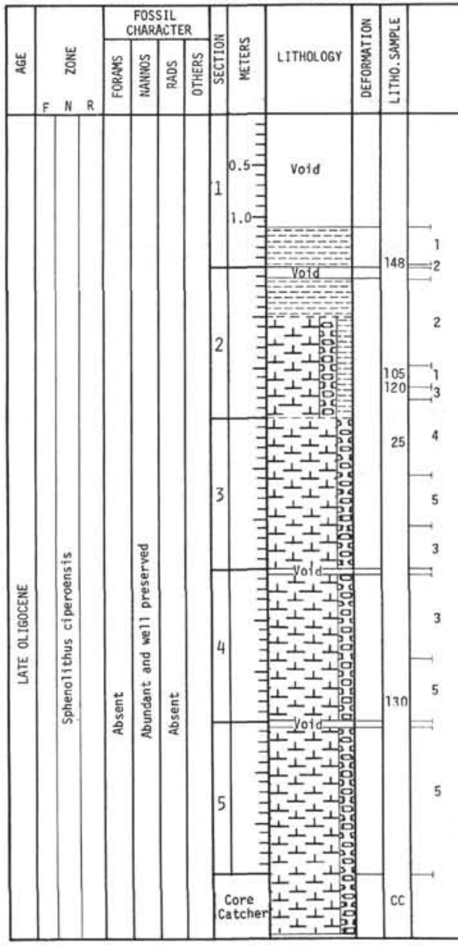

LITHOLOGIC DESCRIPTION

Gray CLAY and yellow MICARB RICH NANNO OOZE.

Clay interval is thickly bedded and bioturbated. The ooze is soft, compact and locally bioturbated.

Dominant lithology SS: Section 1-148 cm
CLAY
Composition:

Clay	90%
Mica	5%
Zeolites	2%
Nannos	2%
Ferromanganese minerals	Trace

Dominant lithology SS: Section 4-130 cm
MICARB RICH NANNO OOZE
Composition:

Nannos	70%
Micarb	15%
Clay	10%
Carbonate needles	5%

Minor lithology SS: Section 2-105 cm
MICARB CLAY RICH NANNO OOZE
Composition:

Nannos	58%
Clay	20%
Micarb	15%
Zeolites	5%
Mica	2%

Remarks: Traces of zeolite and/or volcanic glass throughout the core.

Color legend:

1 = light olive gray	5Y 5/2
2 = olive gray	5Y 4/1
3 = yellow gray	5Y 7/2
4 = dusky yellow	5Y 6/4
5 = gray yellow	5Y 8/4

Shore-based laboratory results

Carbonate
Section 1-136 cm = 1%
Section 2- 35 cm = 0%
Section 2- 60 cm = 75%
Section 4- 55 cm = 71%
Section 5- 60 cm = 90%

Grain size: Section 1-135 cm

Sand	1%
Silt	5%
Clay	94%

Explanatory notes in chapter 2

Site 221 Hole Core 17 Cored Interval: 215-224

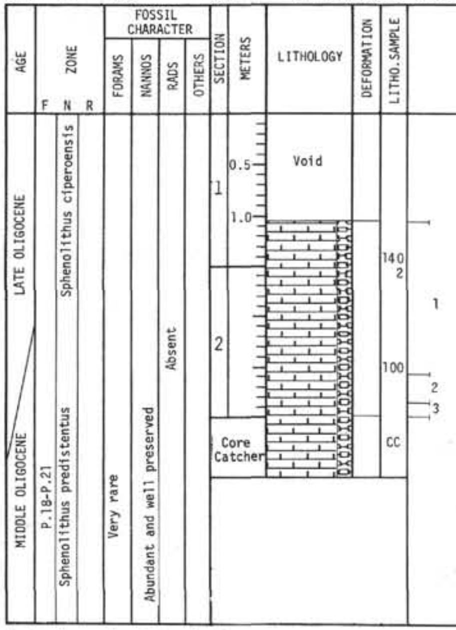

LITHOLOGIC DESCRIPTION

Orange MICARB RICH NANNO CHALK.

Locally thin ooze layers. Traces of zeolite near base. Massive chalk, sometimes thinly laminated or with soft ooze layers. Discoasters are important part of nannofossils.

Dominant lithology SS: Section 2-2 cm
MICARB RICH NANNO CHALK
Composition:

Nannos	78%
Micarb	15%
Clay	5%
Carbonate needles	2%

Color legend:

1 = very pale orange	10YR 8/2
2 = yellow gray	5Y 7/2
3 = yellow gray	5Y 8/1

Shore-based laboratory results

Carbonate
Section 2-82 cm = 83%

Explanatory notes in chapter 2

Site 221 Hole Core 18 Cored Interval: 252-261

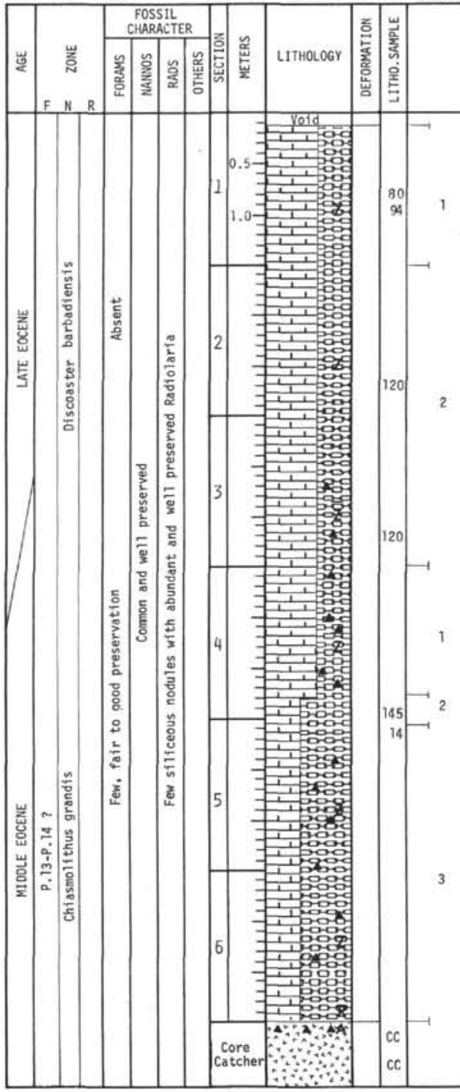

LITHOLOGIC DESCRIPTION

Orange MICARB NANNO CHALK.

Incipient chert nodules. Local volcanic ash and/or zeolite grains. Massive, compact with some bioturbation and streaking. Incipient siliceous nodules and small-scale faulting appear towards base. Core catcher contains chert layer above the volcanic material.

Dominant lithology SS: Section 2-120 cm
MICARB NANNO CHALK
Composition:

Nannos	57%
Micarb	35%
Zeolites	5%
Mica	Trace
Forams	Trace

Minor lithology SS: core catcher 2
MICARB SPICULE RAD RICH NANNO CHALK
Composition:

Nannos	45%
Radiolarians	20%
Sponge spicules	15%
Micarb	15%
Zeolites	5%
Volcanic glass	Trace
Mica	Trace

(The smear slide from the core catcher above the basalt contains 100% volcanic glass)

Color legend:
1 = gray orange 10YR 7/4
2 = very pale orange 10YR 8/2
3 = yellow gray 5Y 7/2

Shore-based laboratory results

Carbonate
Section 1-45 cm = 78%

X-ray mineralogy: Section 1-45 cm

Calcite	95%
Quartz	1%
Clinoptilolite	4%

Explanatory notes in chapter 2

Site 221 Hole Core 19 Cored Interval: 261-270

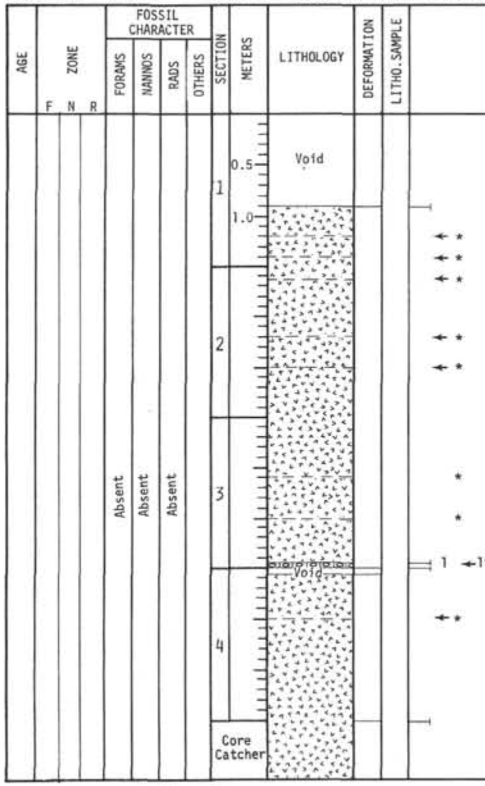

LITHOLOGIC DESCRIPTION

Very dark gray, partially, vesicular. THOLEIITIC DIABASE (with glassy chilled margins between flows) fractures filled by calcite.

Color legend:
1 = very pale orange 10YR 8/2

* chilled margins

Explanatory notes in chapter 2

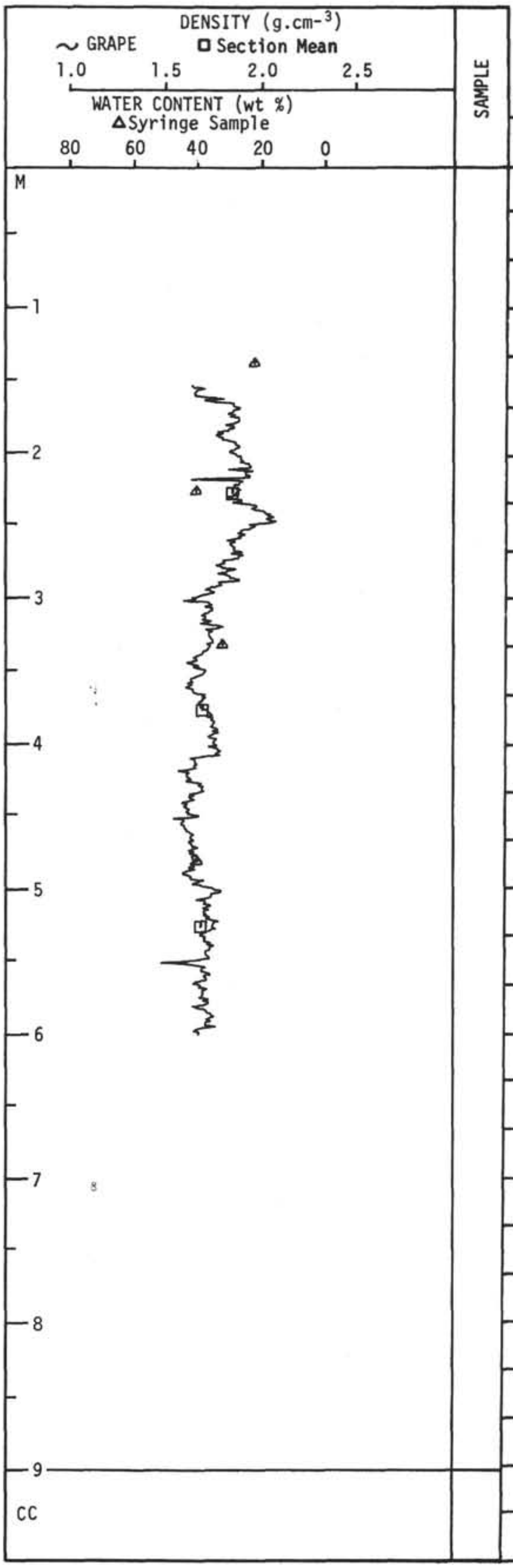

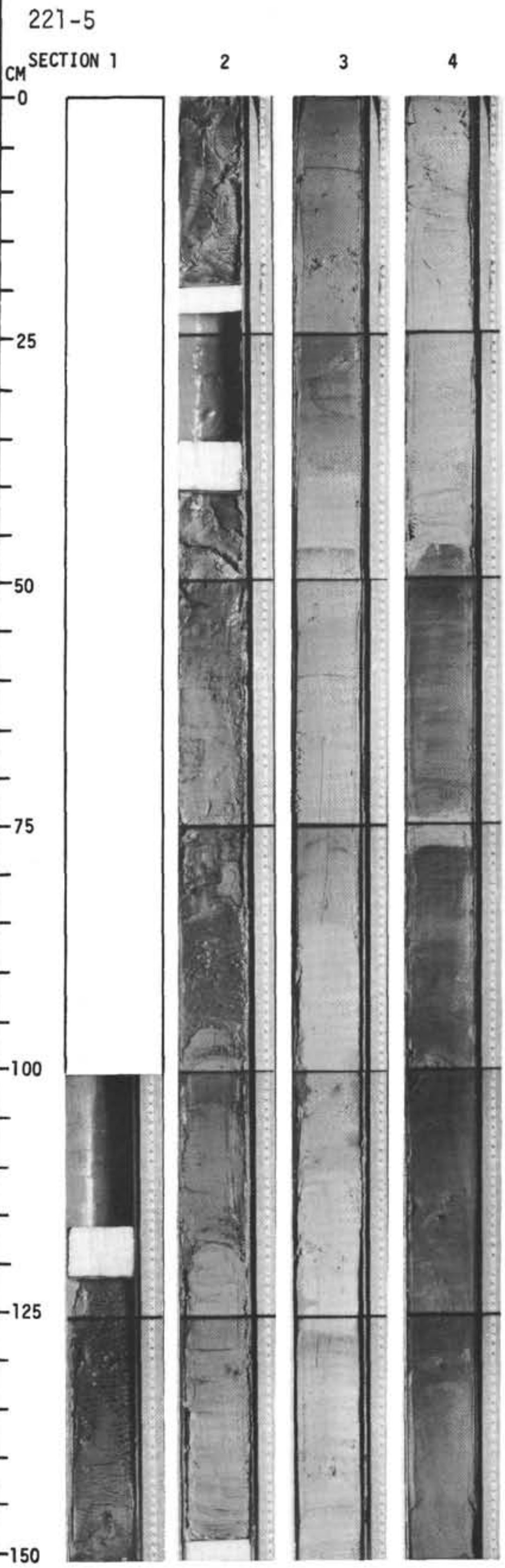

For Explanatory Notes, see Chapter 2

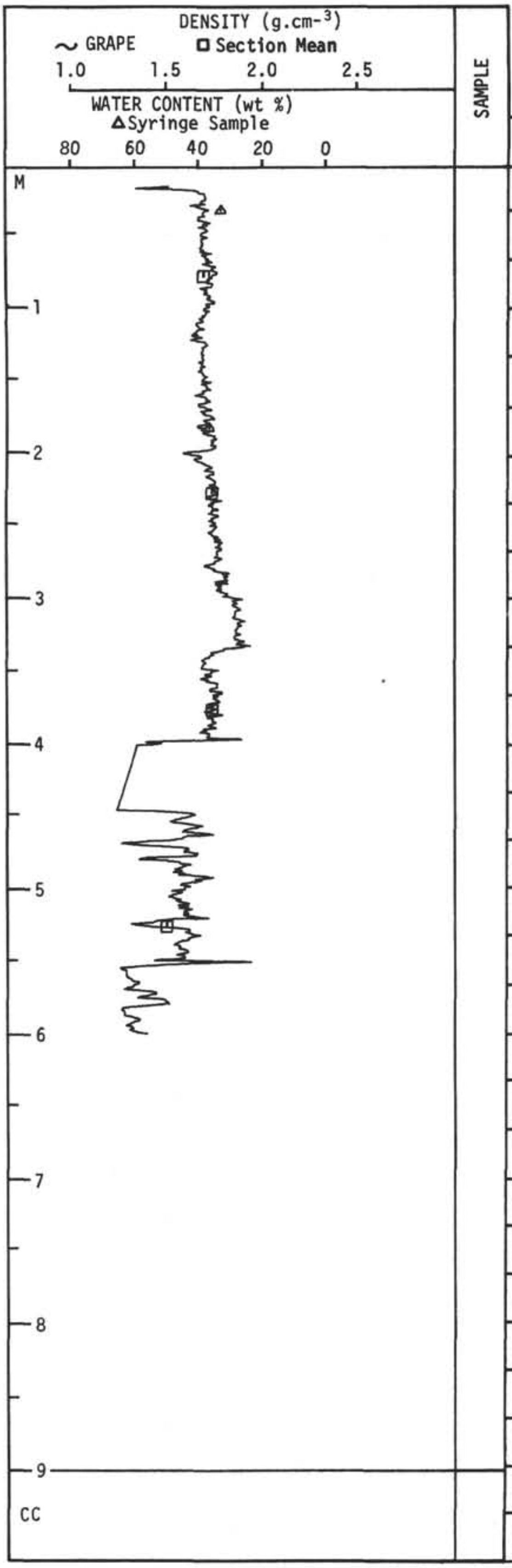

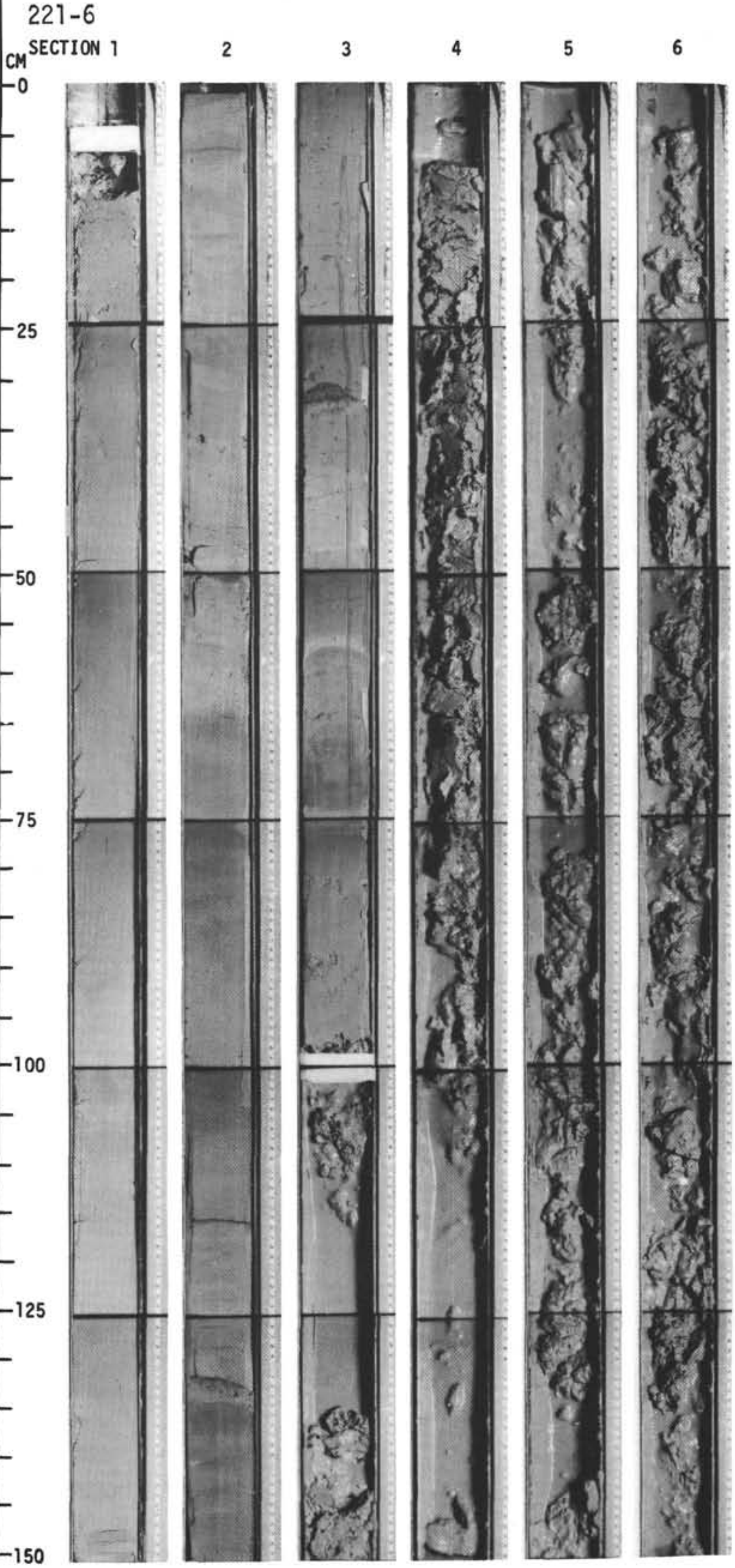

For Explanatory Notes, see Chapter 2

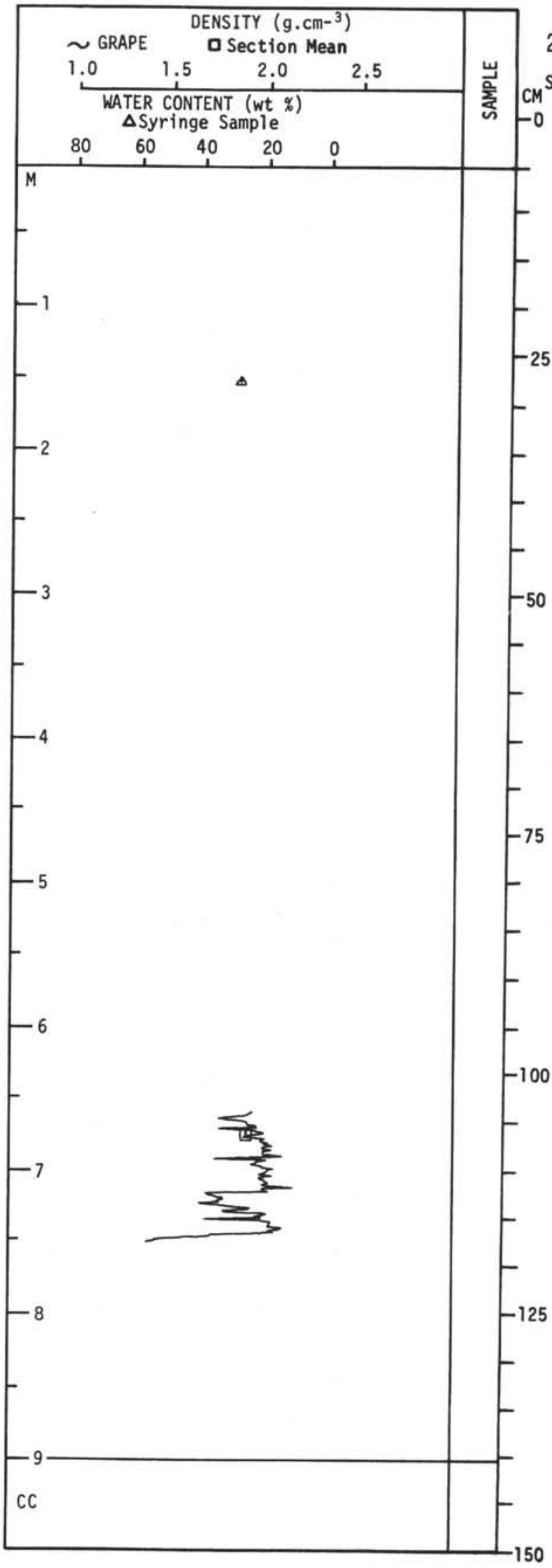

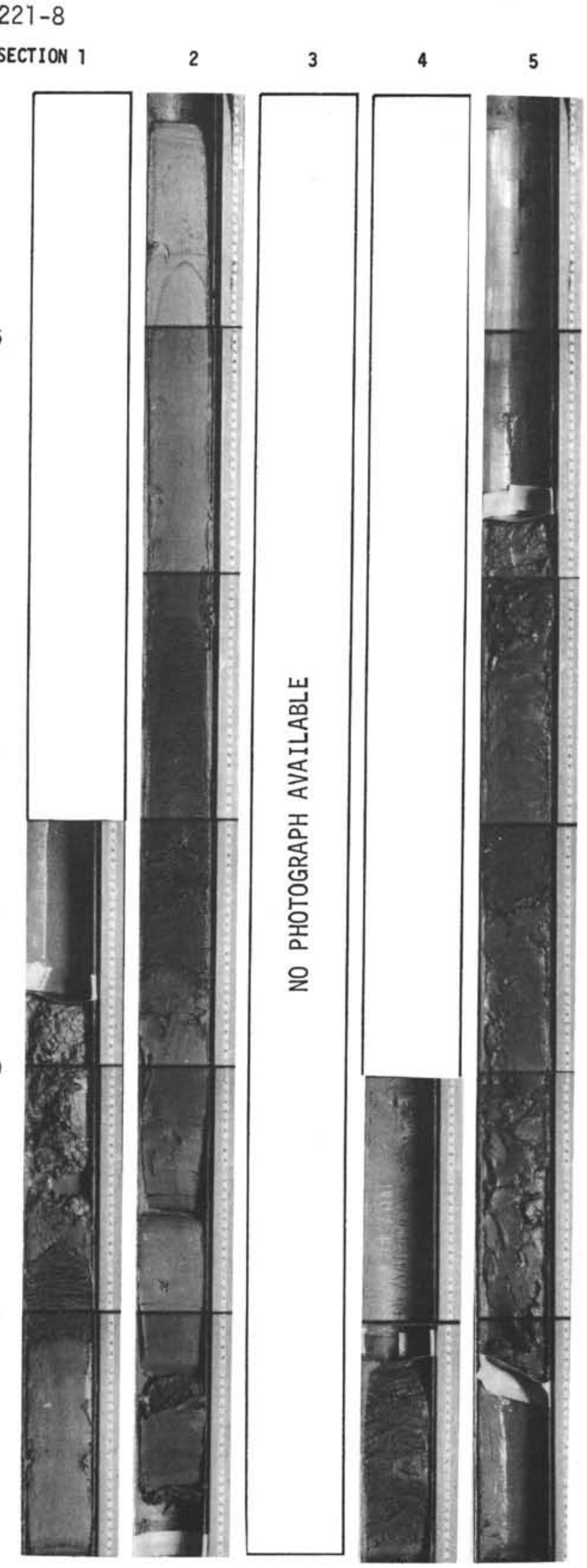

For Explanatory Notes, see Chapter 2

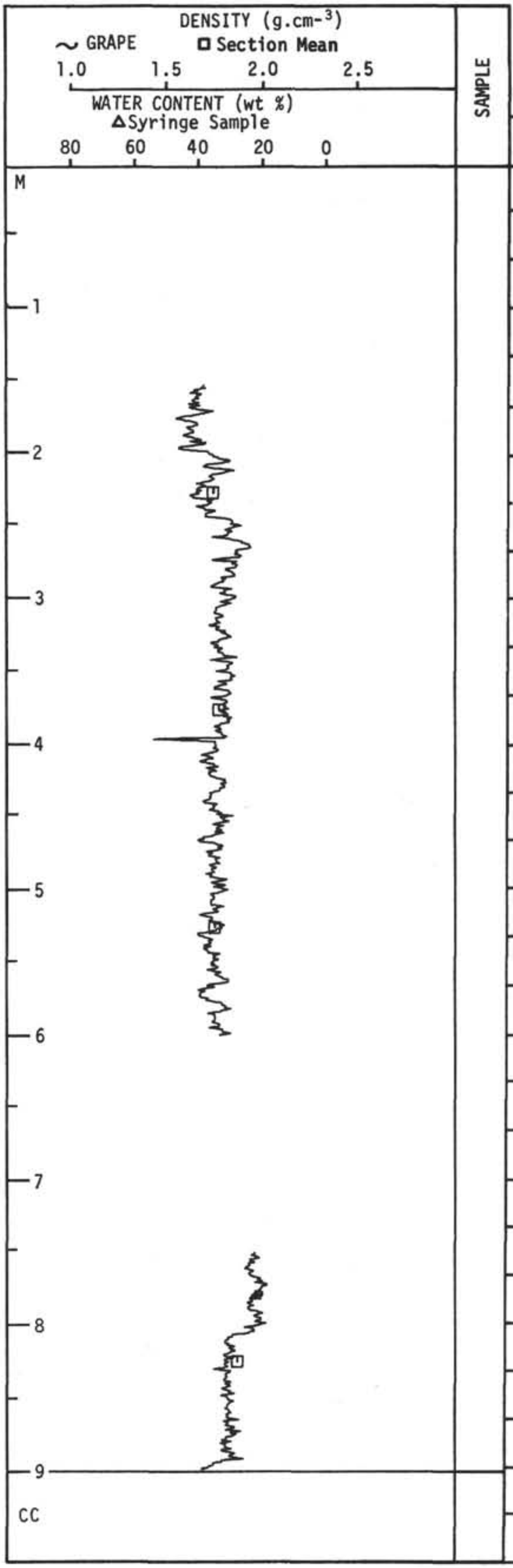

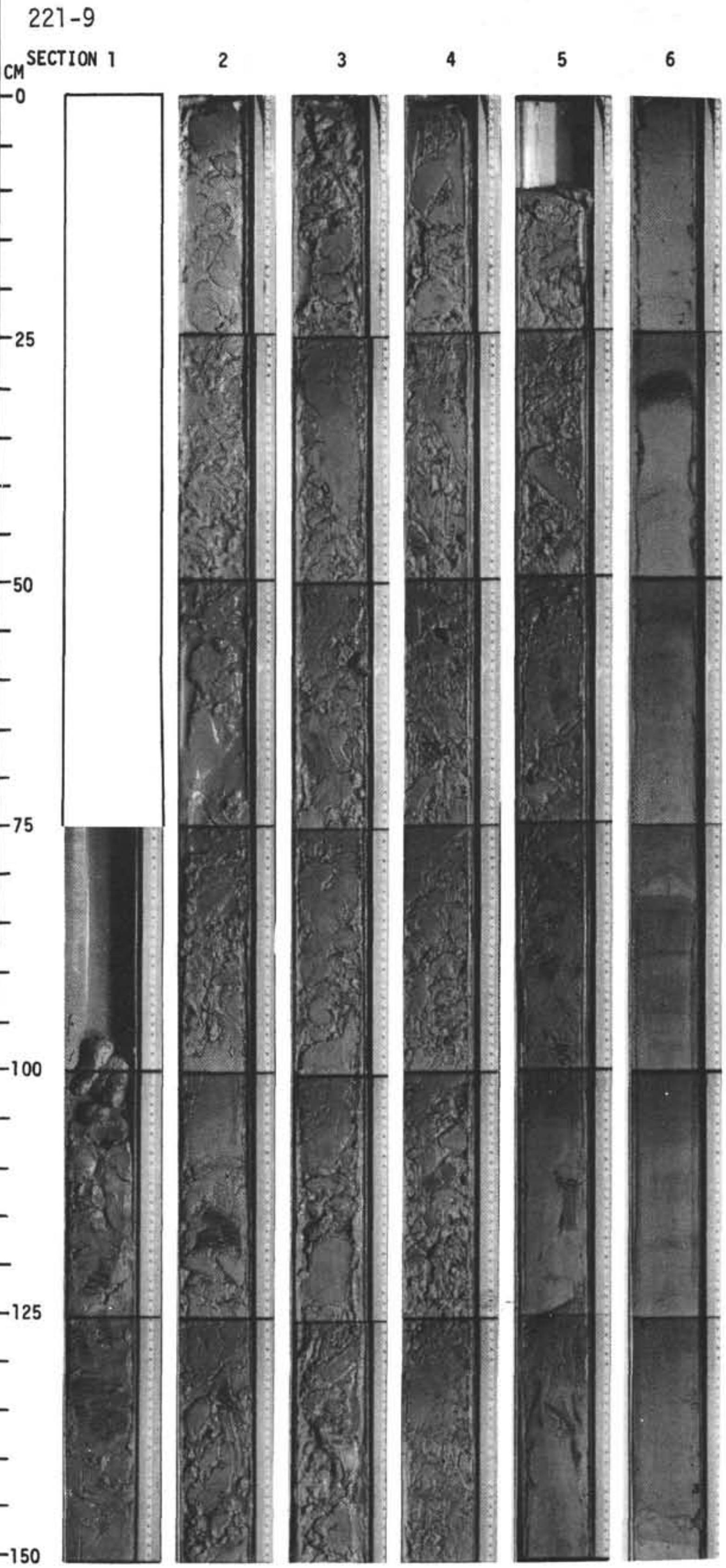

For Explanatory Notes, see Chapter 2

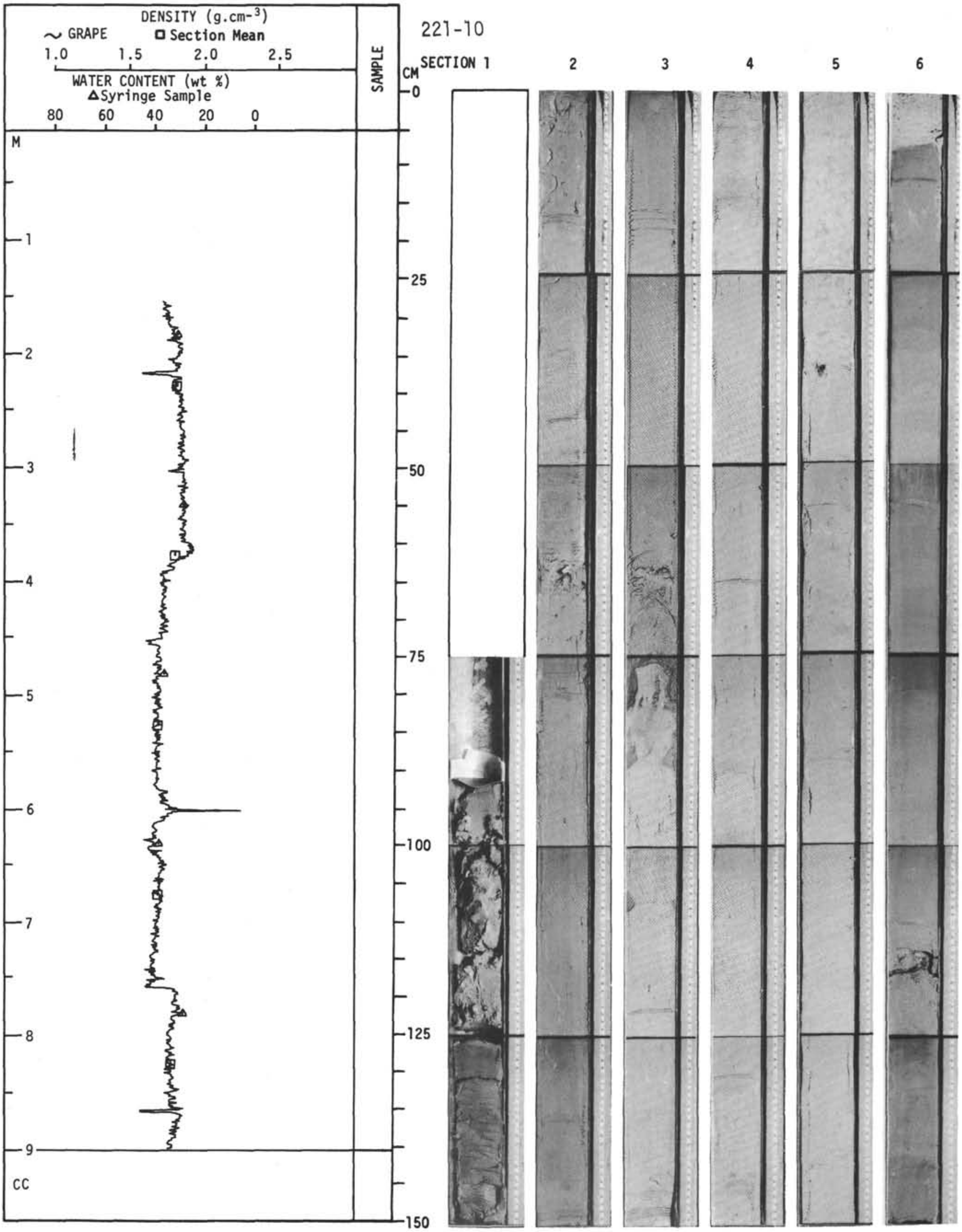

For Explanatory Notes, see Chapter 2

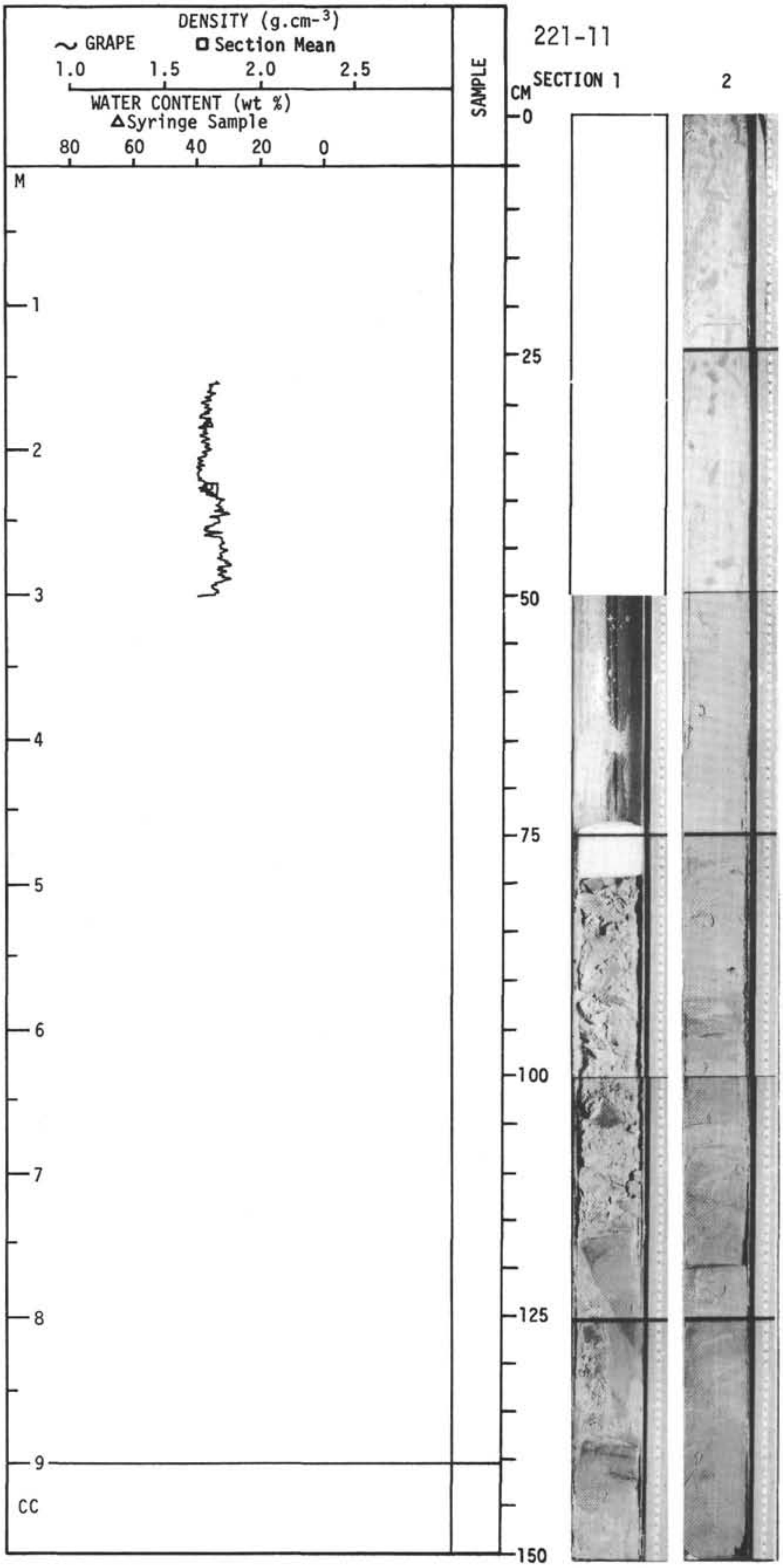

For Explanatory Notes, see Chapter 2

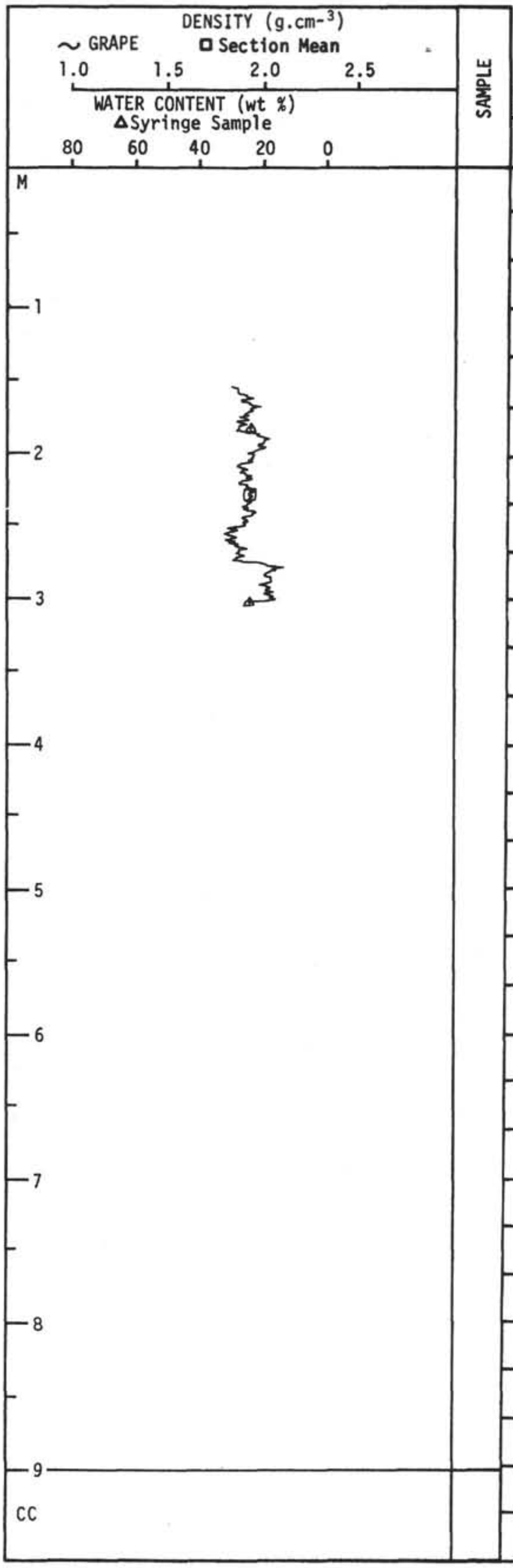

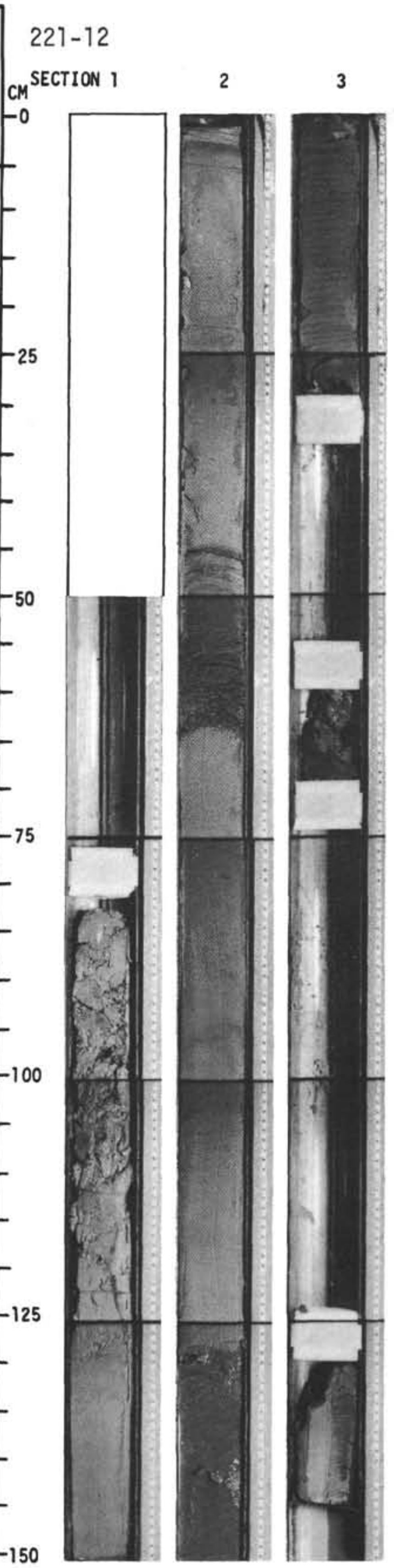

For Explanatory Notes, see Chapter 2

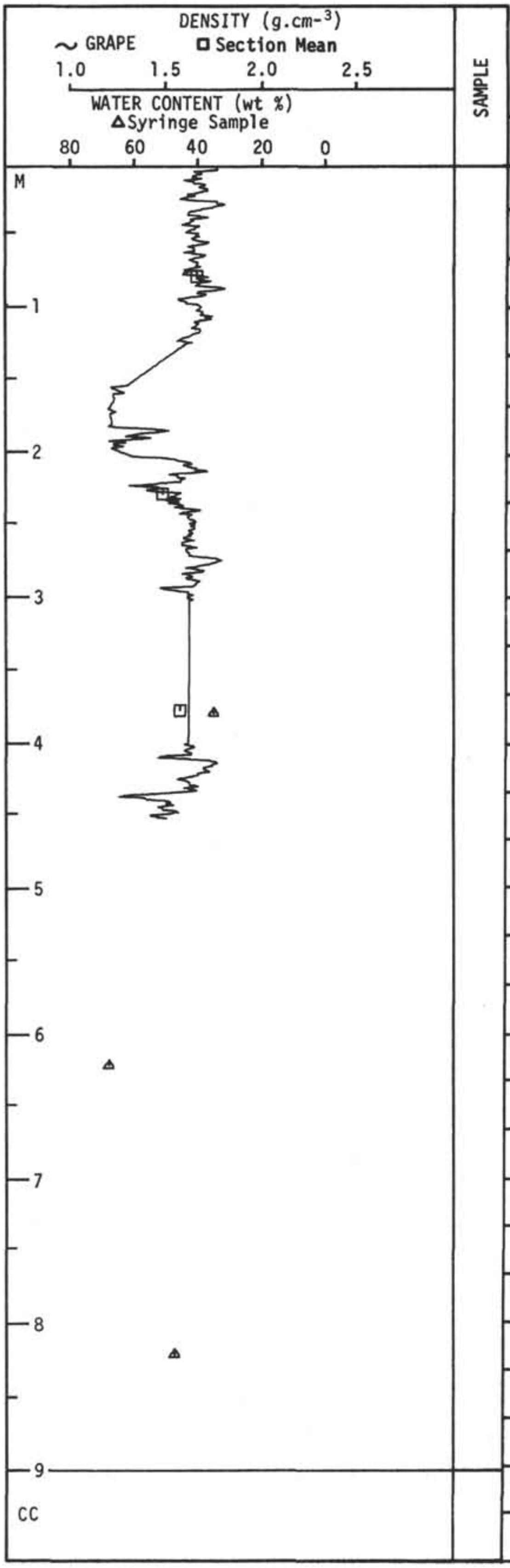

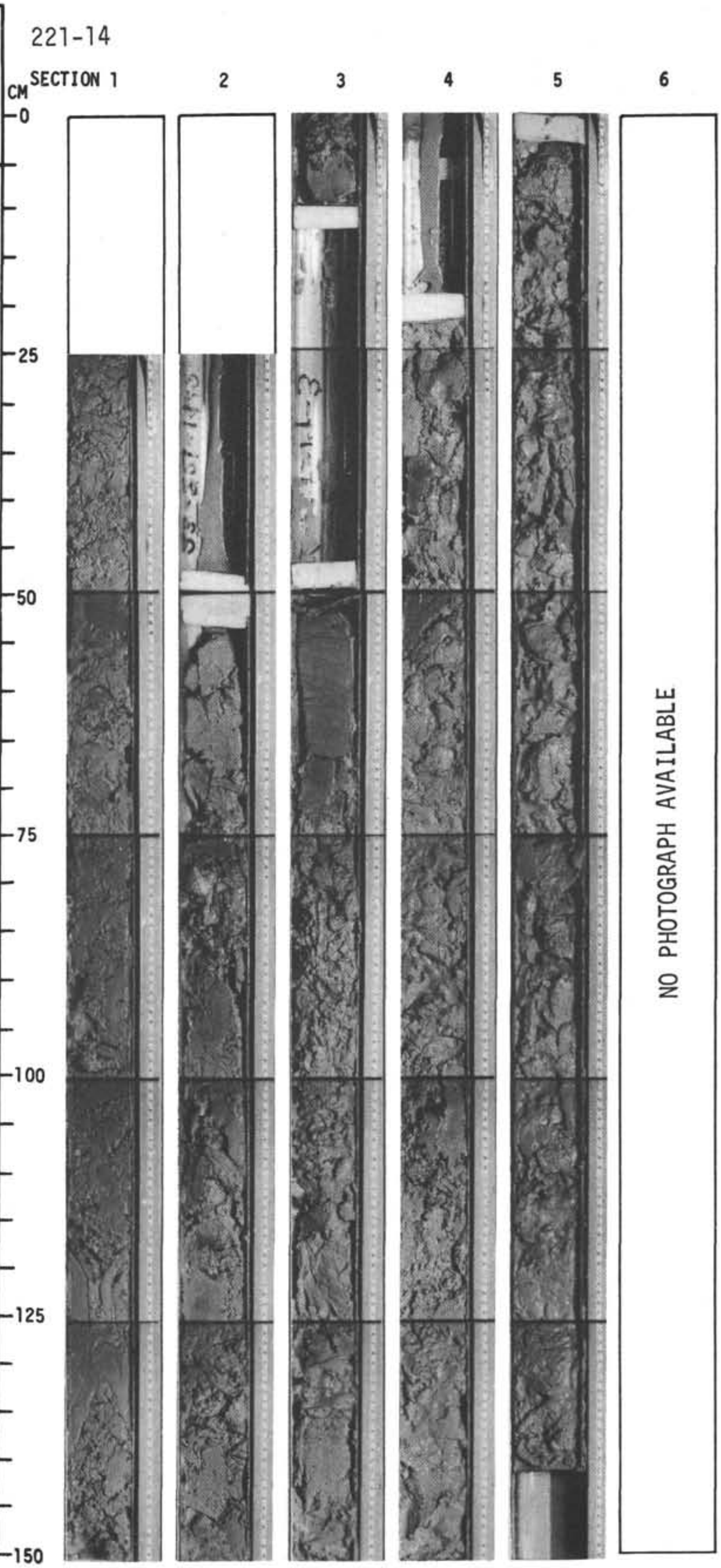

For Explanatory Notes, see Chapter 2

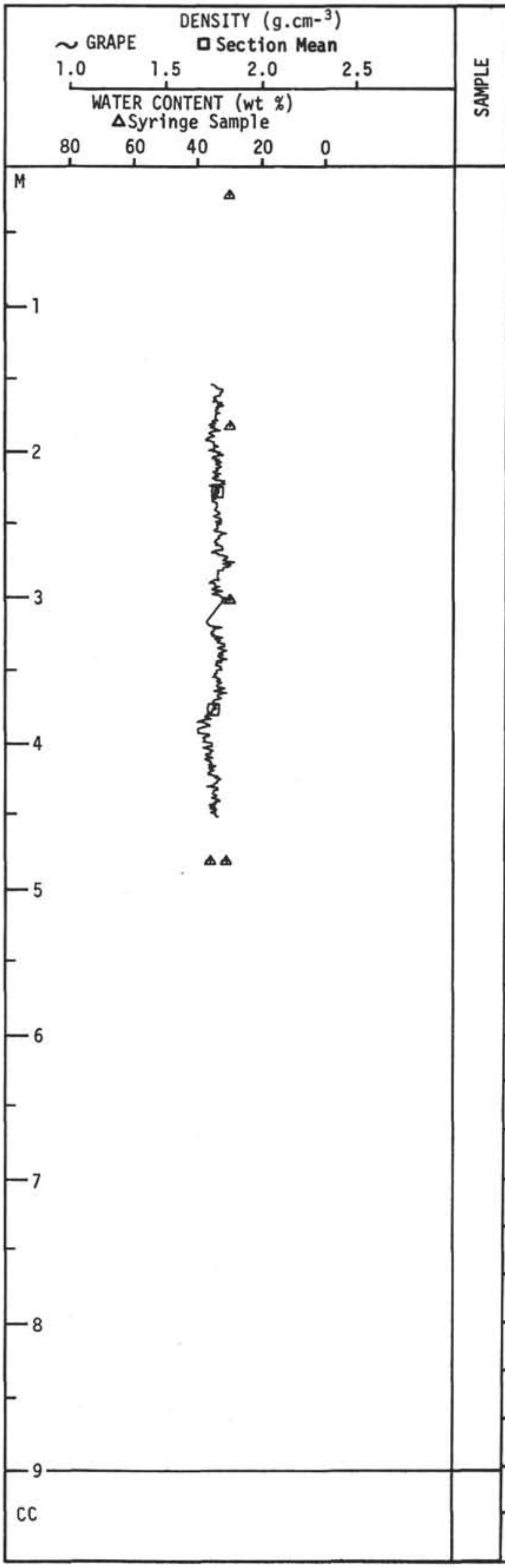

221-15

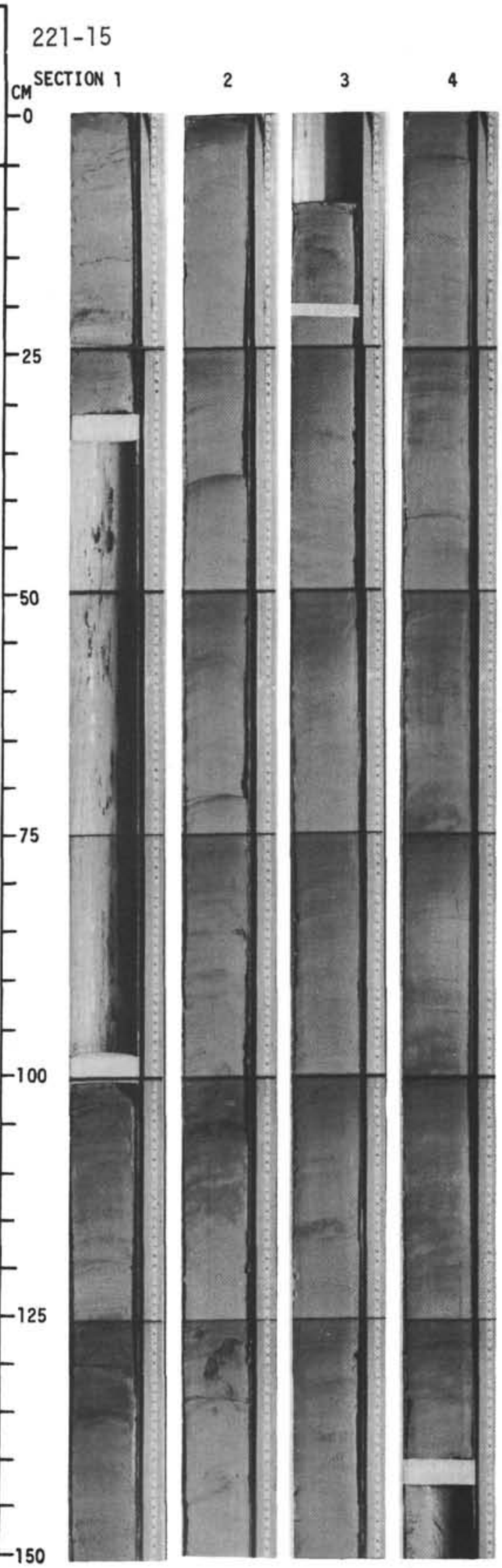

For Explanatory Notes, see Chapter 2

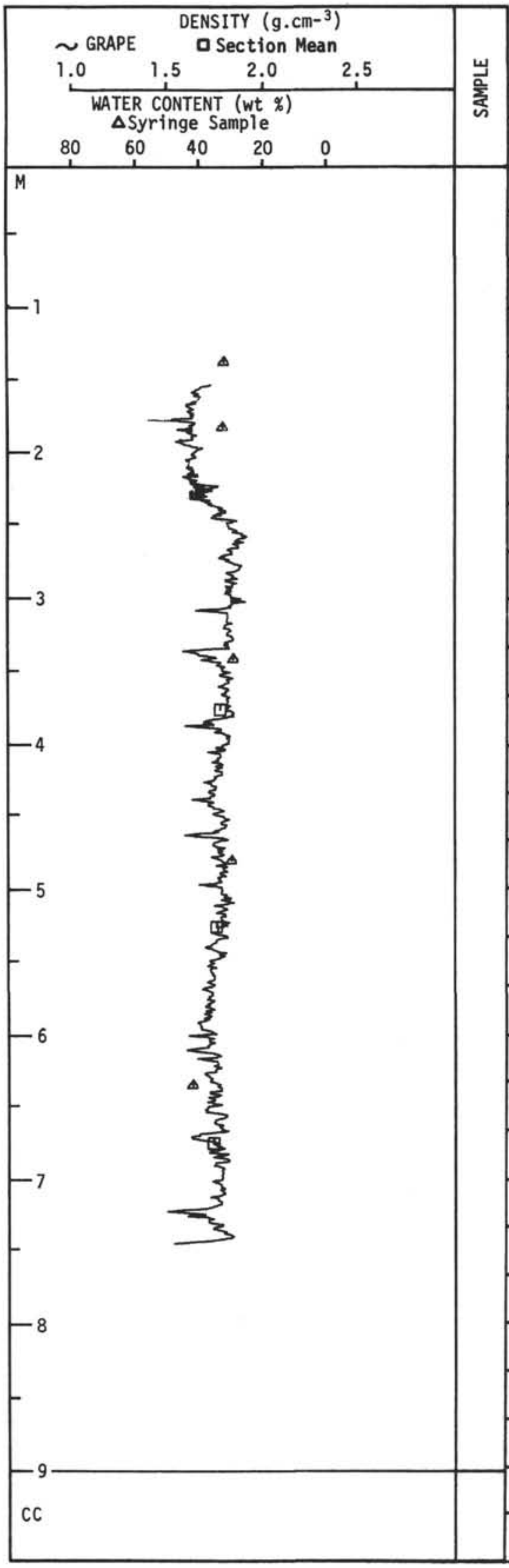

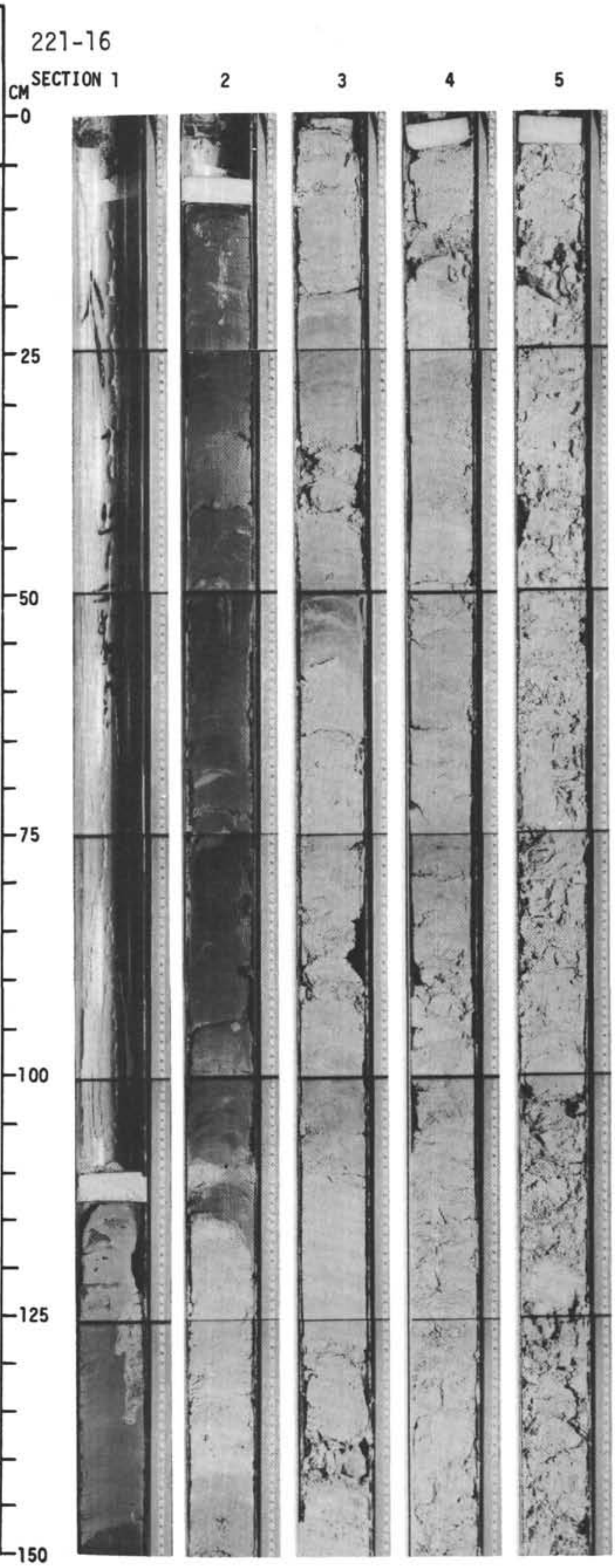

For Explanatory Notes, see Chapter 2

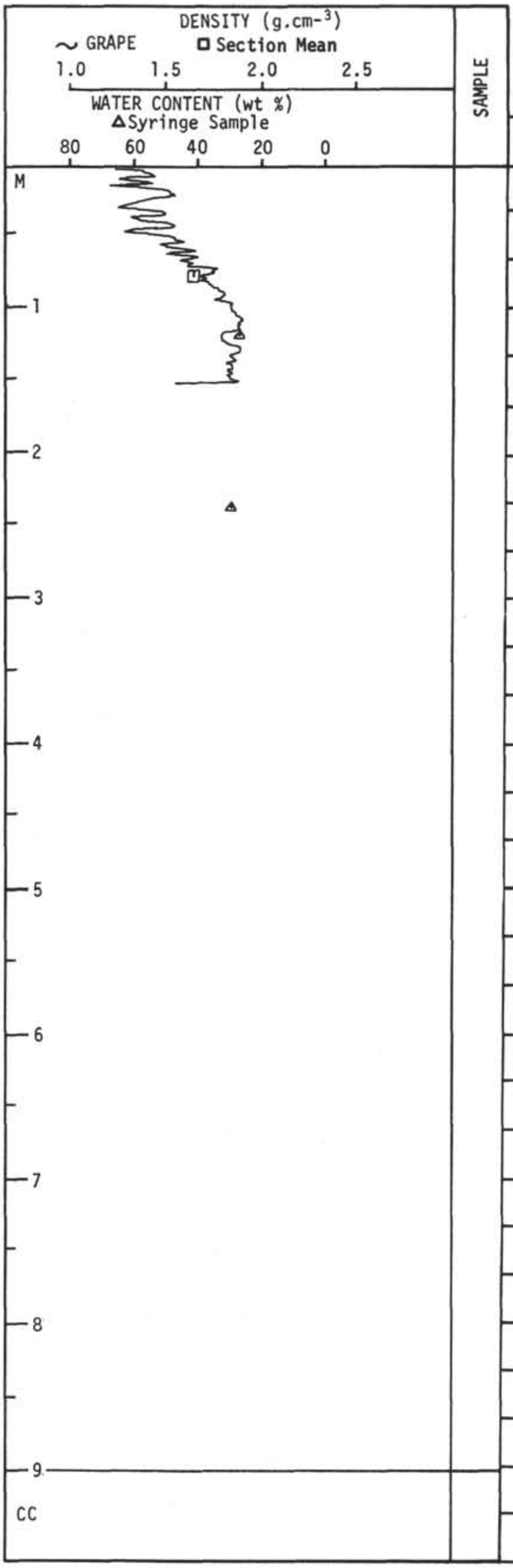

221-17

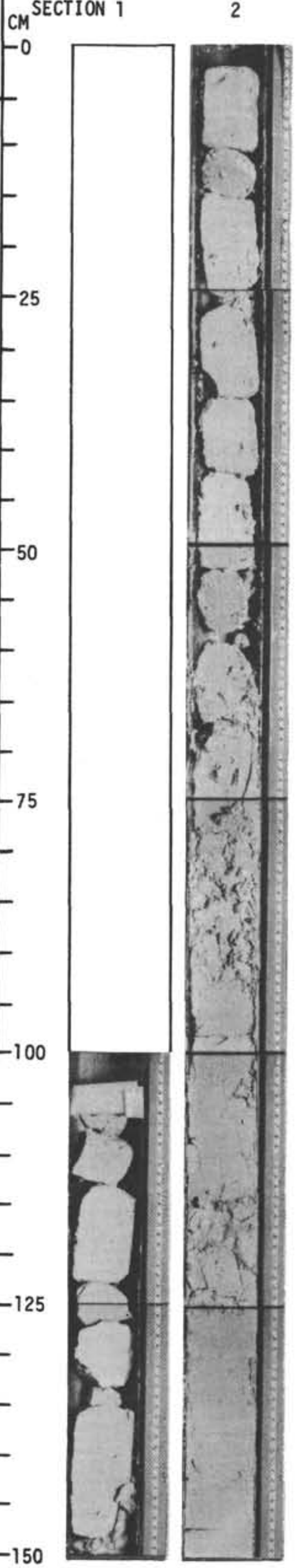

For Explanatory Notes, see Chapter 2

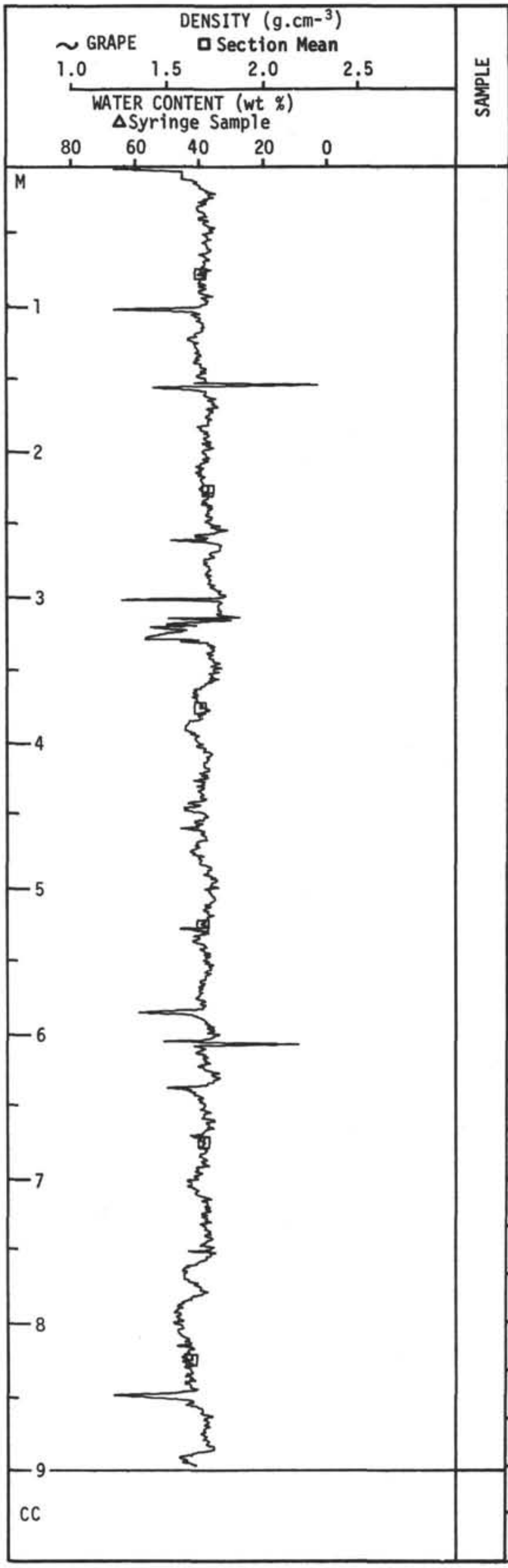

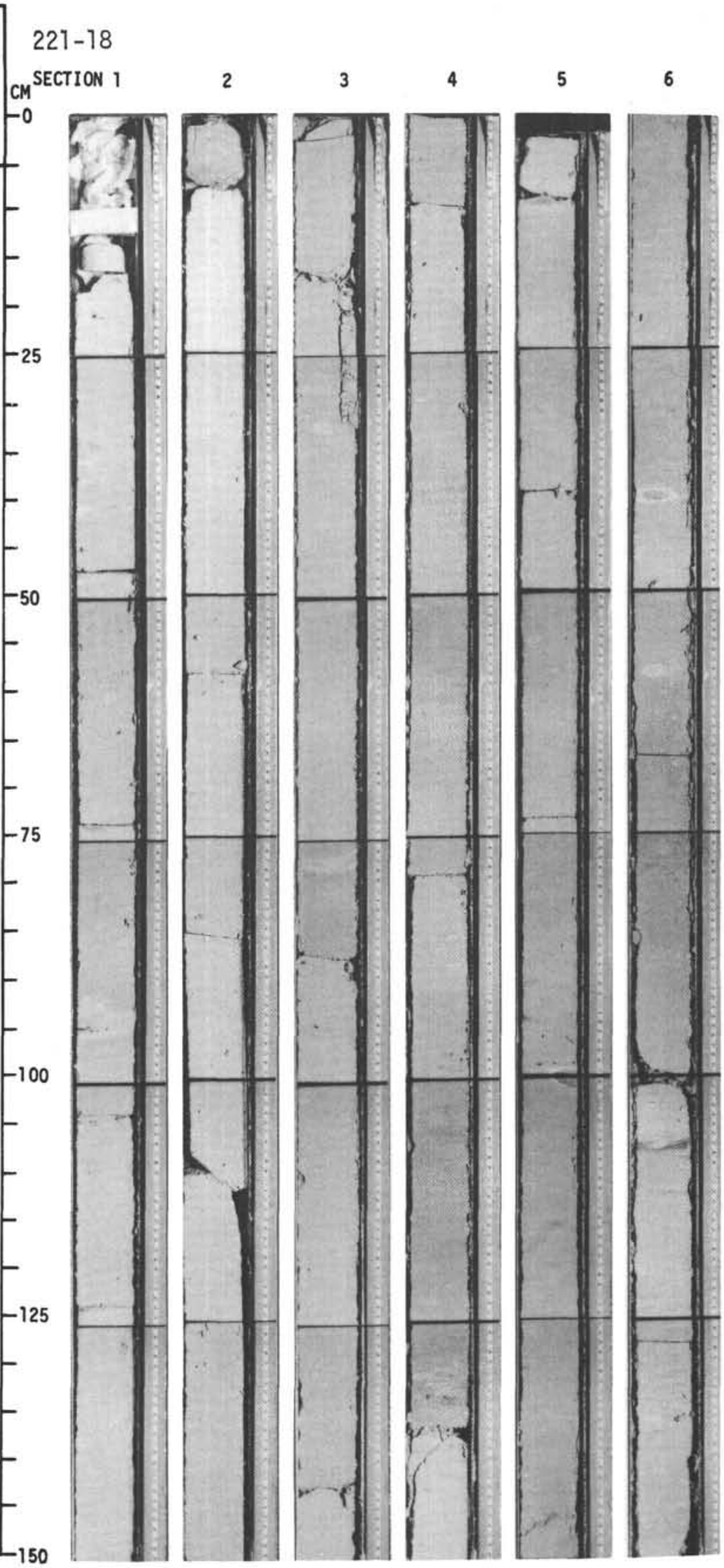

For Explanatory Notes, see Chapter 2

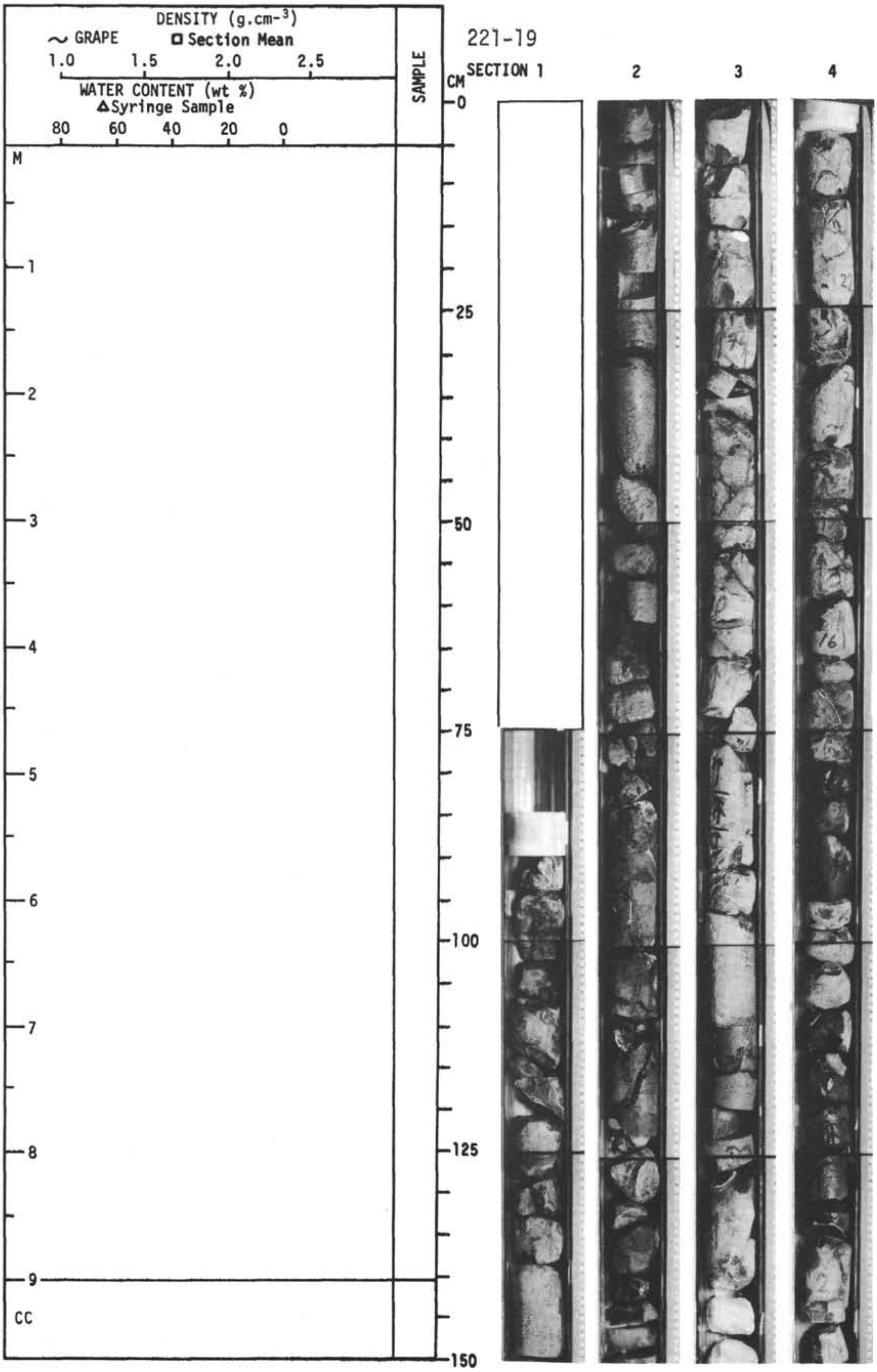

For Explanatory Notes, see Chapter 2